#698

IRAS

CHOPPED PHOTOMETRIC CHANNEL IMAGE

83-004A-03A

IRAS

CHOPPED PHOTOMETRIC CHANNEL IMAGE

83-004A-03A

This data set Catalog consists of one magnetic tape. The tape is 9-track, 1600 BPI, ASCII, written in FITS format. The tape contains 3020 files of data.

D#	C#	FILES	TIMESPAN
D-083698	C-028093	3020	02/02/83-11/21/83

83-004A-03A

Laboratory for SPACE RESEARCH GRONINGEN

of the

National Institute for Space Research

IRAS–DAX
Chopped Photometric Channel, Explanatory Supplement

P.R. Wesselius, D.A. Beintema,
A.R.W. de Jonge, T.A. Jurriens,
D.J.M. Kester, J.E. van Weerden,
J. de Vries, M. Perault.

SRON

The National Institute for Space Research is part of the Space Research Organization of the Netherlands.
The laboratories of the institute are located at the universities of Groningen, Leiden and Utrecht.

Address: Landleven 12, PO Box 800, 9700 AV Groningen, the Netherlands.
Telephone: 050 - 11 66 95, telex: 53572 stars nl.

IRAS-DAX Chopped Photometric Channel, Explanatory Supplement

This document has been prepared under the responsibility of the Laboratory for Space Research, Groningen, The Netherlands, by

P.R. Wesselius, D.A. Beintema, A.R.W. de Jonge,
T.A. Jurriens, D.J.M. Kester, J.E. v. Weerden,
Laboratory for Space Research, P.O. Box 800, 9700 AV Groningen,
The Netherlands,

J. de Vries,
Space Science Department, ESTEC, P.O. Box 229, 2200 AG Noordwijk,
The Netherlands,

M. Perault,
Observatoire de Paris, DEMIRM, F92190 - Meudon, France.

Assistance in analyzing the CPC data was provided by:
J.L. Puget, R. Wainscoat.

The drawings have been ably prepared by A. Koning, Laboratory for Space Research, Groningen.

TABLE OF CONTENTS

1. Introduction
    1.1 Functional description of CPC and IRAS
    1.2 Instrument performance
    1.3 Product
    1.4 Document structure

2. Observations
    2.1 Observation modes
    2.2 Control accuracy

3. End products

4. The photometer

5. Instrument performance
    5.1 Detector behaviour
    5.2 Sensitivity
    5.3 Observed beam profile

6. Data reduction
    6.1 Input data base
    6.2 System design
    6.3 Demodulation and deglitching
    6.4 Responsivity variation
    6.5 Pointing reconstruction and regridding
    6.6 Calibration and generation of end products

7. Analysis of reduction techniques
    7.1 Demodulation and deglitching
    7.2 Responsivity variation
    7.3 Attitude reconstruction and regridding
    7.4 Theoretical beam profile

8. Photometric calibration
    8.1 Sensitivity changes and repeatability
    8.2 Linearity and absolute calibration
    8.3 NGC 6543 as reference source

Annex 1. Deglitching algorithm

Annex 2. Discussion of sample maps

Annex 3. Tape format

Annex 4. List of observations

1. Introduction

This document is intended to provide the user of IRAS-CPC observations with the technical information that might be needed in the interpretation of CPC maps.

1.1. Functional description of CPC and IRAS

The main goal of the IRAS mission was to make a complete survey of the infrared sky. The "survey instrument" was used for this. (see the Explanatory Supplement to the IRAS Catalogs and Atlases, 1985 (abbreviated as IRASES)). In addition it was possible to perform pointed observations both with the survey instrument and with CPC.

CPC literally means Chopped Photometric Channel. The instrument measures simultaneously in two wavelength bands, one centred at 50 µm, the other at 100 µm. These bands are shown in Fig 4.1. It has a circular field of view with a diameter of 1.2 arcmin, matched to the diffraction limit of the telescope at 100 µm. The CPC, contrary to the survey instrument, was chopping against a reference blade at a few Kelvins.

The CPC mainly distinguishes itself from the survey instrument by its high spatial resolution. The CPC beam is theoretically predicted in chapter 7.4 and observationally derived in chapter 5.3. The observed beam appears to be significantly larger than expected. This can possibly be ascribed to the responsivity variation phenomenon described below.

Generally maps covered a region of 12 × 9 arcmin. These maps were made by executing "raster scans" (see section 2.1) using the satellite attitude control system. Reconstruction of the map (see section 6.5) gives an accuracy of a few arcsec for relative positions within one map, and an absolute accuracy of about 30 arcsec.

1.2. Instrument performance

A brief overview of the major items is presented. A more extensive discussion is given in chapter 5. Two major instrumental problems were encountered: responsivity variations and glitches. A common origin for these problems is most likely the too low temperature of the focal plane. In order to understand how these problems affect the astronomical interpretation of the CPC maps a few maps are extensively discussed in Annex 2.

In the course of an observation (4 to 7 minutes) the CPC sensitivity changes when significant infrared flux was "seen" by the detector: we interpret this as a responsivity variation of the detector/FET combination. There are at least two time scales involved: an overall gradual increase of the response if sufficiently strong background radiation is present, and a faster response change due to point sources.

An extra complicating factor to the detector responsivity variations is a DC leak in one of the two extra beams present for beam switching (never used in orbit). Regions exhibiting a complicated structure in the infrared can appear quite weird because of the direct gain changes combined with the DC-leak-caused gain changes.

Two kinds of "glitches" severely affect the raw data: induced by high energy particles, and caused by the infrared photons themselves. Their signature is usually much narrower than expected from a point source.

The reproducibility of observations is generally good.

1.3. Product

One of the main requirements on the data processing was that by end '84 a reduced product was available. This inevitably led to compromises in the optimal choice of reduction algorithms and procedures (in spite of the production delay of several months). We are confident about the deglitching, regridding, attitude reconstruction, and calibration, but the correction for the responsivity variations is unsatisfactory at present. Maps that clearly suffer from this effect, after our (too) simple gain-correction procedure, are omitted from the set of maps offered to the IRAS community. We advise people interested in specific suppressed maps (a complete list of observations is added as Annex 4) to contact the Laboratory for Space Research. Special processing tools are available to analyze such maps.

1.4. Document structure

The document is split in two parts. The first three chapters are essential reading for any CPC user: the major instrumental problems are briefly described, the observational method is outlined, and the data products are presented.

The subsequent chapters 4 to 8, and the Annexes give background information for the interested reader:

- the instrument and its performance in chapters 4 and 5,
- the data reduction and the analyses leading to reduction methods and algorithms in chapters 6 and 7,
- the flux calibration and linearity in chapter 8,
- several special topics in the Annexes.

2. Observations

This chapter describes the observation modes used, and addresses the control accuracy. Characteristics of the CPC instrument are summarized in chapter 1, and elaborately described in chapters 4 and 5.

2.1. Observation modes

The IRAS satellite performed observations by scanning at constant solar aspect angle. Special observations employed a "raster scan". A raster scan consisted of a number of small scans ("legs"). Size and shape of the area of sky covered by the legs (a "map") could be chosen almost at will. Many options were not sensible for CPC. All CPC raster scans (summarized in Table 2.1) covered a "rectangular" sky area and reversed the scan direction between legs.

Table 2.1. CPC science raster scans

Name	area in × cr (arcmin)	samples in × cr	separation in (arcsec)	separation cr (arcsec)	occurrence
CPP00A	3 × 1	78 × 10	2.3	6.0	3
CPPF0A	3 × 1	38 × 10	4.7	6.0	55
CPC03A	3 × 3	78 × 10	2.3	18.0	115
CPCF3A	3 × 3	38 × 10	4.7	18.0	17
CPC09A	9 × 9	38 × 18	14.2	30.0	859
CPCF9A	9 × 9	18 × 18	30.0	30.0	1020

in: in scan; cr: cross scan,
There are two samples in every second for all types of raster scan.
10 extra samples are taken between raster legs during the turnaround. Inclusion of these samples leads to an in-scan extension of the maps of a few arc minutes.

The astronomer/planner had to code his intended raster scan in the Observation Input Language (OIL). Via a number of computer programs running on a computer at the Ground Operations Centre in Chilton, England the raster scan description in OIL was translated into the data words uplinked to the onboard computer program, as part of the Satellite Operations Plan (SOP). (Such a SOP was executed in about twelve hours, between successive passes of the IRAS satellite in its sunsynchronous orbit.)

There were several reasons to define - for science observations - only a limited number of standard raster scans. Allowing astronomers/planners to choose from a very large number of raster scans for thousands of special observations would have made the task of installing the observations in the ground system almost unmanageable. It proved to be very worthwhile to have many observations executed in exactly the same way: the calibration can depend on the specific raster scan used.

In detail, the CPC observations were done as follows. A position calibration star was observed with the visual sensors in the focal plane, then the satellite slewed to the desired region and performed the raster scan, subsequently the detector looked for a minute at the internal (flux) calibration source, finally the satellite slewed again towards a position calibration star and observed it. The position calibrations can occasionally give an erroneous result (wrong star, wrong catalog position of star) or one or both are absent because of planning constraints. Such problems can result in bad reconstructed positions.

2.2. Control accuracy

Astronomers indicated to the planning system the central coordinates (in Ra, Dec) of the region they wanted to study; we refer to "target" position. Of interest to the CPC user is how the coordinates assigned to the processed CPC map are related to this target position.

We defined a fixed grid of pixels on the sky. Attitude reconstruction and regridding (see section 6.5) resulted in surface brightness values being assigned to pixels covered by the raster scan. Within a map the positions are accurate to about 20" with respect to each other.

The accuracy of the location of a map on the sky was derived as follows. We compared for 50 clearcut point sources the position of the source in the CPC map with the target position (assuming that the -usually - optical position coincides with the far-infrared position). This gave a standard deviation of 25" both in-scan and cross-scan. However, the distribution of the position difference values does not resemble a gaussian; it has a more pronounced tail. There are 7 of the 50 observations that have a difference of 60" or slightly more between the target position and the CPC position.

3. End products.

About 2100 scientific observations were done during the IRAS mission. After the reduction about 1500 observations were considered acceptable for publication. All observations done with raster scan types other than CPC09A and CPCF9A were left out. Other observations were recognized as problematic during the reduction (usually because of peculiar responsivity variations), and rejected for that reason. Detailed information about the reduction is given in chapter 6.

One reduced observation is presented as 4 maps of the sky. Two of the maps are the result of the full data reduction scheme, for the 50 and 100 μm channels (the 'clean image'). The other two give the corresponding 'raw image' of the same observational data, but here the deglitching and responsivity variation correction steps of the reduction are skipped. Because of the many assumptions involved in these two reduction steps (see chapter 7), we advise the user of the CPC products to compare the two images in order to get an idea of the nature of these corrections. This may help to identify some of the reduction problems outlined in chapter 7. The discussion in Annex 2 of some sample maps clearly shows the need for the combined use of both 'raw' and 'clean' images.

The images are distributed on magnetic tape in the format known as FITS (Flexible Image Transport System, Wells 1981). The total data volume consists of three tapes, containing 489, 624, and 395 observations (the sky has been divided in three equal right ascension parts). The four maps of each observation are organized as two consecutive files on tape. The 50 and 100 μm 'clean image' maps are combined into the first file as two planes of typically 40×40 pixels on a common 20 arcsec grid. The 'raw image' maps follow in the second file in exactly the same structure as the clean maps. An example of the FITS header is given in Annex 3.

4. The photometer

The photometer has a field of view matched to the diffraction image of the IRAS telescope in the 100-μm range. The image of the field stop in the telescope focal plane is circular, with a diameter corresponding to 1.2 arc-min. The resulting beam profiles are discussed in section 7.4 and observations pertaining to the beam are described in section 5.3.

The optics and the detectors with their pre-amplifiers are in an assembly cooled to 2.4 K.

An absolute chopper, operating at about 15 Hz, is located just in front of the field stop. Thus the infrared signal modulation is proportional to the difference in emission from the sky and from the cold chopper blades. The chopper is of the tuning-fork type, with a shutter blade fixed to each of its tines.

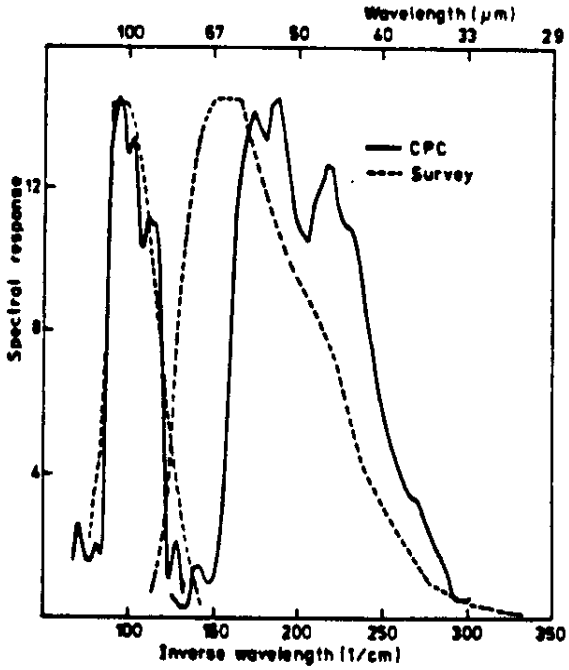

Fig. 4.1. The spectral response of CPC and of the survey instrument.

An optical system consisting of a beam splitter, filters and field optics images the telescope pupil onto the two detectors. The combination of beam splitter, filters and detector cut-offs define the wavelength bands (41-62.5 and 84-114 microns). The resulting passbands are shown in Fig. 4.1. Short-wavelength leaks, if present, are at most at the one percent level, as is evident from observations of Ceres and of stars.

Both detectors were made from Gallium-doped Germanium; they were operated at a bias voltage of 40 mV.

The pre-amplifiers are of the trans-impedance type. They are followed by a spike-suppression circuit (operating in the millisecond domain) and by a

15-Hz bandpass filter. The 15-Hz signals then pass though a zero-clamping circuit, which essentially rectifies without integrating, are converted to a logarithmic scale and finally digitized and sampled at 64 Hz. The digitization steps correspond to increments of 3.5 %.

A third 64-Hz data channel records a reference signal from the chopper drive electronics.

A more detailed description of the instrument is given by Wildeman, Beintema and Wesselius (1983).

The instrument provides options that were not used during the mission, intended to solve potential dynamic-range problems. One of these, a differential chopping mode, is relevant because of a non-modulated optical path via an additional aperture, compounding the problem of responsivity variations. The offending aperture is located at a distance of 2.25 arcminutes; on average, it contributes 40 % of the background radiation.

5. Instrument performance

In the first section there is an extensive discussion on responsivity variation and the effect of glitches. These two detector problems were not expected and seriously affect the quality of the CPC data. The sensitivity of the CPC is described in section 5.2, while section 5.3 addresses the beam profile.

Calibration of the CPC, sensitivity changes, and repeatability are treated in chapter 8.

5.1. Detector behaviour

5.1.1. Introduction

Both CPC detectors behaved anomalously during the flight: their sensitivity was much too low, they exhibited strong signal-dependent spiking and their responsivity was strongly influenced by the incoming flux. These effects must be related to the unexpectedly low instrument temperature (2.4 K instead of 3.5 K): one single observation at the end of the mission, when the cryogen was exhausted and the instrument started to warm up, was of a much higher quality. However, the effects are not understood physically and could not be reproduced under laboratory conditions.

5.1.2. Spiking

The spiking phenomenon is the likely cause of the loss of sensitivity and it is probably connected with the responsivity variations. Most of the spiking was clearly correlated with the amount of incident infrared flux. Moreover, spikes tended to occur during the "open" phase of the chopper cycle: even if phase-sensitive demodulation was applied, spiking would always increase the over-all instrument response. In effect spiking represented an erratic component in the detector responsivity; in an observation on a strong point source, obvious spikes, if left in the data, could contribute 10 % of the observed flux.

The instrument electronics contained deglitching circuits, operating in the kHz domain, intended to suppress spikes due to the incidence of ionizing particles. Before the flight the deglitchers, tested with a radio-active source, proved to remove more than 80 % of the noise energy carried by the spikes. Possibly the deglitchers were less efficient in rejecting flux-induced "spontaneous" spikes, either because of their different signatures or because of a tendency of this kind of spikes to arrive in close bunches.

Quite likely low-level spiking was the major source of noise in the CPC. Spiking at rates in excess of 1 Hz would not be recognizable as such, due to the narrow pass bands of the instrument electronics. Fig. 5.1 shows some spike statistics which support this hypothesis.

There probably is a physical connection between spiking and responsivity

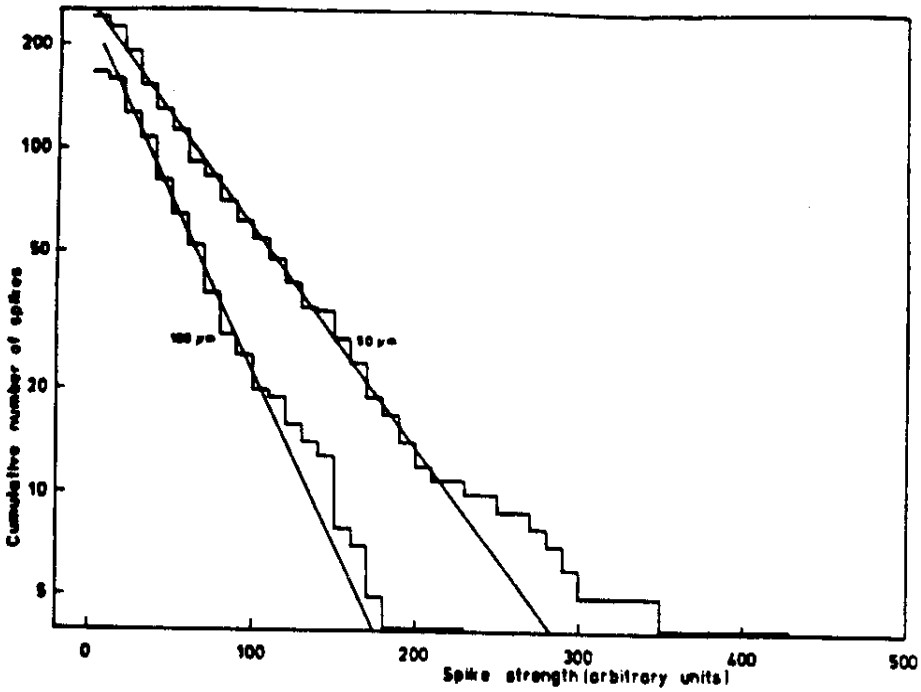

Fig. 5.1. Cumulative number of spikes versus spike strength

These spikes were found by the deglitching algorithm in data on empty fields. Note the excess of strong spikes, and the absence of a cut-off at low values.

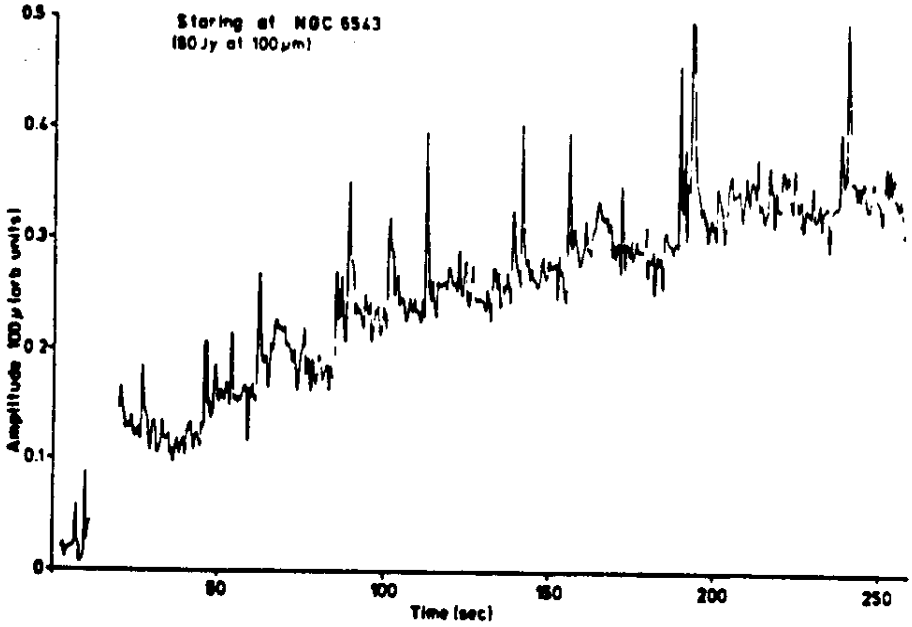

Fig. 5.2. The CPC response during a stare at NGC 6543.

In the first 10 seconds the source was outside the beam. The data have been demodulated but not deglitched. Two effects are evident:

- the response keeps rising until an equilibrium is reached after 200 seconds,
- many spikes appear to coincide with instantaneous responsivity increases.

changes. On a rising signal spikes often appear to co-incide with instantaneous responsivity increases; fig. 5.2 provides an example of this phenomenon.

5.1.3. Responsivity variations

On sufficiently bright sources, strong variations of the photometer responsivity are observed on time scales ranging from a few seconds to several minutes (the maximum duration of an observation is about 7 minutes). These are strongly non-linear effects, as both the magnitude and the time scale of the variations depend on the previous and present input signal intensity. In extreme cases gain variations by a factor of five have been observed.

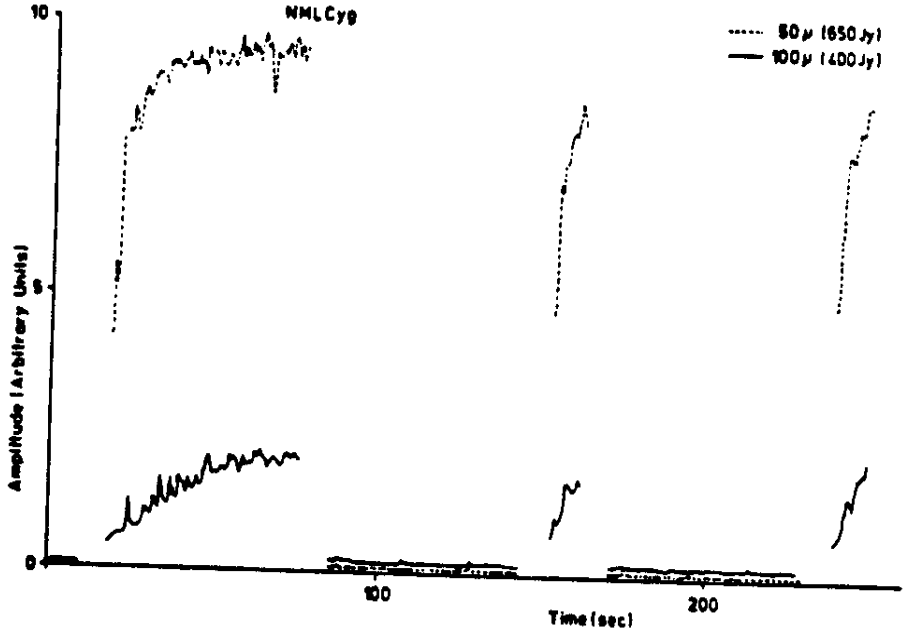

Fig. 5.3. Responses to a strong source (NML Cygni).

The results from three stares on the source, alternated with blank-sky measurements are shown. The transitions from source to sky and back (during which no CPC data were recorded), were sufficiently long for the pointing to stabilize. Raw data have been plotted, after demodulation but before deglitching. At these high signal levels spiking is not predominant. On this very strong source the equilibrium response is obtained after 60 seconds. After a 60-second interruption the responsivity is much reduced but it recovers more rapidly. Weaker sources show much less responsivity variations.

The behaviour is quite complex, but two effects stand out. When a relatively faint point source (about 20 Jy or less) on a low background is moved into the beam, there is a clear signal overshoot, relaxing with a short time constant. This overshoot is usually present in the response to the telescope's internal calibrator (see fig. 5.5). The second effect is a slow responsivity increase, at a rate roughly proportional to the incoming flux, and during a time roughly inversely proportional to this flux. For a constant input an equilibrium state, which depends on the input level, is reached after the detectors have been exposed to about 10^4 Jy.sec / arcmin^2. For exposure levels around 120 Jy/arcmin^2 the responsivity doubles in about 30 sec. The

magnitude of this long-term effect may be as large as a factor 5. A few seconds in darkness are sufficient to lose most of this gain increase, but the high responsivity is recovered very fast if the system has not had enough time to relax.

These effects were recognized as the observing program proceeded. The distortions due to responsivity variations can be very strong, but are quite reproducible. To characterize the effects quantitatively, special calibration observations were performed.

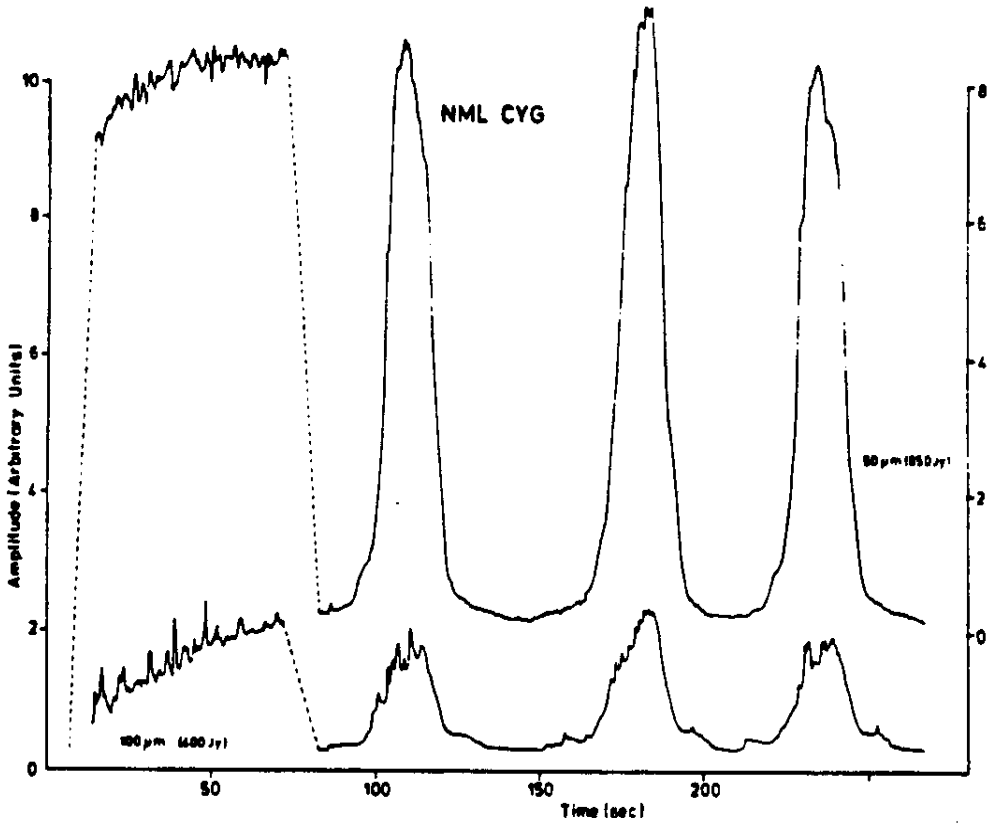

Fig. 5.4. Responses to a strong source (NML Cygni).

The results from a stare on the source, followed by three slow (0.075 arcmin/sec) scans in alternating directions are shown. Raw data have been plotted, after demodulation but before deglitching. The scan direction has a small influence on the response; this must be caused by a leak in one of the two additional CPC apertures meant for a beam-switching mode - radiation through this aperture is not modulated but reaches the detectors.

- One set of calibration observations consisted of pointing measurements alternating between a strong or moderately strong source and a low-level background nearby. Each phase lasted between 10 seconds and a few minutes. Unfortunately, operational limitations precluded recording data during the 7 or 8 seconds slew between the two positions. Examples of results from such observations are given in Figures 5.3 and 5.4.

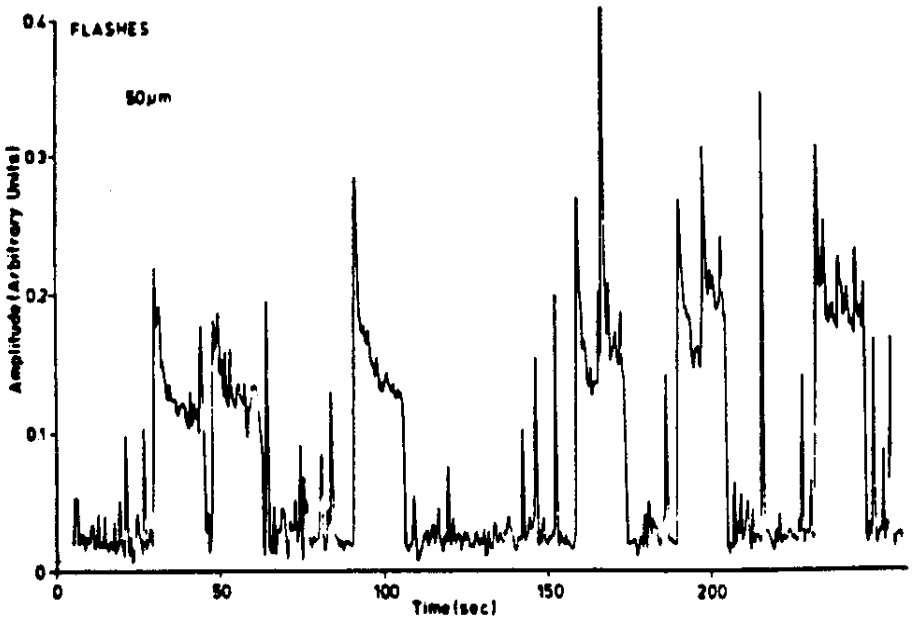

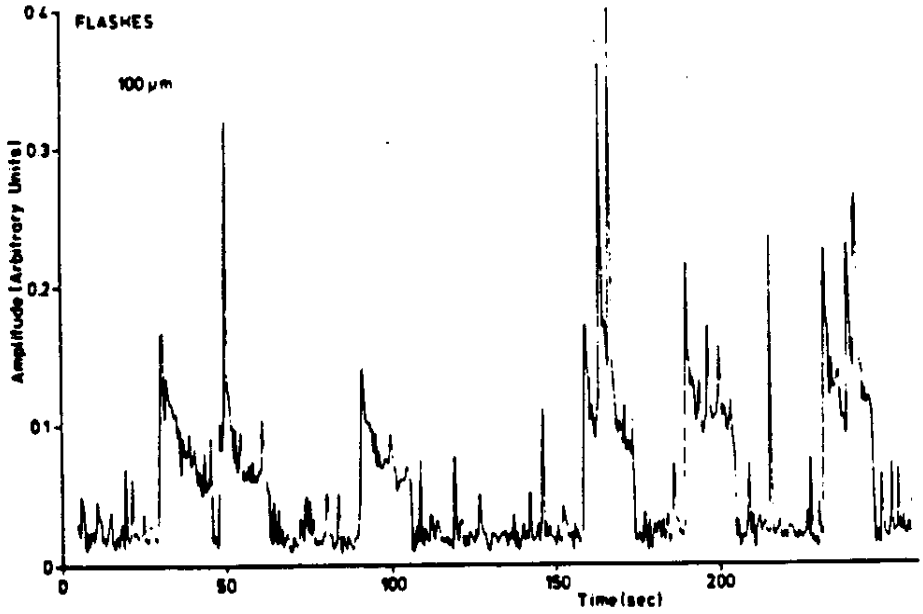

Fig. 5.5. Response to a sequence of stimulator exposures.

While pointing at blank sky, the internal stimulator was activated during 6 15-sec intervals, at t = 25, 43, 86, 160, 185 and 227 sec. The data were demodulated, but not deglitched.

Each flash response shows an initial signal overshoot, a short-term responsivity variation effect. The overshoot on the second flash, which followed closely on the first one, is less pronounced. A longer-term effect is the response increase from one flash to the next. The spiking is strong, but does not seriously affect the measurement accuracy.

Similar observations have been carried out on a very low background, using the internal calibrator as a source. Fig. 5.5 shows such an observation. The initial signal overshoot is conspicuous, but it appears only after a sufficiently long interruption (the threshold is between 4 and 16 seconds). The integrated exposure is insufficient to show the long-term responsivity increase.

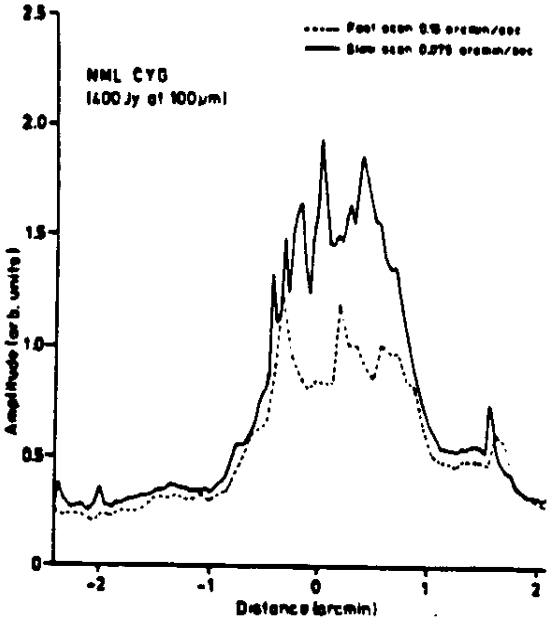

Fig. 5.6. Scan-rate dependence of the response to a strong source (NML Cygni).

Long-term responsivity increases are of course dependent on the scan rate. During a slow source crossing the responsivity build-up can be appreciable. This effect is more pronounced at 100 μm than at 50 μm. It is much less severe for sources of 100 Jy or less.

Repeated scans at various speeds across sources of various brightness show the beam profile distortions resulting from the responsivity variations (Fig. 5.6). The maximum response reached in a fast scan is generally lower than the value obtained after a long integration on the source. The profile is usually asymmetric, and the peak may be shifted forward or backward, due to the overshoot effect or to the long-term effect, depending on the scan speed and on the source intensity.

5.1.4. Attempts at modeling the responsivity variations

The reproducibility of the anomalous gain effects made us hope that we might be able to characterize the detector behaviour sufficiently to enable us to devize a correction procedure. We constructed a phenomenological detector model, described below, that can reproduce the results of the calibration measurements reasonably well. However, using this model to reconstruct the IR signals on the detectors turned out to be impractical, for reasons that are

probably fundamental. In the first place, such a reconstruction process is very sensitive to noise, particularly when superimposed on signal gradients. A second problem is its high sensitivity on the assumed initial state of the detector in terms of model parameters. Finally, the model predicts much too small responsivities at low input signal levels. In view of the inherent instability of a direct correction procedure and of the reasonable agreement between CPC and survey fluxes over a large dynamic range, we decided not to attempt any correction based on a detector model.

In the phenomenological detector model the state of the detector is defined by two quantities, a gain factor G and a saturation level F_s. The input signal F_{in} and the response F_{out} are related by

$$F_{out} / F_s = 1 - e^{-G \times F_{in} / F_s}$$

The values of both G and F_s are variable, controlled by first-order differential equations. The behaviour of G determines the long-term responsivity variations, F_s accounts for the short-term effects.

The differential equation for the gain factor is

$$dG/dt = A \times F_{in} \times (G_{max} - G) - B \times (G - G_{min})$$

where the constants A, B, G_{max} and G_{min} are chosen to fit the experimental data.

G tends to an equilibrium value

$$G_{eq} = (A \times F_{in} \times G_{max} + B \times G_{min}) / (A \times F_{in} + B)$$

with a time constant equal to

$$\tau = 1 / (A \times F_{in} + B)$$

An analogous differential equation applies to the saturation level F_s, with F_{in} replaced by $(g \times F_{in})$.

5.1.5. Laboratory tests

Laboratory tests on Ge:Ga detectors from the same supplier failed to reproduce the detector behaviour experienced during the flight. In these tests the electrical configuration and the temperature of the detector and the pre-amplifier were the same as during the flight, while the signal levels were in a range where strong effects have been observed. Signal-related short-term responsivity variations remained below the 5 % level. Stronger gain variations accompanied by spiking were observed occasionally, but only after strong electrical disturbances.

5.2. Sensitivity

In this section we will discuss the sensitivity of the CPC observations. The responsivity changes discussed in the previous section affect the sensitivity. The ability to detect point sources depends on the previous signal detection history of a detector. If there is much infrared flux in a map, the ensuing distortions in the infrared image will effectively make the signal to noise worse.

We analyze a few CPC images with relatively little flux. Such low-flux images reasonably well represent the real infrared distribution on the sky, and the noise can be determined quite well. A sizable number of CPC maps fall in this category, e.g. all images obtained outside the galactic plane and the LMC.

We first selected an "empty" image; this one was a large planetary nebula at high galactic latitude, too weak to be detected. A histogram of the surface brightness values can be approximated quite well by a gaussian. The standard deviation of this gaussian, B_σ, is interpreted as the uncertainty in the surface brightness for a single pixel.

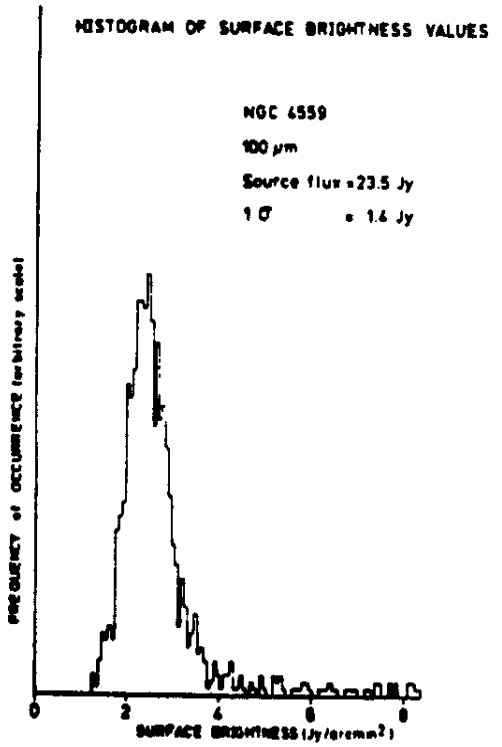

Fig. 5.7. Surface brightness distribution in a map around NGC 4559.

The histogram is dominated by blank-sky samples; the values above about 3.5 Jy per sq.arcmin are due to the source NGC 4559. The noise, although probably dominated by low-level spikes (see fig. 5.1), apparently has a nearly Gaussian distribution.

In images containing relatively little flux the histogram of surface brightness values exhibits also a gaussian shape at the low surface brightness values, with a tail extending to large values. An example is shown in Fig. 5.7; B_σ can be determined quite well.

Table 5.1. Examples of total flux determination.			
Source Name	CPC Band (μm)	Source Flux (Jy)	B_g (Jy/arcmin^2)
Empty Field	50	0.6	0.3
	100	0.9	0.4
NGC 4559	50	3.4	0.3
	100	23.5	0.4
NGC 1961	50	10.1	0.4
	100	50.6	0.5
M 81	50	13.0	0.5
	100	33.9	0.7

Even for images containing not too much flux spread out over the image, B_g can be determined. E.g. for the image of M 81 the histogram is too skewed to be represented by a gaussian. By using only the part left of the maximum, which does resemble a half-gaussian, B_g can be estimated reasonably well, and it is only slightly larger than the empty map noise.

Converting B_g into an uncertainty estimate for total flux determinations (e.g. to use as a point source detection limit) is not straightforward, because the regridding process causes the noise in adjacent pixels to be correlated, in a way that depends on the exact scan path for the observation.

We used the procedure outlined in sections 8.2 to determine the fluxes of a number of weak sources (see table 5.1). The result on an empty field, or on an empty area in the map, is indicative of the reliability of the so determined fluxes. Fluxes down to a level of a few Jy can be determined.

5.3. Observed beam profile

Knowledge of the CPC beam profiles can serve at least three purposes:
- to estimate the extent of an isolated source,
- to separate sources lying very close to each other,
- to determine the flux of an isolated point source from its peak surface brightness.

Note that the beam profile plays no role in the photometric calibration of the instrument; all maps are given in terms of surface brightness, and fluxes of sources can be found by integrating their surface brightness.

Determining the beam profiles observationally requires a true point source sufficiently bright at the CPC wavelengths. There exist very few sources that meet these requirements; most bright 50 and 100 μm sources have extents that are significant compared to the 1.2 arcmin diameter of the CPC's entrance aperture. The asteroid Ceres was selected for this purpose; at the time of observation its flux was 200 and 105 Jy at 50 and 100 μm, and its diameter about one arcsec. We obtained 8 9 × 12 arcmin maps of Ceres; the results of the observations are summarized in Table 5.2. To characterize a profile width, we use the effective solid angle of the profile, i.e. the total

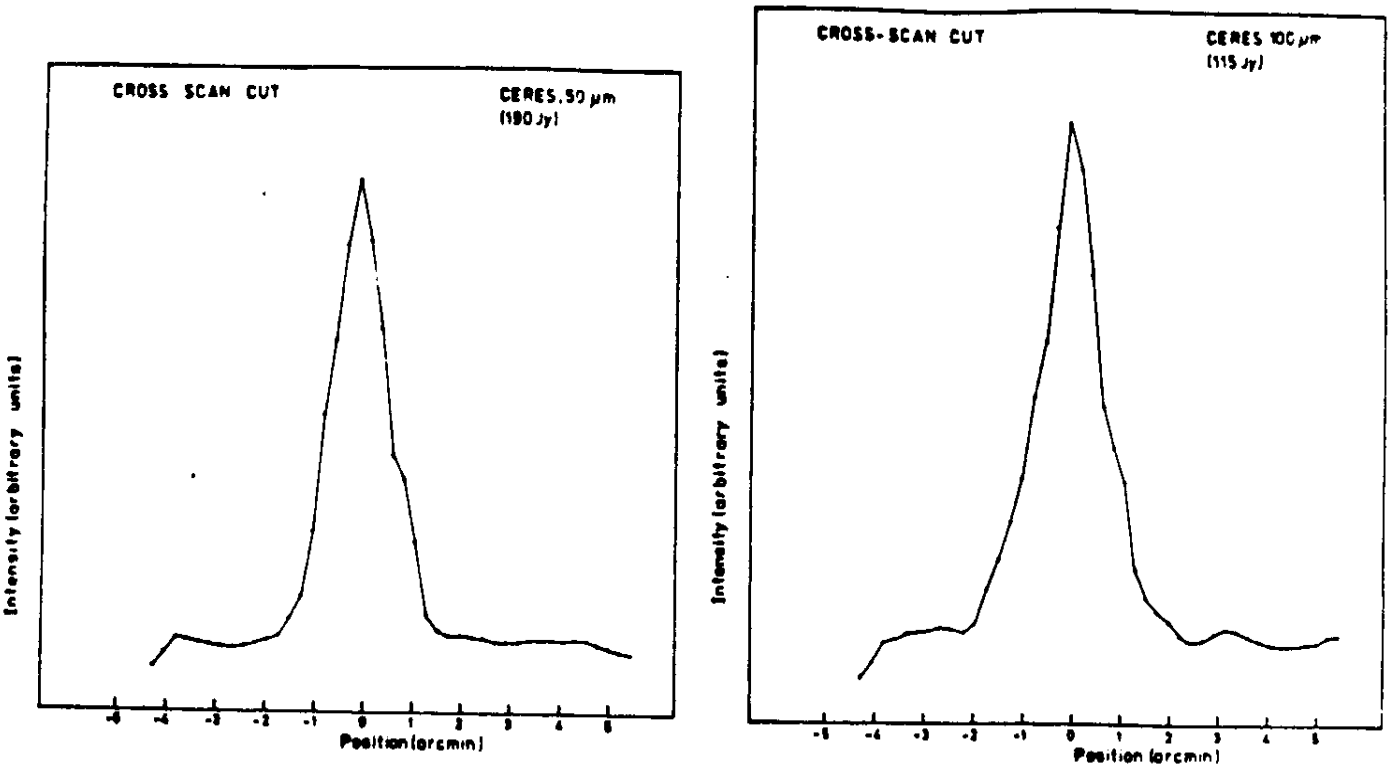

Fig. 5.8. Observed beam profile

Cross-scan cuts through images of Ceres at 50 and 100 μm are shown (a CPC09A observation, see table 2.1). The FWHM at 50 and 100 μm is 1.4 and 1.6 arcmin respectively. Average values from all Ceres observations are presented in Table 5.2.

flux divided by the peak surface brightness, and the full width at half maximum (FWHM). Figure 5.8 shows cross-scan cuts through the best image of Ceres.

Table 5.2. Beam characteristics from observations of Ceres

The quoted uncertainty is the r.m.s. deviation of a single observation from the mean.

Band	Solid Angle (arcmin²)	FWHM (arc sec)
50 μm	2.5 ± 0.2	88 ± 4
100 μm	3.3 ± 0.2	100 ± 3

The internal consistency of the Ceres measurements is somewhat misleading; the observed short-term responsivity variations (see section 5.1) cause flux-dependent distortions of the source profiles. This might explain the inconsistency of the results on Ceres with the theoretical beam profile (section 7.4).

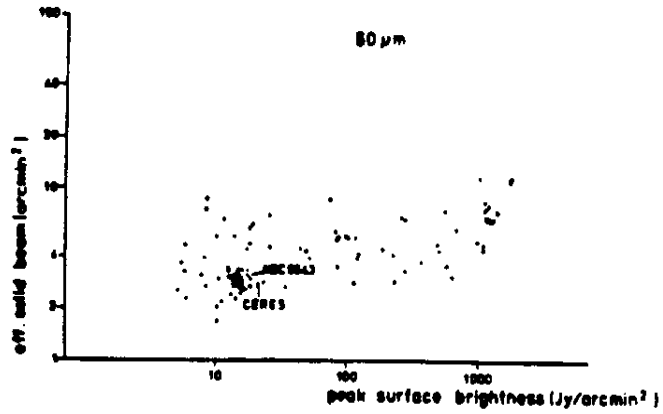

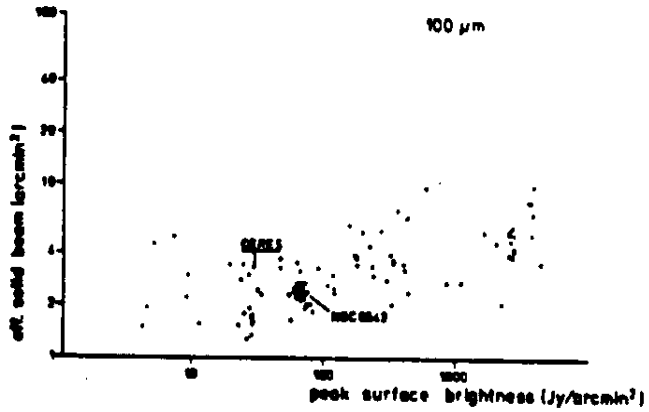

Fig. 5.9. Peak surface brightness and flux density

These figures show the effective solid beam (the ratio of measured flux density and measured peak surface brightness) and the peak brightness for a number of point sources. The scatter indicates that peak brightness is an unreliable indicator of source strength. The slight tendency of the effective solid beam to increase with source flux is undoubtedly caused by short-term responsivity variations.

Indeed when we compare the Ceres observations with other observations of likely point sources , we do find a correlation of the apparent width of the beam profile with the source peak surface brightness. Figure 5.9 shows the results of the comparison. In producing these data we needed a scheme to estimate the background in a map; for this purpose we used the median value of the surface brightness (cf. section 5.2). The apparent beam size tends to increase with the source brightness, but there is an appreciable scatter. One cause for this scatter is undoubtedly that the background surface brightness also influences the responsivity variations.

The main conclusion from the beam profile measurements must be that great caution is required in interpreting the extent of sources in the CPC maps. Also, peak brightness is an unreliable basis for a flux estimate; the photometric calibration of the CPC is based on integrated fluxes.

6. Data reduction

6.1. Input data base

The CPC images were produced from a data base set up during the mission at the ground station. The contents of this data base are as follows:

- a complete log of the observational schedule;
- assorted satellite data not transmitted in the high-speed telemetry, notably the results of the attitude calibration measurements;
- alignment and calibration parameters of the satellite attitude system;
- satellite board clock calibration;
- status of telemetry quality;
- for the whole period covered by the telemetry from the satellite, once per second the status of the DAX instrument (temperatures, voltages etc.);
- the CPC 64-Hz digital data, for the periods the satellite was commanded to CPC data handling.

About three hours after the completion of each 12-hour observing period (SOP), a tape containing these data in 6 files, was delivered to a ROG crew at the ground station. The contents of this tape were then immediately processed for data quality verification, quick-look reduction and archiving (combining several SOP's worth of data to an single tape). The total comprises about 800 MBytes of data on 32 tape volumes.

6.2. System design

The software system for production of the CPC images is designed around two special file formats, DAX files and image files. The different steps in the reduction are performed by about half a dozen programs which repeatedly process files in these formats. The relation between programs and files is shown in Fig. 6.1.

Both file formats were designed to contain a complete subset of the data base, in the sense that all the relevant information for processing was present in each file. This avoided the construction and maintenance of auxiliary data bases, at the cost of about 10 % overhead in file size, due to the presence of multiple copies of global information structures. Also some derived quantities had to be recomputed for each file anew, instead of being globally available. The main profit of this setup was the production flexibility. For all reduction steps we could choose a compromise method between two extremes. At one end we could run large volumes of data in batches through a single program and store the intermediate results, at the other end we could generate a single observation end product by running a single file through all programs in a pipeline connection.

The DAX file is capable of holding all data pertinent to a few observations, usually the 12-hour operational period (SOP) is kept together. The

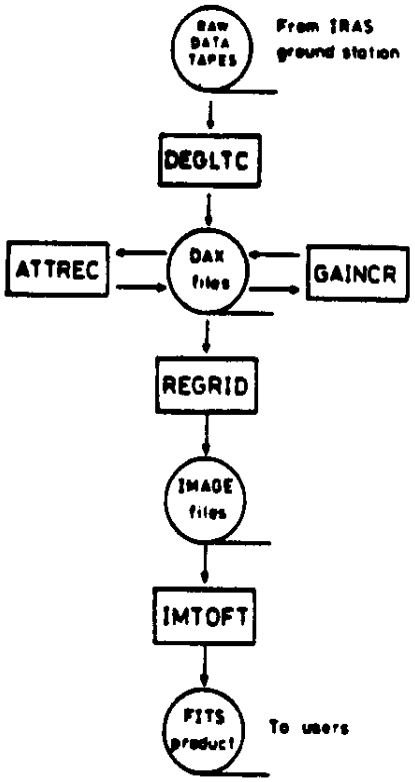

Fig. 6.1. Schematic data flow of the CPC reduction system.

See text for a description of the various parts.

data are maintained in time order in an intermediate stage of reduction, while various programs derive and add calibration parameters without changing the DAX-file format. This setup enabled us, at least to a certain extent, to exchange the order in which some programs operated on the DAX files, or even to reprocess DAX files without having to regenerate an intermediate product.

The image files are used for the intermediate reduction stage where the time order is lost and the results are stored as images, i.e. estimated surface brightness values at a regular grid on the sky. Each image file contains the data for one observation.

6.3. Demodulation and deglitching

The first program in the reduction scheme is DEGLTC, which creates a DAX file for one SOP from the data tapes received from the ground station. The data are processed by DEGLTC in three steps.

a. The consistency of the input files is verified and the DAX-file format is set up.
b. The digital data stream of the CPC is decompressed. The 64 samples per second of the detector output values are reconstructed from the digital 8-bit data stream by table lookup. Demodulation is done by correlating 8 consecutive samples with a sine function at the known fixed chopping frequency of 15.062 Hz, with the phase as free parameter. This resulted in 8 samples of modulation amplitude per second per detector.
c. To suppress the spiking behaviour of the detectors, a deglitching algorithm is applied to the 8-Hz data, independently for each detector. The deglitching algorithm recognizes spikes by a sudden increase in response,

followed by a decrease to the original level on a time scale of 0.5 seconds. When a spike is detected the estimated amplitude of the spike is subtracted. Both the deglitched data stream and the original 8-Hz data stream are then smoothed by averaging over half-second intervals. The resulting two values per second are stored in the DAX file for further processing.

Side effects of the demodulation and despiking methods are discussed in section 7.1, a detailed description of the algorithm is given in Annex 1.

6.4. Responsivity variation

Correction for gradual changes in detector responsivity ("gain") during the observation is done by the program GAINCR, usually the third step in the reduction process. The algorithm is based upon the following assumptions.

- The demodulated and deglitched response of the detector is equal to observed sky surface brightness multiplied by a gain function.
- The gain changes slowly in time, on time scales comparable to the duration of a leg of the raster scan.
- In the part of the sky covered by the raster scan, a background region of constant surface brightness is present, crossing the scan legs, thereby providing a reference level that is observed several times during the observation.

After selecting a number of samples representative for the background, the change observed in this background is modelled and used to derive the gain function. The instrumental causes of the gain variations are described in section 5.1, the validity of the correction method is discussed in section 7.2.

The background region is determined by taking the despiked response values for one detector as a function of time from the input DAX file, two values per second of observation. The lowest values from each pair of legs are selected as background samples, until the summed response in the selected points reaches a value of 1 Instrumental Unit (= 100 Jy/arcmin^2), or until 20 points in this pair of legs are chosen.

The gain variation is then modelled by fitting polynomials of degree 0 to 4 through the response values in the background region (see Fig. 6.2). The residual variances of these fits are compared, and if two polynomials have a difference of less then 20%, the higher-order one is rejected as being unnecessarily complex. The remaining polynomial with the highest order is considered to model the gain variations.

Finally the gain function is determined by normalizing the gain variation polynomial so that its value for the maximum response in the whole map is equal to one. The despiked data values are then divided by the gain function for that detector, while the 'raw' data values are unchanged. The resulting data stream is stored in the same DAX file format as the input data.

The gain correction procedure was considered to be dubious when one or more of the following cases applied.

- There is no clearly recognizable background region: less then 10 % of the

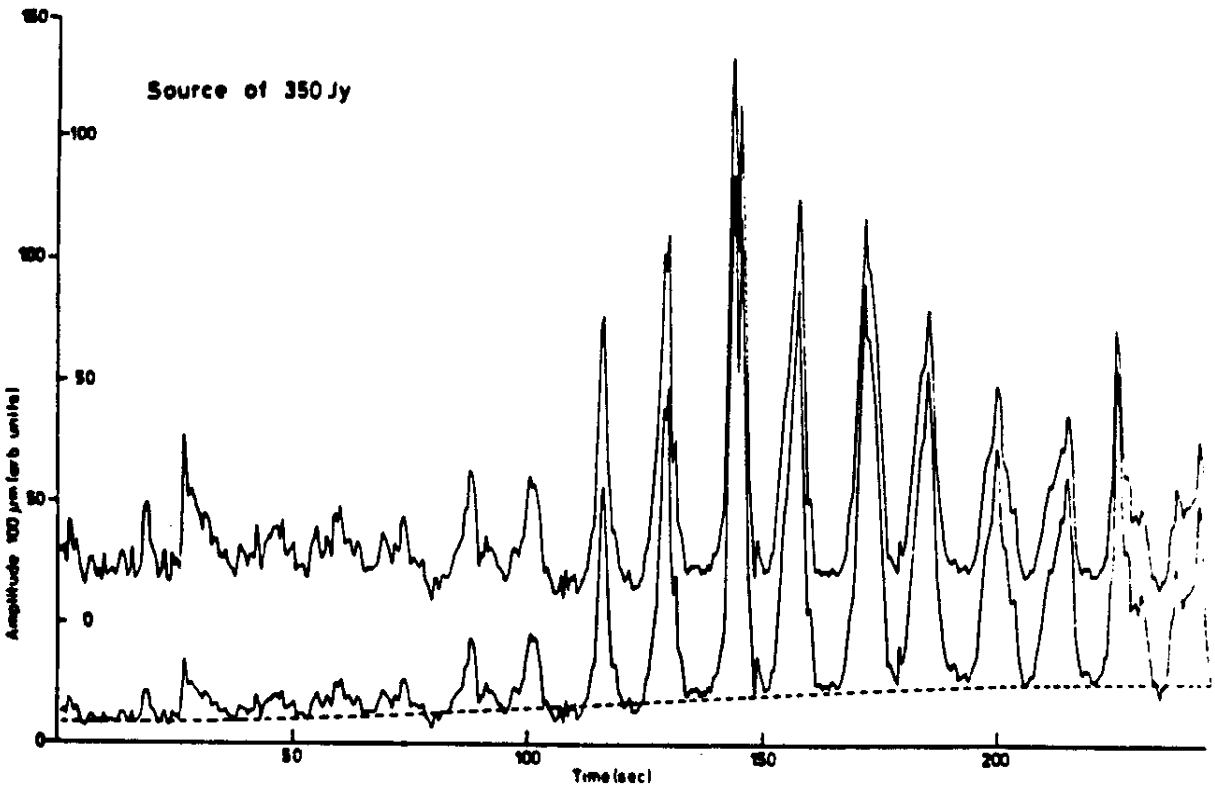

Fig. 6.2. Long-term responsivity variation correction

The lower plot shows the original observation: the background increases slowly due to the long-term increase in gain. The background was fitted by a function represented by the dashed line. The gain function is normalized at the peak (at about 145 sec) and the resultant plot is the higher one (shifted upward for sake of clarity).

samples in the whole map are selected as belonging to the background.

- The minimum and maximum values of the gain variation have a ratio of 6 or more.
- A χ^2 test reveals that the response variations on the background cannot be fitted by the chosen gain variation polynomial. The χ^2 test uses the mean absolute difference between successive samples in the whole map as an estimate of the standard deviation σ. The fit is rejected whenever χ^2 exceeds the 0.1 % probability limits meaning that of the cases where the model was valid, 1 in 1000 will be falsely rejected.

A dubious gain correction at either wavelength is taken to affect the whole observation; a remark is then added to the output file, which will prevent the appearance of this observation in the current end products.

6.5. Pointing reconstruction and regridding

The program ATTREC reconstructs the viewing direction of the CPC hole at the sky from the satellite attitude information:

a. the satellite position as commanded by the ground station,
b. the servo error (difference between commanded and observed position) as used in the attitude servo loop and reported back by the satellite,

c. an inversion of the algorithm used by the ground station to convert celestial coordinates to satellite position commands,
d. the slow changes in the attitude control system as measured and reported by the satellite upon execution of an attitude calibration scan.

The conversion of satellite position commands to celestial coordinates needs the position of the sun, which is assumed constant for the duration of the raster scan. It is computed for the the time halfway the raster according to the prescriptions of Newcomb (1895) to about 1 arcsec accuracy. For the misalignment parameters which describe the viewing direction of the CPC hole with respect to the satellite attitude control coordinate frame, we use the nominal values provided by the ground station for the optical axis of the telescope, with a fixed correction for the relative position of the CPC hole.

The attitude calibration measurements were used to determine the mispointing of the attitude system by scanning special visual sensors over a star with known position. During the CPC raster scans, the onboard software corrected the commanded attitude for difference between achieved and intended viewing direction as computed from the last succesfully executed attitude calibration scan. The reconstruction, done in ATTREC with the originally commanded attitude in combination with the nominal misalignments, amounts to using the misalignments actually valid at this latest attitude calibration. Routinely, attitude calibration scans were requested before and after each CPC raster scan.

The second attitude calibration, done after the raster scan and the flux calibration measurement, was used to determine the change in misalignment correction. The change was usually negligible in the cross-scan direction, being the mechanical misalignment between the sun sensor and the telescope. In the in-scan direction the change is mainly caused by the error in the integration of the gyro readouts. This occurred chiefly during the slew manoeuvres (e.g. going from the attitude calibration track to the raster scan). The change in misaligment between the two attitude calibrations is interpolated by ATTREC in proportion to the number of slews performed, and assumed constant during the raster scan.

The reconstruction of the raster scans uses an in-map coordinate system. The axes of this system coincide with the in-scan and cross-scan directions. The origin of the in-map coordinates is established by determining the commanded sky position for a sample halfway the middle leg, and rounding the result to a point on a predetermined 1 arcminute grid in RA/Dec. The rounding to a fixed grid facilitates superposition of overlapping maps. Right ascension, declination of the origin of the in-map coordinate, and position angle system are recorded in the DAX-file.

For each leg of the raster scan the commanded positions of the first and last sample on the in-map coordinate system are computed and stored. The servo errors, giving the recorded deviations from the commanded scan are already stored in the DAX-files on a one-second basis.

The program REGRID computes the sky surface brightness at a regular pixel grid. In doing so, the information is converted from the time domain to the image domain, the result is of necessity in a different format. The grid is always at 20-arcsec pixel size, oriented in RA/Dec, with the center position

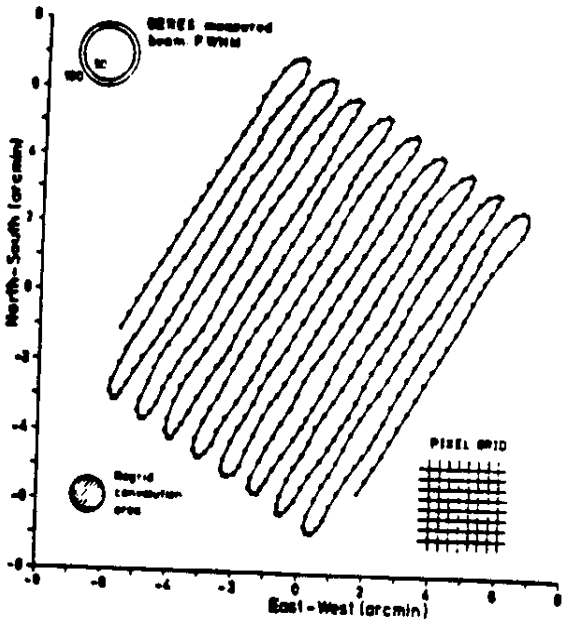

Fig.6.3. Movement of CPC diaphragm over the sky during a CPCF9A raster scan.

The scan starts in the lower left corner. Dots indicate the viewing direction at half-second intervals. For comparison, the FWHM observed beam diameter, the convolution diameter used in regridding, and the pixel grid size are shown.

at the origin of the in-map coordinate system. Correcting the reconstructed commanded position with the control errors, both available at one-second intervals, gives the actual track of the CPC diaphragm over this grid.

By quadratic interpolation a position is assigned to each half-second surface-brightness sample. The surface brightness at each pixel of the grid is computed as the average of all samples that are within 32 arc seconds of the pixel position. This amounts to a convolution of the data by a circular beam of the same radius and rectangular cross section. The surface brightness is considered undefined for pixels where no sample is taken within the 32 arc second radius. The procedure is (partly) depicted in Fig. 6.3.

A conventional astronomical object name, usually provided by the requester of the observation, is added from a manually maintained list, as an aid in identification.

6.6. Calibration and generation of end products

Program IMTOFT is the final step in the reduction process, reformatting the regridded images to FITS format. The surface brightness B_{int} is kept in internal units up to this stage, where it is converted to B_{stnd} in MJy/ster. The overall calibration factor A and the sensitivity change time scale T, derived in sections 8.1 and 8.2, are given in table 6.1. The conversion applicable at the time of observation t (in years) is then given by the formula:

$$B_{stnd} = \frac{A}{1 - (t-1983.0) / T} \times B_{int}$$

In order to make the difference between 'clean' and 'raw' images (see section 3) visible, a margin is added to the images, which is filled with undefined data values for clean images. For the raw images the margin contains

Table 6.1.
Calibration of instrumental units.

Wavelength λ (µm)	Calibration Factor (Jy/arcmin^2 per I.U.)	Calibration Factor (Jy/pixel^A per I.U.)	Timescale T (year)
50	70	7.8	3.5
100	105	11.7	3.0

the character pattern 'RAW IMAGE' (or the part of it which fits).

When finally preparing the tape, dubious observations as described in the previous sections, are prevented to appear in the current product. Each file on the resulting FITS tape contains two images at 50 and 100 µm, stored as two planes in a three-dimensional data array. The clean and raw images are paired as two files of identical size, and the observations are sorted to Right Ascension.

The FITS header section is built upon a rather rigid template, where only the values needed for a quantitative interpretation of the data are given as FITS keyword parameters:

- type, amount and organization of the data on tape,
- scale of the maps and position on the sky,
- calibration of the FITS tape values to MJy/ster,
- epoch of observation and of tape generation.

Other parameters, which assist in a qualitative interpretation, are passed in COMMENT fields. If numeric values appear in comment positions, they must not be used for detailed computations. E.g. we give the beam position for the first and 10th second only to convey an impression of the execution of the raster scan.

7. Analysis of reduction techniques

7.1. Demodulation and deglitching

The potential side effects of the chosen demodulation technique result from the choice of ignoring the phase information. This can reduce the measurement accuracy at signal-to-noise ratios of order 1 or less; at such low signal levels the noise tends to get rectified and thus adds to the amplitude estimates, and any sign reversals in the modulation remain undetected. In a number of test cases we computed the phase for each 8-Hz demodulation interval. This showed that, apart from a systematic influence of the signal level and except on strong glitches, the phase is quite stable, even at the lowest signal levels. In other words, the 15 Hz modulation is always present with a relatively high signal-to-noise ratio and taking account of the phases would not significantly affect the results. Strong glitches are rectified and therefore systematically over-estimated, but do not pass the deglitching process anyhow. The results of the quick-look processing of CPC data, which employed phase-sensitive demodulation at 2 Hz without deglitching, confirm the conclusion that the phase information in the CPC data is irrelevant.

7.2. Responsivity variation

As explained in section 5.1, it is quite difficult to reconstruct the gain variations of the CPC detectors. When the gain drops to a low value, reconstruction of the corresponding surface brightness means dividing the response by a number close to zero, with disastrous effects on the result. This prevented us from applying the model given in section 5.1, instead we 'measured' the gain variations by fitting a smooth function to the background of each observation (section 6.4). As the method searches for a minimum response on each pair of scan legs, it relies on the existence of an area of constant surface brightness crossing the scan legs. This assumption is all right for relatively isolated objects.

When an area with extended emission is observed, the gain variation can not be disentangled from the true background variations. The gain as 'measured' on the lowest values of each leg pair, will then not reflect the true gain variation. Because we normalize the gain to be unity at the maximum response, the effects are limited in the cases where a relatively bright source was observed on a low but non-constant background. The major effect on the resulting map is then a pseudo-background strip, oriented across the scan legs, where the surface brightness is forced to be constant. For relatively weak sources embedded in complex emission structures, the gain variation becomes almost impossible to reconstruct. Annex 2 discusses in detail a few good and bad cases of our gain correction method.

7.3. Attitude reconstruction and regridding

Each step in the attitude reconstruction can conceptually be assigned to one of two levels. The first level deals with the local geometry of the executed raster pattern ; the second level deals with the location and the orientation of the raster on the sky.

At the local level, which determines the relative positions in the map, the dominant error stems from neglecting changes in the attitude control system parameters during the raster scan. A slow, linear drift in these parameters would cause scale errors or shear in the map. From the consistency in the attitude calibrations bracketing most CPC observations, we conclude that such distortions will not exceed 5 arc seconds. Although the executed scanning rasters have significant irregularities, particularly near the transitions between scan tracks, the relative attitude reconstruction enables the use of all photometric samples in the regridding process.

At the second level, where absolute positions are determined, the main error is again related to the uncertainty in the attitude system parameters. The special attitude calibration scans with the visual star sensors, bracketing the raster scan, usually provide a net value for the in- and cross-scan errors at the moment of the star sightings. The attitude reconstruction algorithm uses a fixed fraction of the difference between the two values to compensate for drift in the system parameters, but it is not clear whether this is the best procedure. From tests on known objects (see section 2.2) we find that the absolute position error is about 25 arc sec r.m.s..

The input data of the regridding routine is a time sequence of brightness measurements at intervals of 0.5 seconds. With the results of the pointing reconstruction the regular one-dimensional temporal grid is translated into a slightly irregular two-dimensional spatial lattice. The separation of the lattice points is typically 25 arc sec, 30 % of the beam diameter, so that the the sky brightness is always adequately sampled.

The regridding routine transforms a map to a regular lattice with a spacing of 20 arc sec. The interpolation algorithm simply assigns to each lattice point the mean brightness measured at all points of the original grid within 30 arc sec. If the original grid were regular, the interpolation would amount to a two-dimensional convolution with a "pill box" function. From this point of view, significant irregularities are found only at the edges of the observed fields; everywhere else proper spatial convolution occurs. As is demonstrated in the next section, the employed interpolation function combines well with the optical beam profile.

7.4. Resultant Beam Profile

Accurately known significant contributors to the over-all beam profile applicable to the CPC maps are :

- diffraction at the telescope aperture,
- the CPC aperture geometry,

- telescope motions during the 0.5-second integration time,
- the regridding algorithm.

Imaging defects are unlikely to have played a significant role. The Low-Resolution Spectrometer, housed in the same instrument package as the CPC, requires much higher optical quality and its results gave no evidence of any optical defects (the spectrometer employed a 15-arcsec slit and operated at wavelengths down to 8 μm). The relay optics in the CPC that image the telescope focal plane onto the entrance stop are simple and not critical.

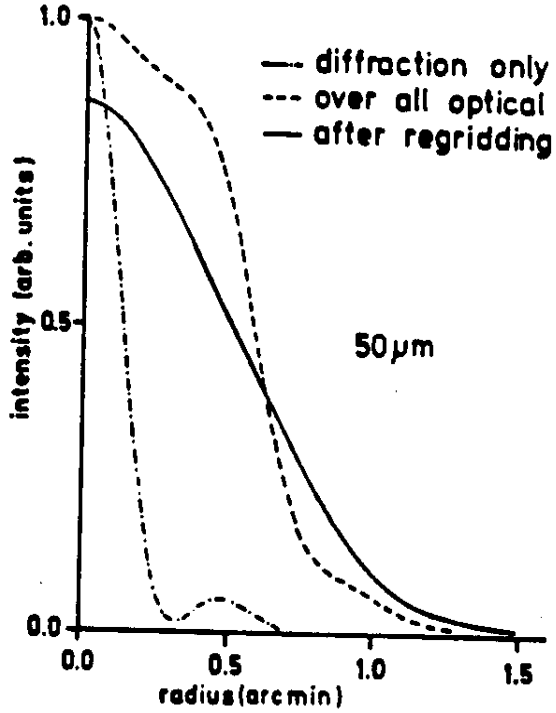

Fig. 7.1. Theoretical beam profile in the 50 μm band.

The optical beams at the telescope focal plane, with and without the effect of the finite CPC aperture are also shown. The over-all optical profile and the profile after regridding have been normalized to the same two-dimensional profile integral.

In practice the beam profile can be distorted by short-term responsivity variations. The most noticeable effects can occur on strong sources, particularly in combination with high backgrounds. At low scan rates the gain increase on strong sources can stretch the source image in the scanning direction; a high background underneath a strong point source can be amplified locally to produce the semblance of wings, again extending in the scanning direction. Probably because of such non-linear effects, the point-source profiles in the obtained maps are often broader than the predicted beam profile.

Figure 7.1 shows the predicted CPC beam profile at 50 μm. To indicate the importance of the various contributors, the figure also shows the Airy function representing the telescope diffraction, averaged over the wavelength band, and the optical beam profile, which is the convolution of the Airy function with the CPC aperture function. After regridding, the profile has a nearly Gaussian shape. The regridding does not change the half-width of the profile and reduces the peak response to a point source by only 13 % (optical and over-all profiles are shown on the same scale). At 100 μm, the Airy function is twice as broad and the optical profile is much smoother; the effects of the regridding on profile width and contrast are quite similar.

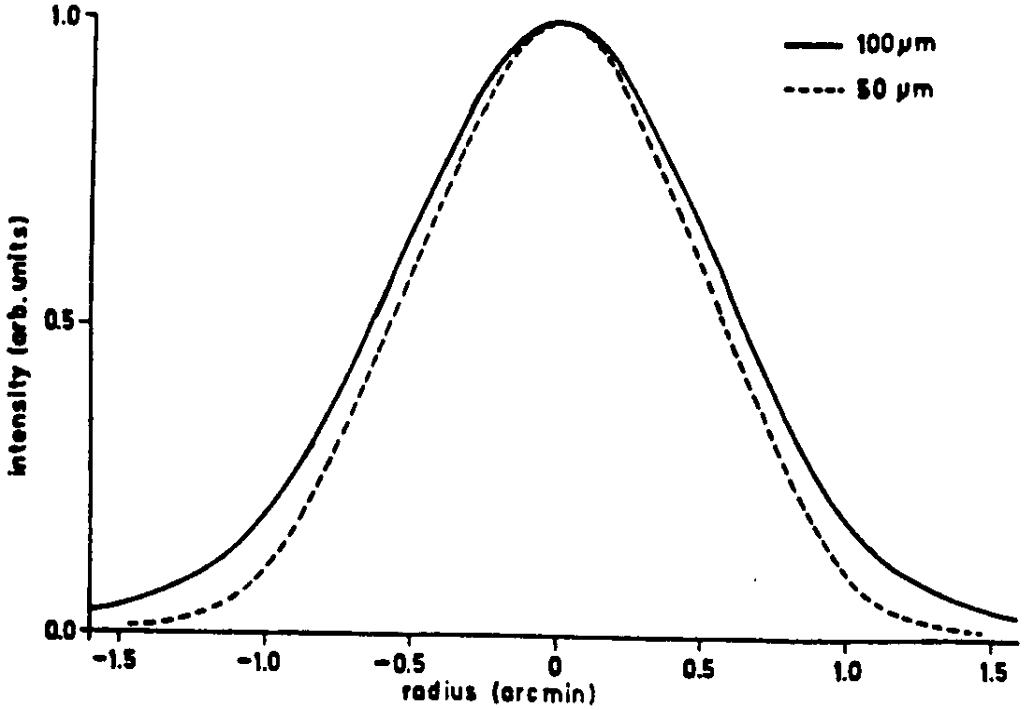

Fig. 7.2. Theoretical beam profiles at 50 and 100 μm.

For the fastest raster scans (CPCF9A macro) an additional in-scan broadening by 3 % is predicted.

Figure 7.2 shows the over-all beam profiles for both CPC channels, normalized to unity peak amplitude.

The figures do not show the additional smoothing in the scan direction due to the finite integration time. At the highest scan rates, in the CPCF9A observations, an in-scan broadening of the profile by only 3 % is predicted.

8. Photometric calibration

For the photometric calibration of the CPC observations we used three sets of observations.

- After each CPC observation the "internal stimulator" in the IRAS telescope was used to produce a 15-second long stimulus signal, thus serving as an internal calibrator. The short-term responsivity variations prevented the use of these measurements to calibrate individual observations, but they served to monitor the long-term responsivity changes.
- The planetary nebula NGC 6543, which was used as a photometric reference for the survey instrument, was observed daily with the CPC. These measurements also monitor the long-term responsivity changes, allow a direct assessment of the repeatability of the observations, and firm-up the absolute calibration.
- A large number of point sources were observed both with the survey instrument and with the CPC. These observations provide a check on the linearity of the CPC brightness scale, allow an estimate of the reliability of CPC fluxes, and provide a tie-in with the survey observations. The results of this comparison did play a role in choosing the normalization procedure in the routine used to reduce the effects of signal-induced responsivity variations.

We have no absolute calibration of background levels. To arrive at a meaningful calibration we would need a much better model of the responsivity variations than we can distill from the available material. The widely different beam sizes of CPC and survey array prevent us from using the survey calibration for this purpose.

8.1. Sensitivity changes and repeatability

8.1.1. Internal stimulator

We study in this section "flashes" of 15 seconds duration observed after each scientific and calibration observation of CPC. From the response of the survey detectors we know that the flash intensity was constant to a few percent during the whole IRAS mission. Thus flashes seem ideal to establish the absolute level of each CPC observation. This is not feasible because the responsivity variation (described in section 5.1) makes the tie-in of the CPC response to a flash and to an astronomical object uncertain due to the time lag of at least 30 seconds (on average a few minutes). In addition, on high backgrounds the signal-to-noise ratio of the flash response is low. In spite of these problems the flash response as a function of time can be used to study long-term responsivity changes of the CPC detectors.

In Fig. 8.1 we show the flash intensity versus time for 829 flashes. The routine flash measurement consisted of 8 seconds background, 15 seconds stimulator on, 7 seconds background. The response of the detectors on the stimulator is shown in Fig. 5.5. Note the predominance of flux-induced spikes; the software deglitcher was not used on these measurements. As a measure of the flash amplitude the difference between the medians of the stimulator and background samples is used, to minimize the influence of spikes.

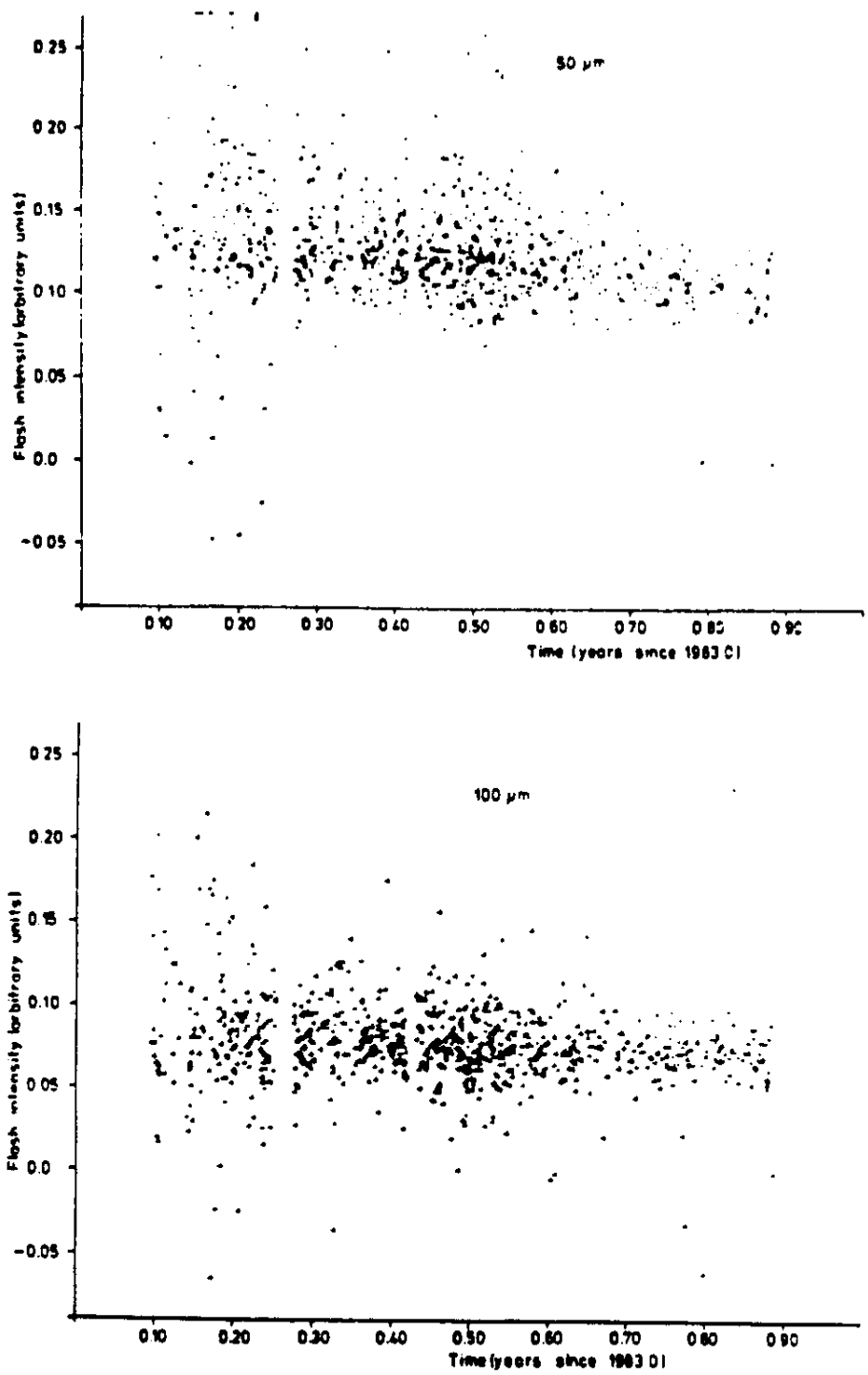

Fig. 8.1. Photometric stability and repeatability, from internal calibrations.

The results of several hundred measurements on the internal stimulator are plotted in this figure. The spread is considerable: about 25 % r.m.s. The slight downward trend is consistent with results obtained on NGC 6543. The mean stimulator signal corresponds to the peak signal from a point source of 21 or 26 Jy at 50 or 100 μm respectively.

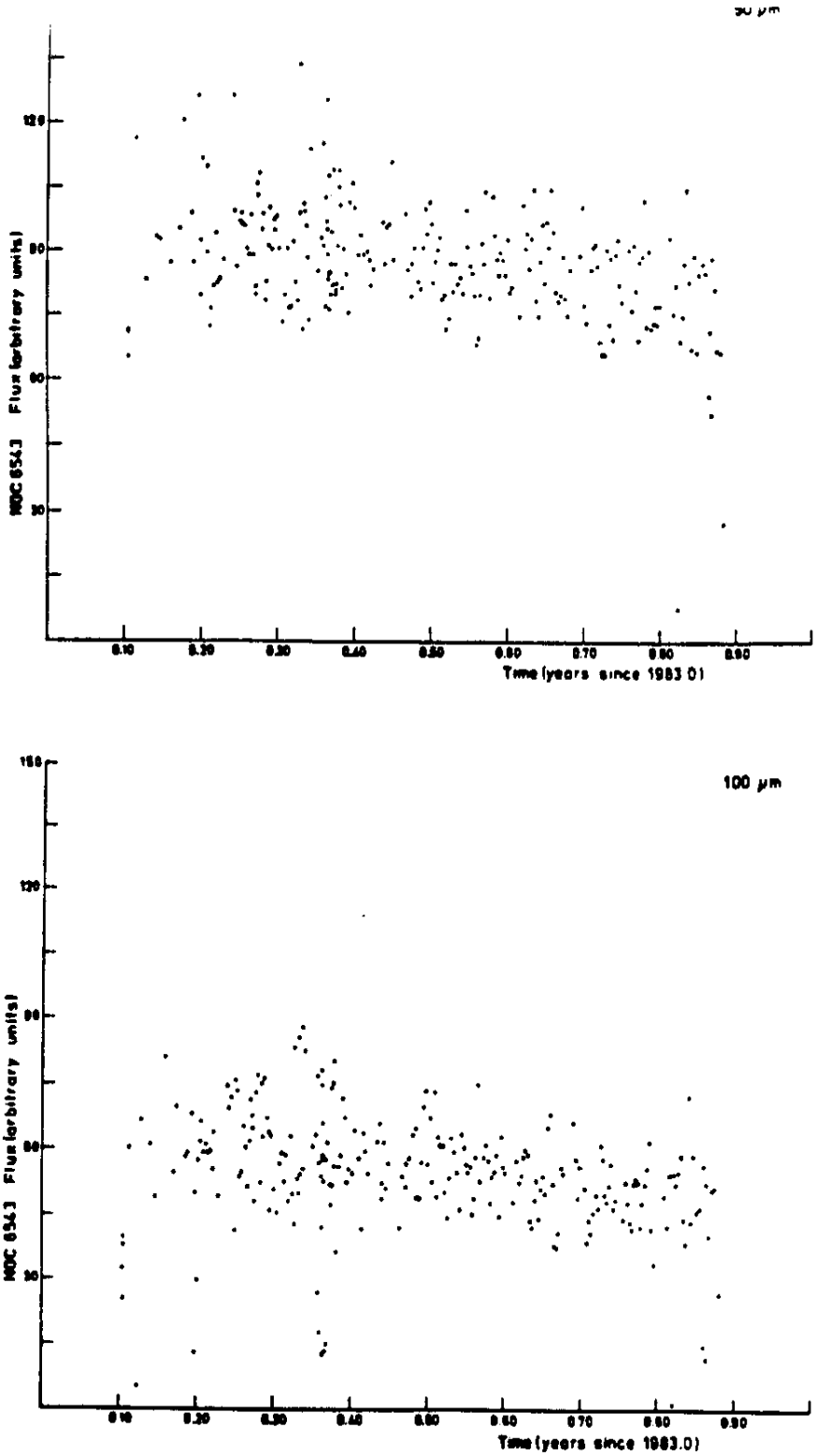

Fig. 8.2. Photometric stability and repeatability, from external calibrations.

Responses to the transfer photometric reference source, NGC 6543, are plotted versus time. In both bands the responsitivity dropped by 30 % per year, an effect that was accounted for in the final calibration procedure. The internal accuracy of these observations is about 15 % r.m.s.

Before t = 0.30 years the scatter in the flash intensity is rather large because the flashes were observed on the source. Therefore we fitted a straight line to the flash intensities beyond t = 0.30, and found a r.m.s. deviation of about 25 % for both bands. This value can be interpreted as an estimate of the repeatability of CPC observations of low signal-to-noise.

There is a barely significant decrease of the response of CPC to the flashes in the course of the mission, confirming the decrease found on celestial sources (see below).

8.1.2. NGC 6543

A similar plot as Fig. 8.1 is shown in Fig. 8.2 using NGC 6543 as a constant source. (The NGC 6543 observations used have not been fully processed: the correction for long-term responsivity variation has not been applied.) A histogram of the flux values indicates that the distribution of flux values resembles a gaussian, and there are about 20 of the 247 flux values that lie very far from the average value. Ignoring those 20 values we have derived one sigma values of 12 % and 17 % at 50 and 100 µm respectively. These values can be interpreted as the repeatability of CPC for sources like NGC 6543:

- lying far away from the galactic plane, and
- not observed just after a passage over the South Atlantic Anomaly.

There clearly is a decrease of long-term responsivity in the course of the mission. Because of the large scatter precise numbers cannot be derived. For the data reduction (see section 6.6) we have used a linear decrease, arbitrarily normalised to 1 at epoch 1983.0, derived from a best fit in Fig. 8.2.

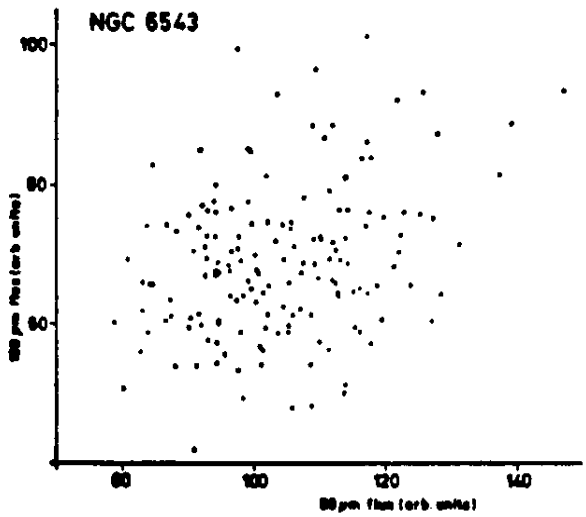

Fig. 8.3. Repeatability of the ratio of the 50 and 100 µm responses to NGC 6543.

Clearly there is very little correlation between the responsivity variations observed in the two channels.

The fairly bad reproducibility derived above is quite probably due to the responsivity variation effect. In figure 8.3 the 100 µm flux is plotted versus the 50 µm flux of each individual NGC 6543 observation. The scatter is considerable indicating that the responsivity variations of the 50 and 100 µm bands of a simultaneous observation are not correlated.

8.2. Linearity and absolute calibration

To determine the linearity and absolute calibration of the CPC a number of observations on point sources were compared with the results of IRAS survey observations.

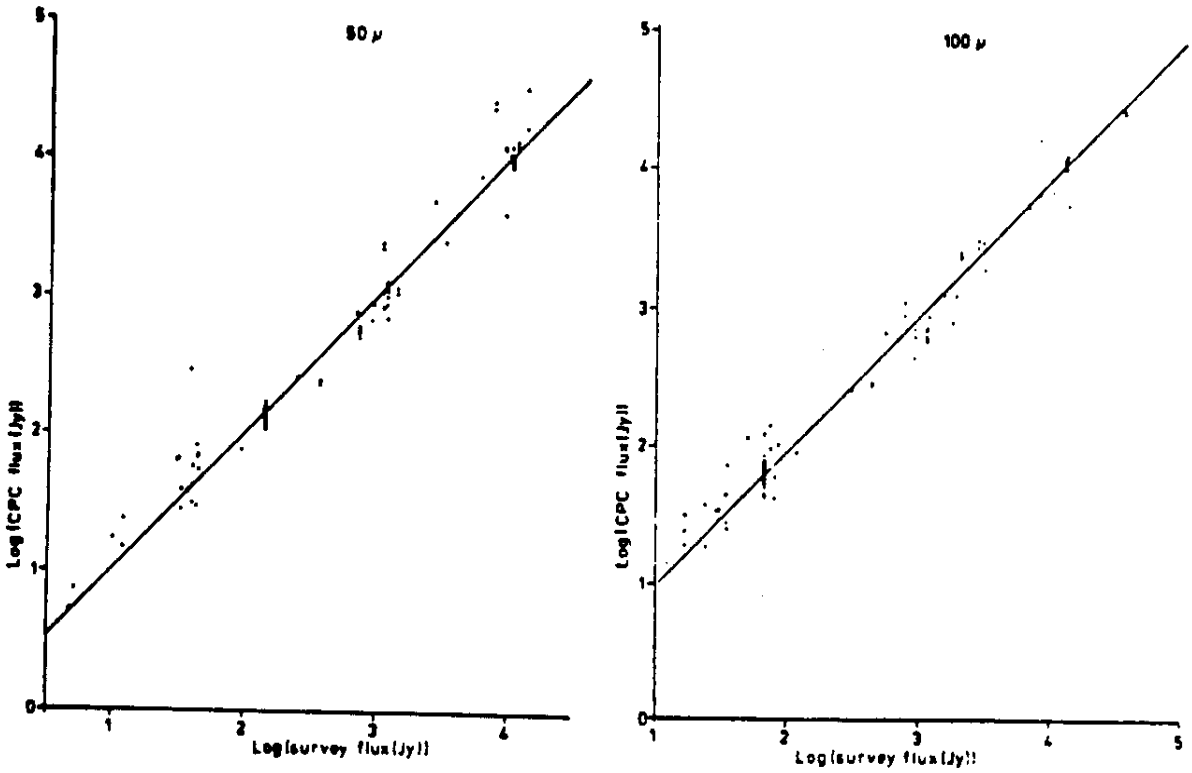

Fig. 8.4. Absolute calibration of the CPC.

For 50 point sources this figure shows the correlation between flux densities from CPC observations and from the IRAS Point Source Catalogue. Apart from a scatter of about 50%, the data can be fitted with a linear relation, indicated in the figure. This relation defines the calibration of the CPC results.

About 50 sources were selected from the CPC maps as being completely mapped by the CPC observations, i.e. FWHM less then about 2 arcmin at both 50 and 100 μm. The point source flux density as observed by CPC was determined in instrumental units, by integrating the surface brightness over the whole map with subtraction of the background level. The background surface brightness was taken as the median of the distribution of brightness values in the map. For the selected type of sources, the distribution of brightness values is dominated by the background pixels, and the median value is accurate as background level to within 3 percent. The results were plotted against the IRAS survey point source catalog fluxes (see Fig. 8.4). The CPC 50 μm flux density was compared with the survey 60 μm flux density, and the CPC 100 μm with the survey 100 μm. No color corrections were made to allow for deviations from a flat spectrum.

From these plots three conclusions can be drawn.

1. The CPC photometers are linear as compared with the survey instrument over a dynamic range of 4 decades.
2. The calibration of the instrumental units can be derived by determining the best fitting straight line of slope 1 in the plots of fig. 8.4. A correction factor of 50/60 was used to convert flux densities at 60 μm to 50 μm, i.e. sources with a flat spectrum in νf_ν were assumed in this calibration. The result is given in table 6.1.
3. For individual objects, a CPC-based point source flux density can deviate by 50 percent, even though the CPC maps for repeated observations of a single source reproduce the surface brightness to about 15 percent (see section 8.1).

The disappointing reliability of the CPC surface brightness calibration for single observations may partly be explained by the fact that we did not use any color corrections in the comparison, partly by systematic effects in the different methods of flux determination: for the CPC we integrated surface brightness over the source area, whereas the catalog result is based on a template fit.

We think however that the major part must be ascribed to responsivity variations. We recommend that the flux calibration of individual CPC observations be compared with IRAS survey data results. This can be done by determining the point source flux density as outlined above, and comparing with the point source catalog flux density. As an alternative, the surface brightness in the CPC map may be compared with the extended emission products of the IRAS survey.

8.3. NGC 6543 as reference source

The planetary nebula NGC 6543 was chosen as reference source for the IRAS mission, as it appears to be a sufficiently strong non-variable IR source. Daily measurements of this object allow determination of the repeatability of observations and of long-term variation in the responsivity of the CPC. The response on NGC 6543 was also used as a check on the absolute calibration.

Several properties of NGC 6543 may have influence on the final calibration. Situated at galactic latitude 29°1, the risk of confusion with galactic sources is low. Inspection of Skyflux maps of the region around NGC 6543 confirm that NGC 6543 is an isolated IR source.

Optically, NGC 6543 is a bright compact HII region of approximately 10 arcsec in radius, surrounded by a weak halo of 190 arcsec radius (Millikan, 1974). The IR emission distribution as observed by CPC in the 50 μm band is shown in figure 8.5. With the effective solid CPC beam derived in section 5.3 the nebula appears unresolved. Moseley (1980) has attempted to determine the size of NGC 6543 in 37 μm continuum radiation; he found little flux outside his beam of 20 arcsec diameter. There is no evidence in single CPC images that a halo is present at 50 and 100 μm.

Planetary nebulae do not only emit IR continuum radiation, but also line radiation in forbidden lines. Known planetary nebula emission lines in the survey and CPC passbands are [OIII] at 52 μm, [NIII] at 57 μm and [OIII] at

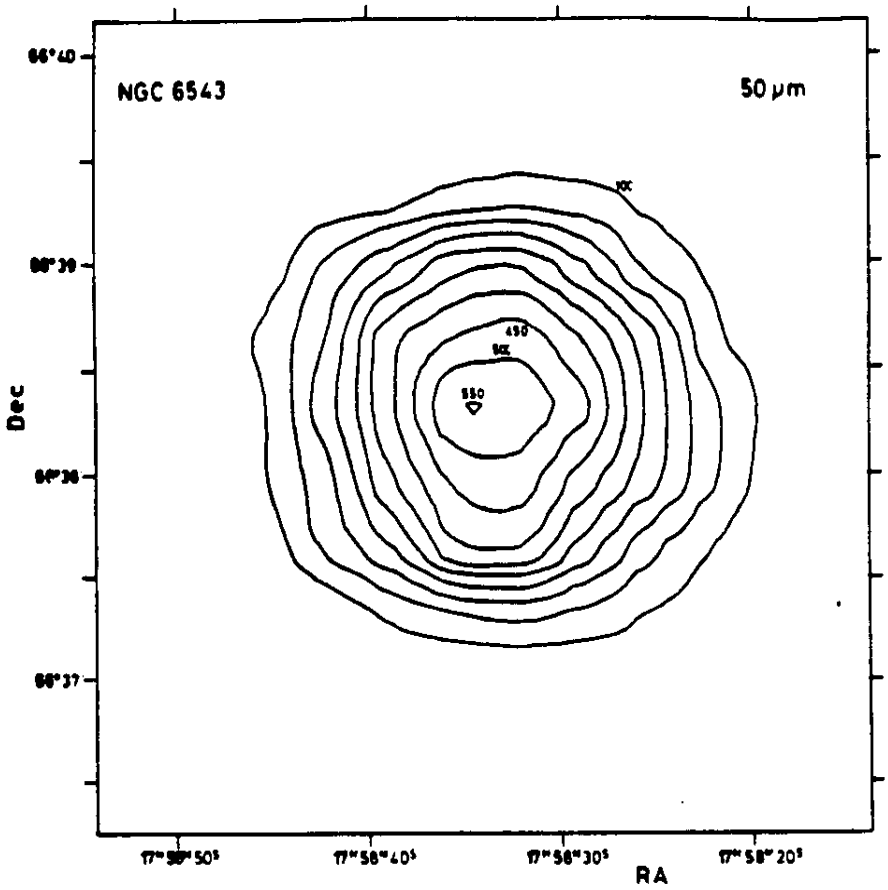

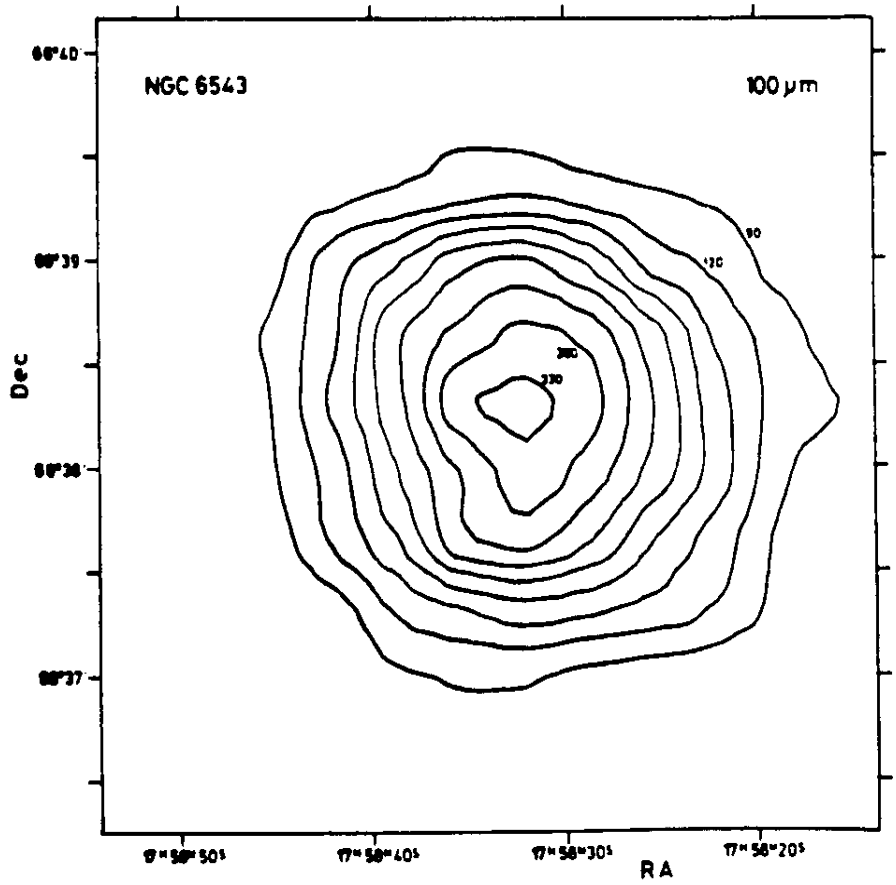

Fig. 8.5. Contour plots of NGC 6543 at 50 and 100 μm.

An arbitrary observation of this planetary is shown. The brightness unit is 1 MJy/sr. An individual observation does not show any extended structure.

88 μm.

The 52 μm and 57 μm lines appear in both the CPC 50 μm band and the survey 60 μm band (see figure 4.1). Watson et al. (1981) measured the 52 μm line intensity in NGC 6543 as 2.6×10^{-13} Wm^{-2}. An upper limit on the intensity of the 57 μm line can be derived by assuming (i) a cosmic nitrogen abundance, (ii) all N is ionized into N^{2+}, and using known parameters such as electron density and temperature (Pottasch et al.,1984). The 57 μm line intensity is then at most 8.5×10^{-13} Wm^{-2}. The in-band flux at 60 μm was found to be 3.4×10^{-12} Wm^{-2} (IRASES 1985), which is considerably larger than the estimated flux in the lines. Since both lines are located well inside both the 60 μm survey and 50 μm CPC bands, their influence on the calibration of the 50 μm CPC measurements is negligible.

The strength of the 88 μm line can be estimated from the 52 μm line intensity, the electron density and temperature in the nebula. In this way an intensity of 5×10^{-14} Wm^{-2} is derived. As the in-band flux in the 100 μm survey band is 7.6×10^{-13} Wm^{-2}, and the line again appears both in the CPC and survey 100 μm bands, the influence on the comparison of CPC and survey fluxes of NGC 6543 is negligible.

We assume, upon the arguments presented above, that the contributions of line radiation are about equal in the survey and CPC bands. We also assume that the underlying continuum can be represented closely enough by a 135 K blackbody curve for computing color corrections. The survey flux densities can then be converted to the following flux densities at the CPC wavelengths:

$$F_{50\ \mu m} = 140\ Jy,$$
$$F_{100\ \mu m} = 67\ Jy.$$

In conclusion, the measured fluxes within the broad photometric bands of the CPC and survey instrument are mainly due to thermal continuum radiation from heated dust particles. It was therefore justified to use NGC 6543 to monitor the calibration, repeatability, and stability of both instruments.

References.

Harten, R.H., Grosbol, P., Tritton, K.P., Greisen, E.W., Wells, D.C., 1984, Astronomical Image Processing Circular 10, 14, (Space Telescope Science Institute).

Infra Red Astronomical Satellite Explanatory Supplement (IRASES), 1985, Catalogs and Atlases, Joint IRAS Science Working Group (JISWG).

Millikan, A.G., 1974, Astron. J., 79, 1259.

Moseley, H., 1980, Astroph. J., 238, 892.

Newcomb, S., 1895, Tabels of the Sun (Ast. Pap. Amer. Eph., Vol. VI, Pt. I)

Pottasch, S.R., Beintema, D.A., Raimond, E., Baud, B., van Duinen, R., Habing, H.J., Houck, J.R., de Jong, T., Jennings, R.E., Olnon, F.M., Wesselius, P.R., 1985, Astroph. J. Lett., 278, L33.

Watson, D.M., Storey, J.W.V., Townes, C.H., Haller, E.E., 1981, Astroph. J., 250, 605.

Wells, D.C., Greisen, E.W., Harten, R.H., 1981, Astron. Astroph. Suppl., 44, 363.

Wildeman, K.J., Beintema, D.A., Wesselius, P.R., 1983, J. British Interplanet. Soc., 36, 21.

A.1. Description of CPC Deglitch Routines.

The deglitch routines have two main functions: the demodulation of the raw data and the removal of the frequently occurring glitches. Both functions will be described in some detail below.

Capitalized words refer to procedures or functions of the deglitch software.

A.1.1. Demodulation

The photometric data as they came from the satellite were modulated with a frequency $f_m = 15.062$ Hz. They were sampled 64 times per second ($f_s = 64$ Hz). In a trade-off between high time resolution versus computing time and unwanted beat frequencies, we settled on a demodulation of 8 data-points in one turn, bringing the data frequency down to 8 Hz.
For the k-th point we can write:

$$X_k = b + a \cos(\phi + k\ \Delta\phi) \qquad (1)$$

where b is the dc-value, a is the amplitude and ϕ is the phase of the modulated signal. $\Delta\phi$ is $2\pi f_m/f_s$.
Equation (1) can be written as a linear equation in b, a $\cos\phi$ and a $\sin\phi$:

$$X_k = b + a \cos\phi \cos(k\ \Delta\phi) - a \sin\phi \sin(k\ \Delta\phi) \qquad (2)$$

From this set of 8 equations the amplitude, a, can easily be solved.

FILMAT sets the constants $\cos(k\ \Delta\phi)$ and $\sin(k\ \Delta\phi)$ and fills the inverted matrix; DEMOD performs the demodulation of 8 raw data points, yielding one point for 1/8 sec.

A.1.2. Deglitcher

A.1.2.1. Definition of a Glitch

Glitches come in two kinds: random glitches and photon induced glitches. Both kinds have positive and negative representatives, of which the positive ones are in the majority.

The random glitches are presumably caused by particle hits on the detectors. They occur independent of what the detector is looking at. The cause of the photon induced glitches is less clear. They only occur when a certain amount of flux is shining on the detector. By lack of a more apt name they are called photon induced glitches. Although these two kinds clearly occur, there is a large overlap area where glitches cannot be ascribed to either kind.

In general a glitch is characterized by a fast rise time and an exponential decay. Mostly the top is reached within 0.1 second. Sometimes strange starting effects occur e.g. a deep negative trough just before a positive glitch which are caused by the dc restorer. Negative glitches do not have these strange starting effects. After reaching the top the glitch decays within 1 second to half the top value; it is not possible to define one characteristic decay time. The random glitches seem to be faster than the photon induced ones. Some characteristic glitches are shown in figures A.2 and A.3

A.1.2.2. Removal of a Glitch

The routines for removal are operating on a window of 4 seconds; Fig. A.1 defines the terms: backend, frontend and point.

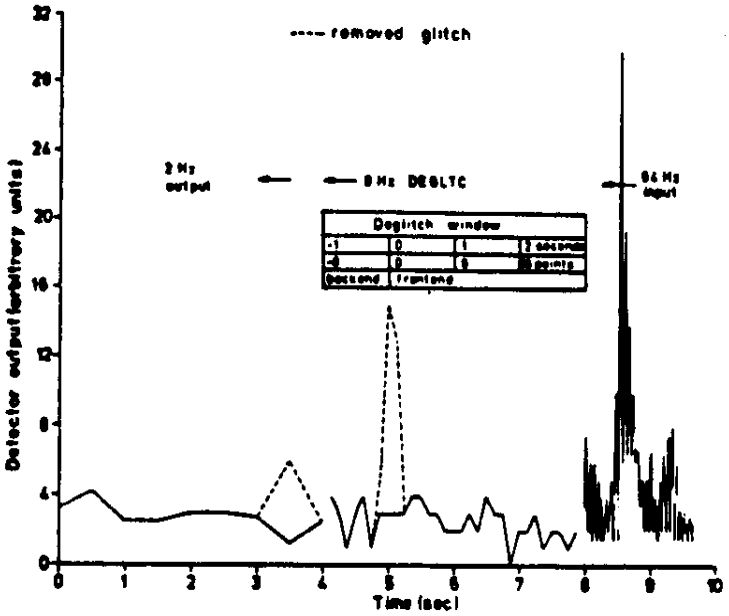

Fig. A.1. Removal of a glitch

The removal method uses a window of 4 seconds. The terms "backend", "frontend" and "point" are explained.

At the start the window is filled (FILWINDOW). The data in the backend are used to determine the background level and its noise. A linear equation is fitted to these points which are weighted with a geometric decay. For computational reasons this particular weighting scheme was chosen: in a scheme where all points on a certain stretch of the backend have equal weight, computational errors tend to accumulate just enough to be noticeable at the end of one measurement (about 400 seconds). The geometric decay avoids this nuisance.

The weight is $\tau^{|i|}$, where i is counted from zero and τ is chosen to be 0.8. Effectively the fit is made to only 5 points but a τ equal to 0.9 (10 points effectively) yields a fit that reacts too slow on a fast crossing of a source. The noise is determined from the sum of the squared deviations. A minimum value on the noise is necessary as the subtracting mechanism in the deglitcher diminishes the number of degrees of freedom in the noise. The value of 0.0001 Volts is taken as it is the smallest value the raw data could at-

tain.

From here on the background to a point is an extrapolation of the linear fit to that point. The noise is supposed to be constant over this extrapolated region.

As the actual filtering of glitches starts at point zero, the first second of every measurement or after a gap in the datastream, is not deglitched. In all other situations the background and noise are determined from deglitched data of the backend.

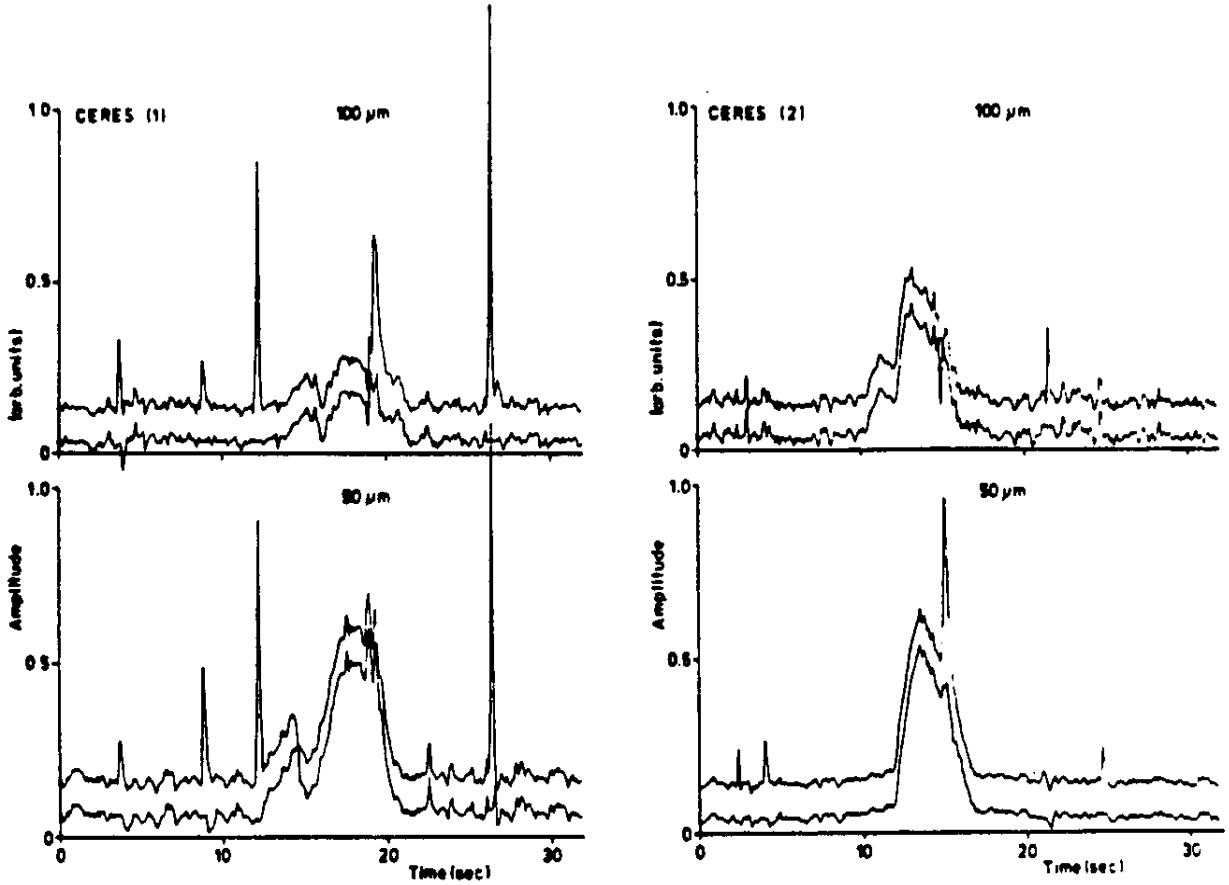

Fig. A.2. Examples of CPC data before and after deglitching.

The figures show 8 Hz data, original (top trace, shifted upward) and deglitched.

- Figure Ceres (1).
  Some random glitches can be seen, often correlated between both channels. Ceres is visible between 12 and 20 sec.
- Figure Ceres (2).
  Some random glitches are present. A nice example of a strong negative glitch occurs at 100 µm at 15 sec; it is correlated with a very strong positive glitch at 50 µm.

In order to be recognised a glitch as defined above has to fulfill 4 conditions. (Note that for negative glitches all signs have to be reversed.)

1. At point 2 the strength of the glitch i.e. the signal minus the back-

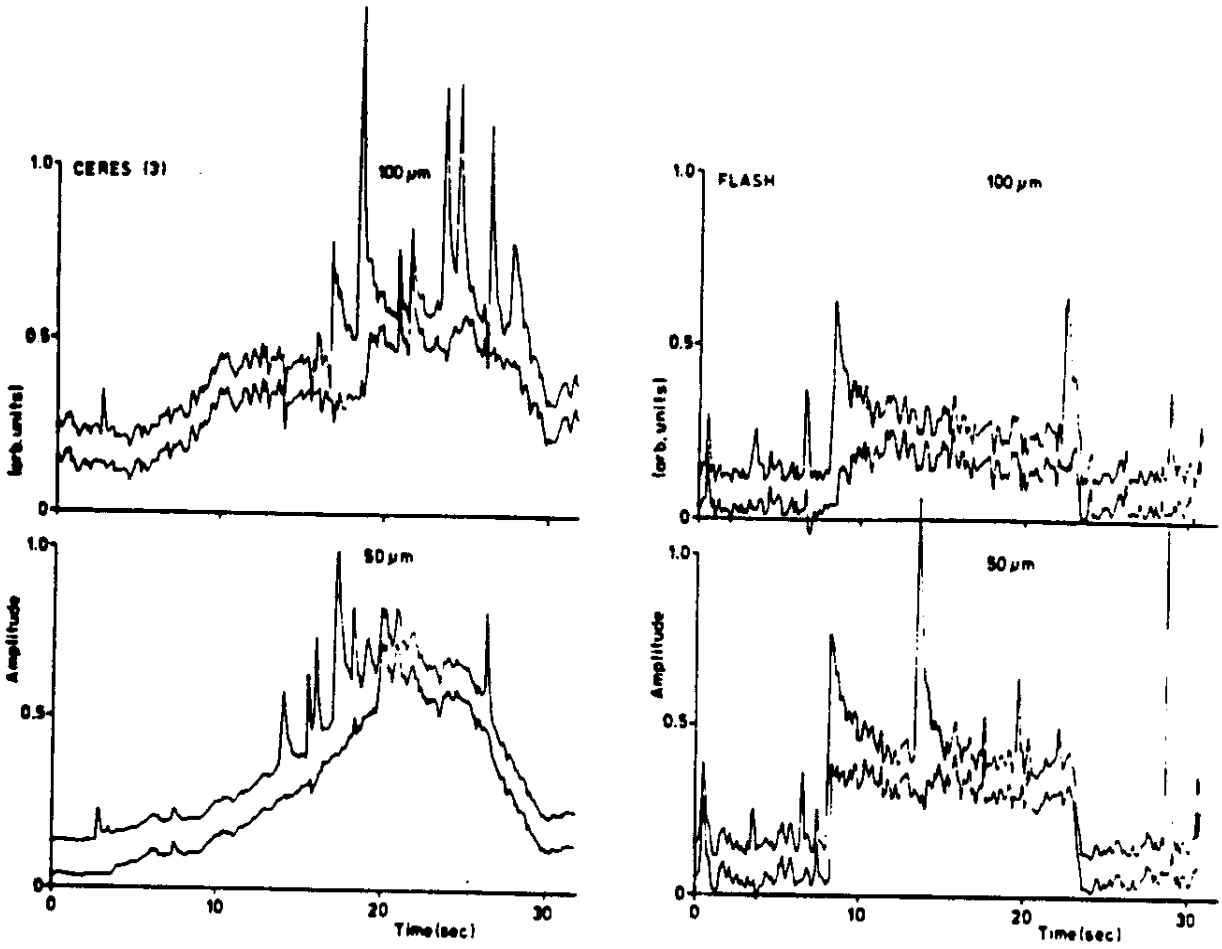

Fig. A.3. Examples of CPC data before and after deglitching.

The figures show 8 Hz data, original (top trace, shifted upward) and deglitched.

- Figure Ceres (3).
  Conspicuous photon-induced glitches appear on the leading wing of Ceres. They are somewhat broader than the random glitches. Note that at 50 μm at 20 sec a complicated 'double' glitch occurs which the deglitcher could not handle. At 26 sec a positive glitch shows a negative start (100 μm).
- Figure Flash.
  At the beginning of a flash usually a photon-induced glitch is seen. This kind of glitch can be removed by the feature described in Annex.1 (condition 4).

ground, has to be greater than 7 times the noise. Point 2 was chosen to step over the strange starting behavior of some glitches (FORNEXTTIME). Seven as a glitch recognition constant is a compromise between cutting in the noise (at 5) and leaving conspicuous glitches untouched (at 10).

2. When earlier in time the subtraction of a glitch already occurred at point 2, we don't want to subtract other glitches which could be artefacts of our own manipulation. More stringent rules have to be applied now. The candidate glitch has to be greater than 4 times the difference between the original and the manipulated signal which allows a glitch in the tail of a previous one to be subtracted, or it has to be greater than 14 times the noise; it has to be really huge. The values of both constants have a certain amount of arbitrariness (CONFUSION).
3. A candidate glitch has to have a top within a certain (time)interval i.e.

a point which is higher than the previous one and the next one. The interval is confined to the points 2 or 3 which limits the rising time to 0.25 seconds (NOTOP).

4. After having a top a candidate has to decay to half of its strength within a certain (time)interval (less than 6 points). When no decay within this interval is found it is tried again with a new glitch strength equal to half of the old one. This is repeated until the new strength is less than 7 times the noise, in accordance with condition 1 or, of course a decay is found. This last feature gives a handle on e.g. glitches at the beginning of a flash. See figure A.3.
   Here also the decaytime from the top is calculated. The exact time of half signal strength is linearly interpolated between the two encompassing points. The decay time equals half signal time minus top time (in seconds). For very short glitches with a decay within one point, the decaytime is determined by fitting an exponential to the first point after the top (NODECAYTIME).

If a candidate glitch fulfills all 4 conditions it is supposed to be a genuine one and it can be subtracted. From the begin to the top the signal is set to the background. From the top to 6 times the decaytime an exponential is subtracted with strength and decaytime as determined (FILTER).

After a search for a glitch, succesful or not, the window is shifted one point (ROLLOVER), the background is determined anew (NIVEAU) and the conditions for a glitch are applied to the next zeropoint. After 8 of those shifts the backend of the window is full of new points. Of both the original and the deglitched signal half-second means are taken which are returned to the main program with the corresponding satcal and a quality measure. The quality measure is defined as the number of points which were left unchanged by the deglitcher; so it runs from 0 to 4. (TAKEMEAN)

When a gap in the data stream occurs the window is emptied first via FILTER, ROLLOVER and TAKEMEAN, after which the window can be filled again with FILWINDOW. The end of the data stream is treated as a gap with the exception that the window is not filled again. The steering between normal and 'gap' performance is done by DGLSTEER.

A.2. Discussion of some sample maps

A.2.3. NGC 6543

This is one of the many observations of the planetary nebula, NGC 6543, our photometric reference source. It is a source of reasonable strength and it is indistinguishable from a point source for the CPC instrument.

The noise is below 5 % and 15 % for the 50 and 100 μ channel respectively. The background lies at 20 MJy/sr for both channels.

Some of the responsivity variation phenomena appear. From the start of the observation (indicated with an arrow, pointing in the in-scan direction) to the end the background increases by about 30 %. The variation is taken out by the gain correction program. The difference between the increasing and the flat background is evident by comparing the 'raw' and the 'clean' map.

Another responsivity variation effect is the distortion in the in-scan direction of the lower contour lines, best seen in the 50 μ 'clean' map. In general features parallel to the in-scan direction should be treated with caution: they could be spurious. In this example map the effect is not very strong; it disappears at the 10 % level and at 100 μ it is not seen at all. For sources fainter than NGC 6543 the effect will be of small or no importance.

A.2.4. NGC 3610

The target of the observation was a galaxy, NGC 3610, but obviously it is not detected.

All 'structure' in the map has a size smaller than or equal to the beam-size. This 'structure' must be noise. The dynamic range is a factor 4 to 6 and the mean flux level is about 13 MJy/sr for both channels. This is approximately the lowest CPC background found. The noise in the map is accordingly (~ 4 MJy/sr per pixel). This noise is dominated by a large number of small to very small glitches which could not be detected by the deglitch program. The larger glitches, present in abundance in the 'raw' map, have been cut out quite satisfactory.

Around the edges of the map the noise is somewhat larger than in the interior. This is due to the fact that at the edges sometimes only one point contributes to the pixel, while in the interior a pixel is always the mean of several points measured.

A.2.5. Ceres

Ceres is an asteroid, and a true point source. It is somewhat more intense than NGC 6543 and all effects described above can also be seen.

Glitches are large and abundant as the observation was done near the South Atlantic Anomaly. The deglitcher is able to take these out.

The gain is increasing with a factor 1.5 and 2.5 for 50 μ and 100 μ respectively. Correcting for it was no problem due to the fact that Ceres is a simple point source on a (presumably) flat background of 50 and 20 MJy/sr.

A.2.6. MRSL 269-01/2

This is a molecular cloud region. The true shape of the cloud is severely distorted by the responsivity variation effect (section 5.1). At the high flux levels of this source glitches are of no importance anymore; they drown in the source flux.

The source is clearly extended, but the true size and shape is difficult to establish from this CPC map. The routine correcting for the long-term increase of the background fails, because the definition of background is moot. The program calculates gain increases of 3 and 5 on 'mean background levels' of 300 and 1100 MJy/sr for 50 and 100 μm respectively.

We decided to exclude maps from the CPC atlas where the gain correction did not meet certain stringent conditions. This particular image is an example of an excluded one.

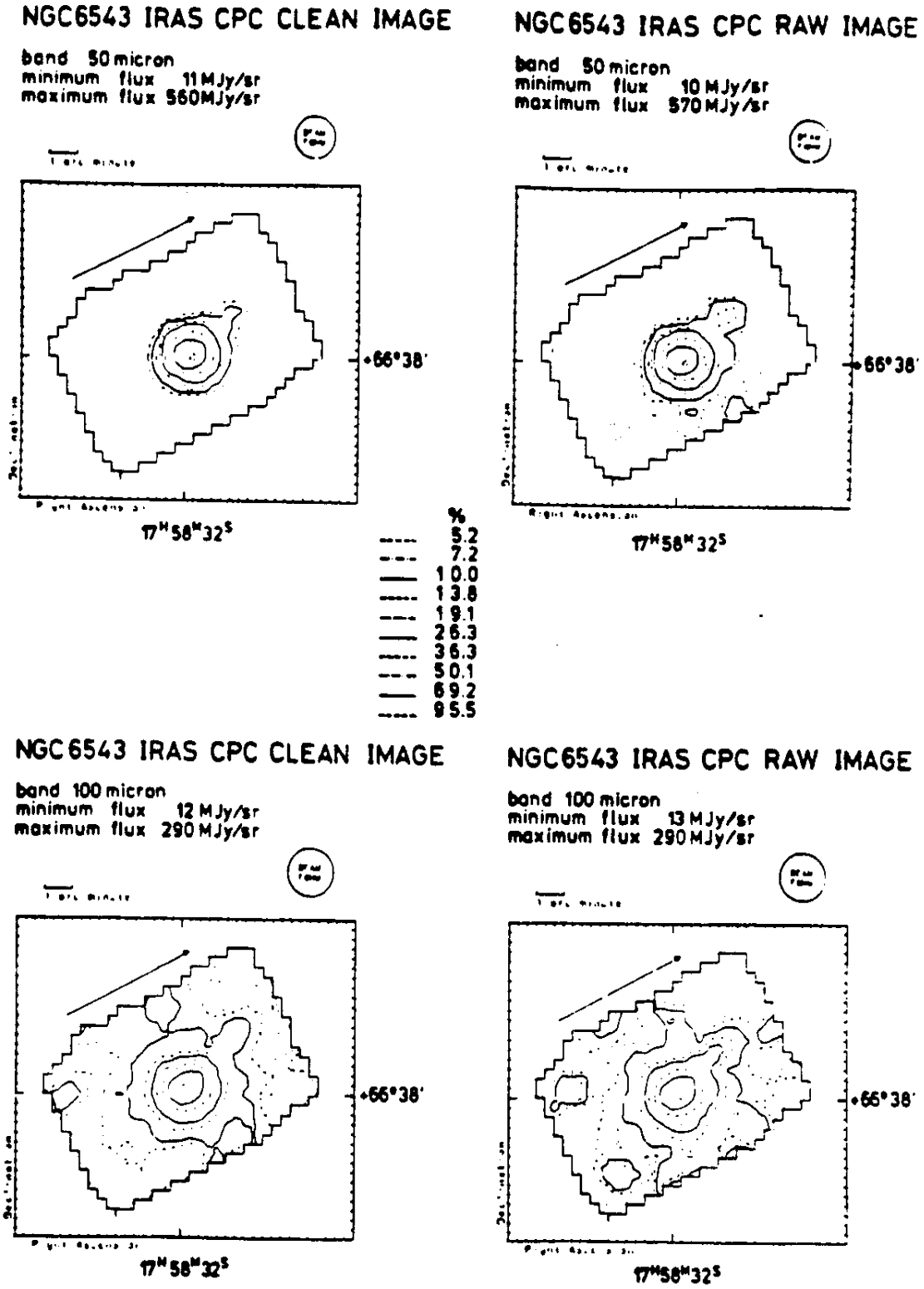

Fig. A.4 Example of a CPC map. See text for a discussion.

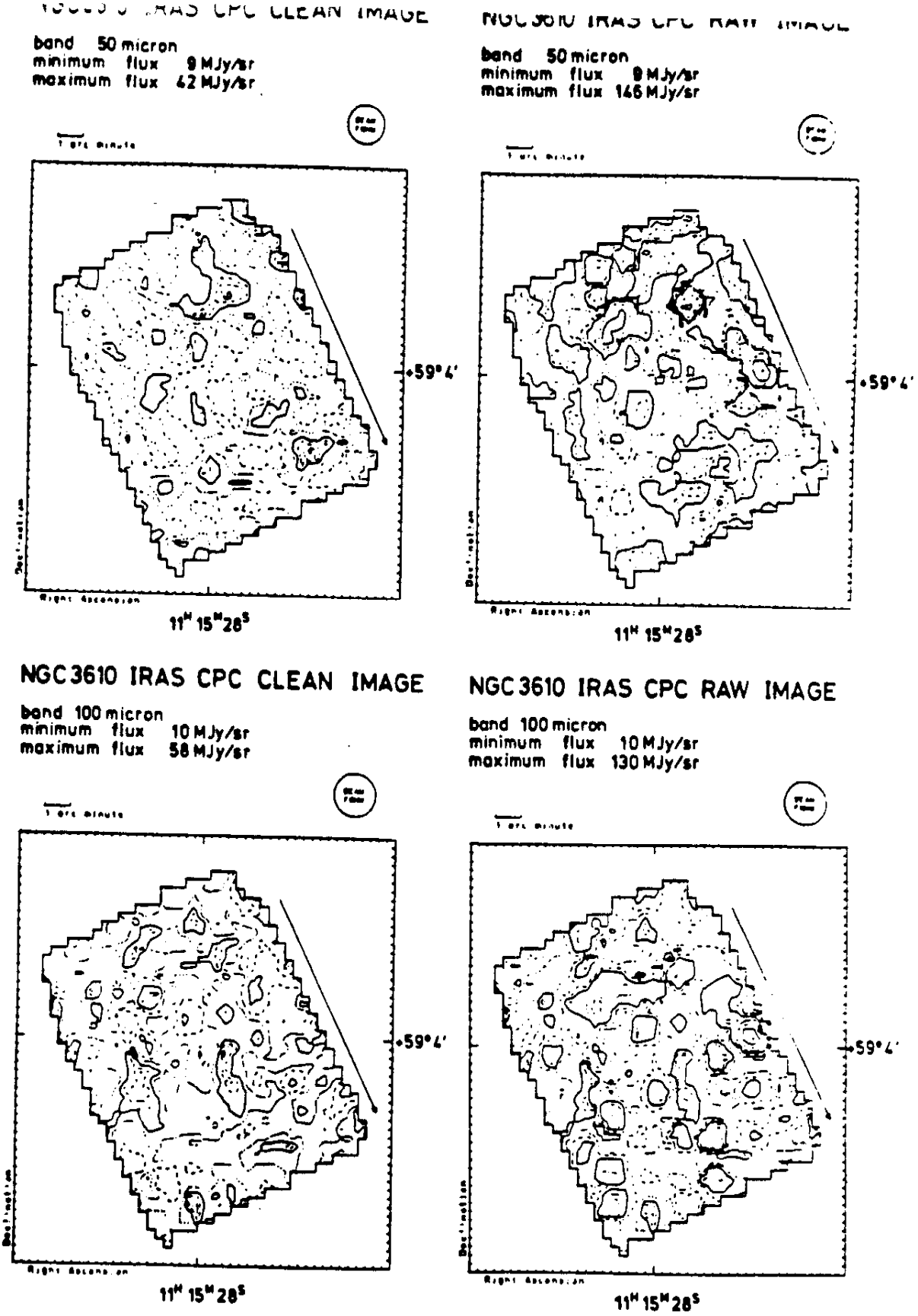

Fig. A.5 Example of a CPC map. See text for a discussion.

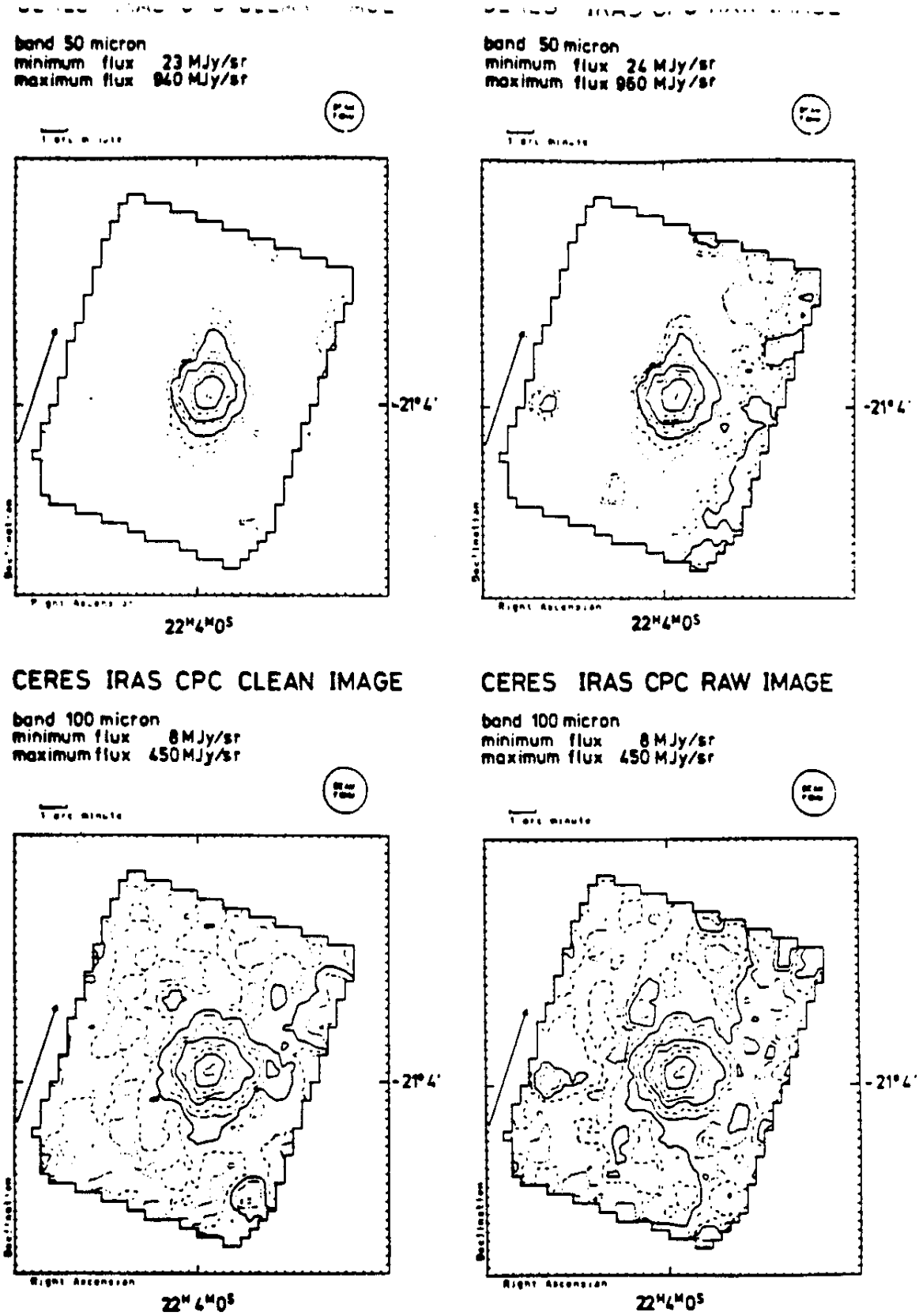

Fig. A.6 Example of a CPC map. See text for a discussion.

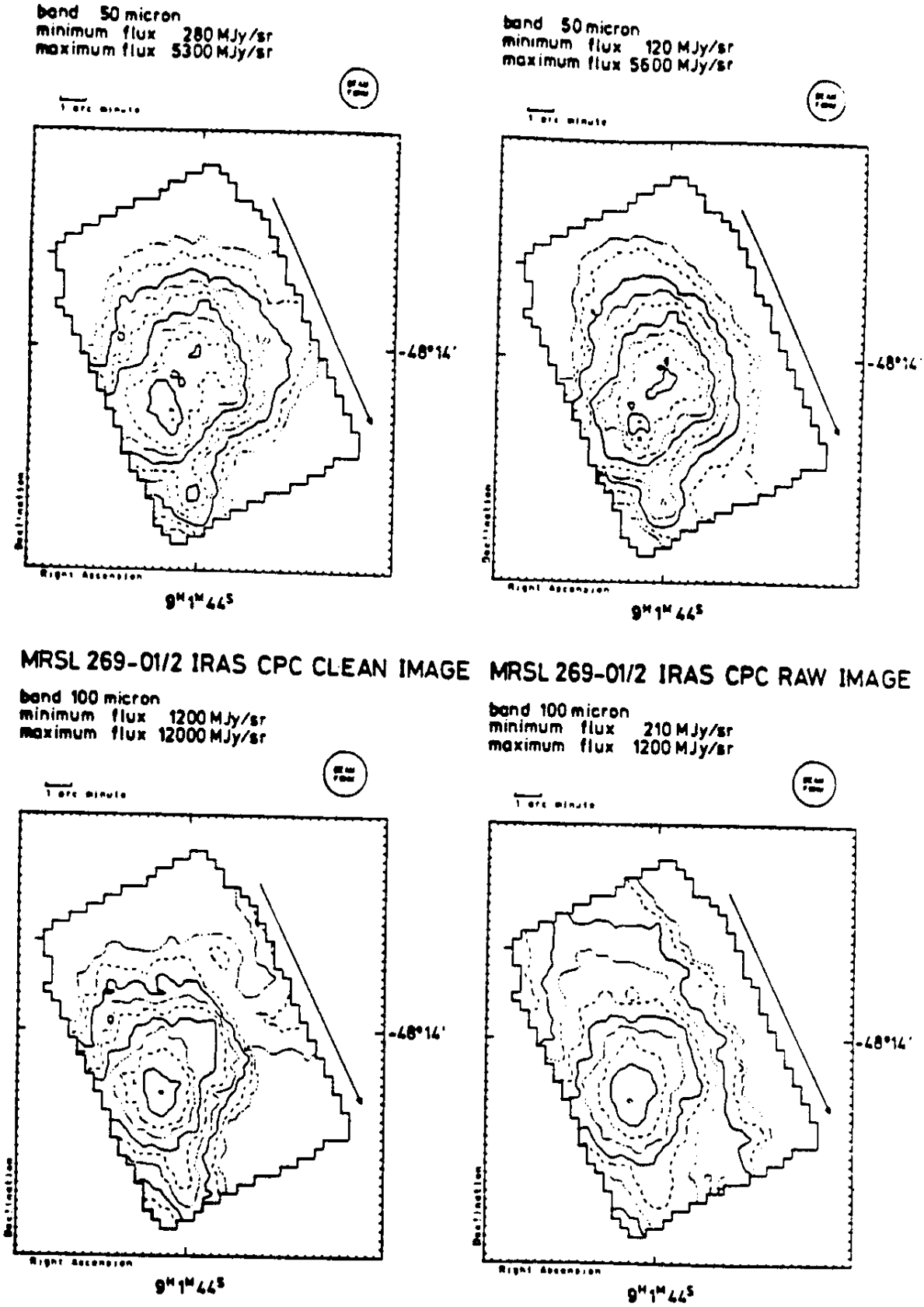

Fig. A.7 Example of a CPC map. See text for a discussion.

A.3. Tape Format

The CPC observations are distributed in on magnetic tape in FITS format, with a corresponding tape density of 1600 bpi and blocksize of 2880 bytes. The FITS format is described in Wells (1980). There are two consecutive FITS files on the tape for each observation, one giving the "clean" and the other the "raw" images (see section 3 and 6.6). In each file two maps (at 50 and 100 μm) are stored in a three dimensional array, where the first axis denotes the right ascension and the second the declination. The third dimension gives the wavelength.

There are 1508 CPC observations distributed on 3 output tapes. For identification purposes, the actual tape in FITS format is preceded by a tape label group, 2 80-byte tape blocks of ASCII characters and a tape mark, written in the format of an ANSI label group. Note that this is at variance with both the FITS standard, which does not specify labelling, and with the ANSI standard, which uses tapemarks only to separate data and label groups, and prescribes trailer label groups as well.

Table A.1. Distributed tapes

Tapelabel	number of observations	RA range (hours)
CPCFT1	489	00 - 07
CPCFT2	624	08 - 15
CPCFT3	395	16 - 23

A list of all observations, sorted on RA/DEC is appended after the FITS images on the tape CPCFT3.

A.3.7. Header of list of observations

The list of the distributed observations, added after the FITS images on the last tape CPCFT3, is written in the FITS table extension format (Harten et al., 1984) The format used is the same as that of column 1-5 of annex 4.

A.4. List of observations

The columns indicate :

1. Conventional astronomical object name (if known).
2. Julian epoch of observation - 1983.0.
3. Map centre Right Ascension 1950.0.
   The list is sorted on Right Ascension.
4. Map centre Declination 1950.0.
5. Observation type used.
   The abbreviations used for the observation types differ slightly from the macro names used in Table 2.1, e.g. CPCF9A = 9*9FF, CPC09A = 9*9F.
6. Declination error warning.
   A "1" in the sixth column indicates that the decoding of the declination sent up to the satellite might be in error.
7. Deleted observation flag.
   "BADGAIN" in column 7 means that the measurement could not satisfactorily be corrected for the sensitivity variation phenomenon discussed in section 5.1. Such observations have been deleted from the processing chain, and can consequently not been found on the CPC tapes. In some cases it might be possible with the help of Groningen experts to interpret the data of such measurements. Interested astronomers should contact P.R. Wesselius.

A.3.8. Header of FITS image

To prevent a proliferation of keywords we give qualitative information in comments. As an example, and to show the keywords we have used, an arbitrary FITS header is shown below.

```
SIMPLE  =                    T / SIMPLE FITS FORMAT ( HEADER VERSION D1 850214)
BITPIX  =                   16 / PIXEL VALUES: 2-BYTE TWOS-COMPLEMENT INTEGERS
NAXIS   =                    3 / NUMBER OF AXES IN THE DATA ARRAY
NAXIS1  =                   47 / NUMBER OF PIXELS/ROW  (RA) (COLUMNS)
NAXIS2  =                   51 / NUMBER OF ROWS        (DEC)
NAXIS3  =                    2 / NUMBER OF WAVELENGTHS (LAMBDA)
CTYPE1  = 'RA      '           /
CRVAL1  =          1.33967E+02 / COORDINATE TRANSFORMATIONS:
CRPIX1  =          2.40000E+01 /  X OF PIXEL = ( COLUMN - CRPIX1 )*CDELT1
CDELT1  =         -5.55556E-03 /  Y OF PIXEL = ( ROW - CRPIX2 )*CDELT2
CTYPE2  = 'DEC     '           / TRANSFORMATIONS BETWEEN (X,Y) AND (RA,DEC):
CRVAL2  =         -4.24833E+01 /  APPROXIMATE (FAR FROM THE CELESTIAL POLES):
CRPIX2  =          2.90000E+01 /   X = (CRVAL1 - RA)*COS(CRVAL2)
CDELT2  =          5.55556E-03 /   Y = DEC - CRVAL2
CTYPE3  = 'LAMBDA  '           /  EXACT:
CRPIX3  =          1.00000E+00 /   X = SIN(CRVAL1 - RA)*COS(DEC)
CRVAL3  =          5.00000E-05 /   Y = ( SIN(DEC)*COS(CRVAL2) ) -
CDELT3  =          5.00000E-05 /       ( COS(DEC)*SIN(CRVAL2)*COS(RA-CRVAL1) )
BSCALE  =          2.58334E-02 / DATA SCALE FACTOR (REAL=TAPE*BSCALE+BZERO)
BZERO   =          9.26282E+02 / DATA OFFSET VALUE
BUNIT   = 'MJY / SR'           / BRIGHTNESS UNITS
BLANK   =                -32767 / TAPE PIXEL VALUE ASSIGNED TO UNDEFINED VALUE
DATE-OBS= '24/06/83'           / DATE OF OBSERVATION       (JE 1983.481044)
TIME-OBS= '22:48:49'           / TIME OF OBSERVATION
INSTRUME= 'IRAS-CPC'           / INSTRUMENT USED IN OBSERVATION
ORIGIN  = 'ROG-GRON'           / NAME OF INSTITUTE THAT PRODUCED THIS FILE
OBJECT  = 'VHE 27B     '       / NAME OF THE OBSERVED OBJECT
COMMENT  IRAS CPC CLEAN IMAGE
COMMENT  NOSSEBEFORE NOSSEAFTER
COMMENT  START OF SCAN AT (COL,ROW)=(22,47) TO (COL,ROW)=(32,39) IN 10 SECONDS.
HISTORY  IMTOFTD1 850309 < REGRIDD2 850127 < GAINCRD3 850127 < CPCATTD3 850127
HISTORY  < DEGLTCD1 841003
COMMENT  THIS TAPE CONTAINS CONFIDENTIAL DATA
COMMENT  PUBLICATIONS BEFORE DEC 1985 ARE RESTRICTED TO IRAS PROJECT SCIENTISTS
DATE    = '09/03/85'           / CREATION DATE OF THIS FITS TAPE FILE
END
```

Remarks:

- When the words 'noSSEbefore' or 'noSSEafter' appear in a COMMENT line, the sighting of a star before or after the rasterscan failed. The attitude reconstruction is not fully reliable.
- The direction and the speed of the scan are indicated in a COMMENT by giving the position of the first sample and the 20th sample. One should not try to reconstruct the details of the raster scan from this information.

NGC 0055	416210	00 12.4	-39 28	9*9FF			
NGC 0055	418954	00 12.4	-39 28	9*9FF			
NGC 0134	505582	00 27.9	-33 32	9*9F			
NGC 0134	459723	00 27.9	-33 32	9*9FF			
M 31	501126	00 37.8	+40 26	9*9FF			
M 31	536988	00 37.8	+40 26	9*9FF			
M 31	561290	00 37.8	+40 26	9*9FF			
M 31	568425	00 37.8	+40 26	9*9FF			
M 31	550495	00 39.5	+41 04	9*9FF			
M 31	601069	00 39.5	+41 04	9*9FF			
M 31	605768	00 39.5	+41 04	9*9FF			
M 31	635943	00 39.5	+41 04	9*9FF			
M 31	537185	00 39.6	+40 54	9*9FF			
M 31	539929	00 39.6	+40 54	9*9FF			
M 31	547751	00 39.6	+40 54	9*9FF			
M 31	551882	00 39.6	+40 54	9*9FF			
M 31	119366	00 40.0	+40 59	9*9FF	1		
M 31	124461	00 40.0	+40 59	9*9FF	1		
M 31	499552	00 40.0	+41 00	9*9FF			
M 31	500531	00 40.0	+41 00	9*9FF			
M 31	502490	00 40.0	+41 00	9*9FF			
M 31	503079	00 40.0	+41 00	9*9FF			
M 31	499943	00 40.4	+41 05	9*9FF			
M 31	510330	00 40.4	+41 05	9*9FF			
M 31	510919	00 40.4	+41 05	9*9FF			
M 31	545416	00 40.4	+41 05	9*9FF			
M 31	636138	00 40.5	+40 55	9*9FF			
M 31	636729	00 40.5	+40 55	9*9FF			
M 31	561681	00 41.5	+41 04	9*9FF			
M 31	567168	00 41.5	+41 04	9*9FF			
M 31	578336	00 41.5	+41 04	9*9FF			
M 31	581079	00 41.5	+41 04	9*9FF			
M 31	592052	00 41.9	+41 10	9*9FF			
M 31	594196	00 41.9	+41 10	9*9FF			
M 31	596359	00 41.9	+41 10	9*9FF			
M 31	598912	00 41.9	+41 10	9*9FF			
	599703	00 41.9	+67 57	9*9F			
M 31	534443	00 42.2	+41 16	9*9FF			
M 31	598715	00 42.2	+41 16	9*9FF			
M 31	600676	00 42.2	+41 16	9*9FF			
M 31	602832	00 42.2	+41 16	9*9FF			
M 31	603025	00 42.5	+41 22	9*9FF			
M 31	633200	00 42.5	+41 22	9*9FF			
M 31	636335	00 42.5	+41 22	9*9FF			
M 31	510525	00 42.7	+41 38	9*9FF			
M 31	549525	00 42.7	+41 38	9*9FF			
M 31	551490	00 42.7	+41 38	9*9FF			
M 31	558731	00 42.7	+41 38	9*9FF			
	592655	00 43.2	+69 59	9*9F			
	596377	00 43.2	+69 59	9*9F			
	603623	00 48.6	+69 03	9*9F			
NGC 0300	435416	00 52.5	-37 57	9*9FF			
NGC 0300	467957	00 52.5	-37 57	9*9FF			
ACK 125-47.1	504266	00 57.3	+15 28	9*9F			
ACK 125-47.1	515290	00 57.3	+15 28	9*9F			
IC 1613	489914	01 02.2	+01 51	9*9FF			

IC 1613	497758	01 02.2	+01 51	9*9FF			
	556371	01 03.8	+12 19	3*3SS			
IRC+10011	537168	01 03.8	+12 19	3*3SS			
IRC+10011	536972	01 03.8	+12 19	9*9FF			
IRC+10011	555580	01 03.8	+12 19	9*9FF			
NGC 0404	523059	01 06.7	+35 27	9*9FF			
NGC 0404	525997	01 06.7	+35 27	9*9FF			
NGC 0474	515409	01 17.5	+03 09	9*9FF			
NGC 0474	520895	01 17.5	+03 09	9*9FF			
	114069	01 20.0	+61 33	9*9FF	1	BADGAIN	
M 33	502098	01 30.4	+30 39	9*9FF			
M 33	506986	01 30.4	+30 39	9*9FF			
M 33	508364	01 30.4	+30 39	9*9FF			
M 33	517177	01 30.4	+30 39	9*9FF			
ACK 127.8-0.0	184454	01 30.5	+62 11	3*3SS	1		
ACK 127.8-0.0	209326	01 30.5	+62 12	3*3SS			
M 33	482102	01 31.0	+30 24	9*9FF			
M 33	484845	01 31.0	+30 24	9*9FF			
M 33	498563	01 31.0	+30 24	9*9FF			
M 33	499347	01 31.0	+30 24	9*9FF			
M 33	501111	01 31.0	+30 24	9*9FF			
M 33	506017	01 31.0	+30 31	9*9FF			
M 33	506793	01 31.0	+30 31	9*9FF			
M 33	508758	01 31.0	+30 31	9*9FF			
M 33	509341	01 31.0	+30 31	9*9FF			
	501306	01 31.6	+30 31	9*9FF			
	503268	01 31.6	+30 31	9*9FF			
	504049	01 31.6	+30 31	9*9FF			
	506598	01 31.6	+30 31	9*9FF			
NGC 0613	502644	01 32.0	-29 40	9*9F			
NGC 0628	531291	01 34.0	+15 32	9*9FF			
NGC 0628	534034	01 34.0	+15 32	9*9FF			
UGC 1176	536778	01 37.5	+15 39	9*9FF			
UGC 1176	541862	01 37.5	+15 39	9*9FF			
NGC 0643B	765965	01 38.4	-75 16	9*9F			
NGC 0643B	773414	01 38.4	-75 16	9*9F			
NGC 650/1	597541	01 39.2	+51 19	9*9F			
NGC 650/1	600285	01 39.2	+51 19	9*9F			
NGC 0660	531486	01 40.4	+13 23	9*9FF			
NGC 0660	539521	01 40.4	+13 23	9*9FF			
NGC 0782	380330	01 56.0	-58 02	9*9FF			
NGC 0782	383074	01 56.0	-58 02	9*9FF			
	233127	01 57.0	-67 04	9*9F			
NGC 0777	555984	01 57.4	+31 11	9*9F			
NGC 0777	564214	01 57.4	+31 11	9*9F			
NGC 0784	587337	01 58.4	+28 36	9*9F			
NGC 0784	599681	01 58.4	+28 36	9*9F			
NGC 0891	577932	02 19.4	+42 07	9*9F			
NGC 0891	580676	02 19.4	+42 07	9*9F			
NGC 0891	125051	02 19.4	+42 07	9*9FF	1		
NGC 0891	142305	02 19.4	+42 07	9*9FF	1		
	198941	02 23.3	+61 38	9*9FF		BADGAIN	
	144853	02 23.3	+61 38	9*9FF	1	BADGAIN	
	190706	02 23.3	+61 38	9*9FF	1	BADGAIN	
NGC 0925	581655	02 24.3	+33 21	9*9F			
NGC 0925	584817	02 24.3	+33 21	9*9F			

NGC 0925	586161	02 24.3	+33 21	9*9F			
NGC 0925	588904	02 24.3	+33 21	9*9F			
UGC 2035	587531	02 31.5	+29 32	9*9F			
UGC 2035	591851	02 31.5	+29 32	9*9F			
NGC 0986	505775	02 31.6	-39 15	9*9F			
MAFFEI 1	206976	02 32.6	+59 26	9*9FF			
MAFFEI 1	209916	02 32.6	+59 26	9*9FF			
MAFFEI 2	207175	02 38.1	+59 23	9*9FF			
MAFFEI 2	212660	02 38.1	+59 23	9*9FF			
	232731	02 43.7	-62 43	9*9F			
NGC 1097	522629	02 44.2	-30 29	9*9FF			
NGC 1097	558293	02 44.2	-30 29	9*9FF			
	631060	02 48.6	+69 03	9*9F			
	633799	02 48.6	+69 03	9*9F			
	595571	02 51.2	+41 23	9*9F			
	633394	02 51.2	+41 23	9*9F			
NGC 1140	582418	02 52.1	-10 14	9*9F			
NGC 1140	585556	02 52.1	-10 14	9*9F			
ACK 255-59.1	499700	02 55.2	-44 22	9*9F			
ACK 255-59.1	502443	02 55.2	-44 22	9*9F			
	150139	02 59.4	+60 16	9*9F	1		
	146219	02 59.4	+60 16	9*9F	1	BADGAIN	
	152291	02 59.4	+60 16	9*9F	1	BADGAIN	
NGC 1169	216980	03 00.2	+46 11	9*9FF			
NGC 1169	219730	03 00.2	+46 11	9*9FF			
	166014	03 03.5	+58 19	9*9F	1		
	168563	03 03.5	+58 19	9*9F	1		
NGC 1291	497737	03 15.5	-41 18	9*9FF			
NGC 1291	500873	03 15.5	-41 18	9*9FF			
	198959	03 16.5	+41 20	9*9F			
	215222	03 16.5	+41 20	9*9F			
NGC 1313	236849	03 17.7	-66 41	9*9F			
NGC 1313	239593	03 17.7	-66 41	9*9F			
ACK 138.0+7.	145431	03 20.7	+65 21	3*3SS	1		
ACK 138.0+7.	147389	03 20.7	+65 21	3*3SS	1		
NGC 1316	199397	03 20.8	-37 23	9*9F			
NGC 1316	199592	03 20.8	-37 23	9*9F			
NGC 1316	514394	03 20.8	-37 23	9*9F			
NGC 1316	517138	03 20.8	-37 23	9*9F			
	145824	03 23.7	+58 36	9*9F	1	BADGAIN	
	152096	03 23.7	+58 36	9*9F	1	BADGAIN	
	112121	03 25.0	+30 00	9*9F	1		
	114278	03 25.0	+30 00	9*9F	1		
	607912	03 25.3	+31 13	9*9F			
	610655	03 25.3	+31 13	9*9F			
	616337	03 25.5	+31 06	9*9F			
	618885	03 25.5	+31 06	9*9F			
	608495	03 25.6	+30 58	9*9F			
	611238	03 25.6	+30 58	9*9F			
	113490	03 25.7	+30 58	9*9FF	1		
	132519	03 25.7	+30 58	9*9FF	1		
	608107	03 25.9	+31 15	9*9F			
	610850	03 25.9	+31 15	9*9F			
	608300	03 26.0	+31 08	9*9F			
	611786	03 26.0	+31 08	9*9F			
	113504	03 26.1	+31 08	9*9FF	1		

	119581	03 26.1	+31 08	9*9FF	1	
	133303	03 26.1	+31 08	9*9FF	1	
	613981	03 26.2	+31 00	9*9F		
	616530	03 26.2	+31 00	9*9F		
	113882	03 26.3	+30 60	9*9FF	1	
	124860	03 26.3	+30 60	9*9FF	1	
	611043	03 26.5	+31 17	9*9F		
	613398	03 26.5	+31 17	9*9F		
	613594	03 26.6	+31 10	9*9F		
	616141	03 26.6	+31 10	9*9F		
	619080	03 26.8	+31 02	9*9F		
	624371	03 26.8	+31 02	9*9F		
NGC 1350	594938	03 29.2	-33 48	9*9F		
NGC 1350	659217	03 29.2	-33 48	9*9F		
ACK 141.7+3.	145627	03 29.4	+60 10	3*3SS	1	
ACK 141.7+3.	147783	03 29.4	+60 10	3*3SS	1	
	232930	03 31.0	-75 23	9*9F		
NGC 1365	584364	03 31.7	-36 18	9*9F		
NGC 1365	587694	03 31.7	-36 18	9*9F		
•	145846	03 40.3	+32 00	9*9F	1	
NGC 1428	582007	03 40.5	-35 19	9*9F		
NGC 1428	658042	03 40.5	-35 19	9*9F		
NGC 1433	569456	03 40.5	-47 23	9*9F		
NGC 1433	577686	03 40.5	-47 23	9*9F		
IC 342	655742	03 41.9	+67 57	9*9F		
IC 342	657697	03 41.9	+67 57	9*9F		
IC 342	671222	03 41.9	+67 57	9*9F		
	150912	03 42.0	+67 56	9*9FF	1	
•	153461	03 42.0	+67 56	9*9FF	1	
	157773	03 42.0	+67 56	9*9FF	1	
NGC 1448	529087	03 42.9	-44 48	9*9F		
NGC 1448	539082	03 42.9	-44 48	9*9F		
NGC 1448	510858	03 42.9	-44 48	9*9FF		
NGC 1448	534179	03 42.9	-44 48	9*9FF		
UCG 2855	641240	03 43.2	+69 59	9*9F		
UCG 2855	643983	03 43.2	+69 59	9*9F		
UCG 2855	783295	03 43.2	+69 59	9*9F		
UCG 2855	199136	03 43.3	+70 00	3*3SS		
UCG 2855	203839	03 43.3	+70 00	3*3SS		
	188157	03 55.0	+66 59	9*9FF	1	
	190901	03 55.0	+66 59	9*9FF	1	
	179942	04 15.0	+41 54	9*9F	1	
	182686	04 15.0	+41 54	9*9F	1	
NGC 1559	458925	04 17.0	-62 54	9*9F		
NGC 1559	463036	04 17.0	-62 54	9*9F		
NGC 1566	528106	04 18.9	-55 03	3*3SS		
NGC 1566	528887	04 18.9	-55 03	3*3SS		
NGC 1566	328769	04 18.9	-55 03	9*9FF		
NGC 1566	331513	04 18.9	-55 03	9*9FF		
NGC 1566	117667	04 18.9	-55 03	9*9FF	1	
NGC 1566	112176	04 18.9	-55 04	9*9FF	1	
	162684	04 21.1	+54 52	9*9F	1	
	165427	04 21.1	+54 52	9*9F	1	
NGC 1569	179533	04 26.1	+64 44	9*9FF	1	
NGC 1569	185413	04 26.1	+64 44	9*9FF	1	
	165820	04 26.9	+54 45	9*9F	1	
	168172	04 26.9	+54 45	9*9F	1	
NGC 1560	174237	04 27.1	+71 46	9*9FF	1	
NGC 1560	179921	04 27.1	+71 46	9*9FF	1	
	190510	04 27.4	+63 30	9*9FF	1	
	193260	04 27.4	+63 30	9*9FF	1	
	640428	04 28.1	+18 01	9*9F		
	646704	04 28.1	+18 01	9*9F		
	737030	04 28.1	+18 08	9*9F		
	743493	04 28.1	+18 08	9*9F		
	160547	04 28.2	+17 53	9*9FF	1	
	163096	04 28.2	+17 53	9*9FF	1	
	222681	04 28.6	+18 09	9*9FF		
	179758	04 28.6	+18 09	9*9FF	1	
	150160	04 28.7	+18 01	9*9FF	1	
	152312	04 28.7	+18 01	9*9FF	1	
	154480	04 28.7	+18 01	9*9FF	1	
	641025	04 28.8	+17 54	9*9F		
	648862	04 28.8	+17 54	9*9F		
	152117	04 29.1	+18 10	9*9FF	1	
	154466	04 29.1	+18 10	9*9FF	1	
	743689	04 29.2	+18 03	9*9F		
	745653	04 29.2	+18 03	9*9F		
	733701	04 29.3	+17 55	9*9F		
	179961	04 29.3	+17 55	9*9FF	1	
	157608	04 29.7	+24 18	9*9FF	1	
	160743	04 29.7	+24 18	9*9FF	1	
	152702	04 30.4	+22 37	9*9F	1	
	157799	04 30.4	+22 37	9*9F	1	
MRSL 155+02/1	217772	04 36.5	+50 15	9*9F		
MRSL 155+02/1	220519	04 36.5	+50 15	9*9F		
	218363	04 37.5	+50 15	9*9F		
	220902	04 37.5	+50 15	9*9F		
	157222	04 38.4	+25 40	9*9FF	1	
	160352	04 38.4	+25 40	9*9FF	1	
	157206	04 38.7	+25 34	9*9FF	1	
	159951	04 38.7	+25 34	9*9FF	1	
CRL 618	179548	04 39.6	+40 01	3*1S	1	BADGAIN
CRL 618	182292	04 39.6	+40 01	3*1S	1	BADGAIN
NGC 1672	593952	04 44.9	-37 35	9*9FF		
NGC 1672	602378	04 44.9	-37 35	9*9FF		
B 026	223265	04 51.5	+30 30	9*9F		
B 026	259135	04 51.5	+30 30	9*9F		
B 026	261295	04 51.5	+30 30	9*9F		
	185434	04 52.1	+30 33	9*9F	1	
	190726	04 52.1	+30 33	9*9F	1	
	183150	04 52.2	-69 27	9*9FF	1	
	191174	04 52.2	-69 27	9*9FF	1	
AB AUR	179162	04 52.6	+30 28	9*9F	1	
AB AUR	181906	04 52.6	+30 28	9*9F	1	
B 028	225623	04 52.6	+30 34	9*9F		
B 028	258939	04 52.6	+30 34	9*9F		
B 028	262082	04 52.6	+30 34	9*9F		
SU AUR	196021	04 52.8	+30 29	9*9F		
SU AUR	199159	04 52.8	+30 29	9*9F		
NGC 1705	160788	04 53.1	-53 27	9*9FF	1	
NGC 1705	164532	04 53.1	-53 27	9*9FF	1	
SG 2.014	217384	04 54.8	+47 53	9*9F		
SG 2.014	219342	04 54.8	+47 53	9*9F		
	181580	04 56.7	-66 29	9*9FF	1	
	184512	04 56.7	-66 29	9*9FF	1	
SCHO 0093	196220	05 00.9	+32 39	9*9F		
SCHO 0093	198766	05 00.9	+32 39	9*9F		
A 7	194481	05 00.9	-15 40	9*9F		
NGC 1784	666478	05 03.1	-11 56	9*9FF		
NGC 1784	759738	05 03.1	-11 56	9*9FF		
NGC 1808	179211	05 06.0	-37 35	9*9FF	1	
NGC 1808	181956	05 06.0	-37 35	9*9FF	1	
ZWG 283.004	217183	05 09.6	+62 31	9*9FF		
ZWG 283.004	219913	05 09.6	+62 31	9*9FF		
NGC 1832	748764	05 09.8	-15 45	9*9F		
NGC 1832	751506	05 09.8	-15 45	9*9F		
	150184	05 10.1	-33 02	9*9FF	1	
	156655	05 10.1	-33 02	9*9FF	1	
	159603	05 10.1	-33 02	9*9FF	1	
	190193	05 10.1	-68 57	9*9FF	1	
	192937	05 10.1	-68 57	9*9FF	1	
	192073	05 12.1	+81 09	3*3SS	1	
	206585	05 12.1	+81 10	3*3SS		
	153532	05 18.4	-45 50	9*9F	1	
	153726	05 18.4	-45 50	9*9F	1	
	183539	05 22.1	-67 60	9*9FF	1	
	188430	05 22.1	-67 60	9*9FF	1	
	184113	05 23.2	-68 05	9*9FF	1	
	189602	05 23.2	-68 05	9*9FF	1	
	783407	05 24.0	-69 45	9*9F		
	784975	05 24.0	-69 45	9*9F		
LH120-N132	283885	05 25.5	-69 41	3*3S		
LH120-N132	286041	05 25.5	-69 41	3*3S		
LH120-N049	456367	05 25.9	-66 08	3*3S		
LH120-N049	465776	05 25.9	-66 08	3*3S		
NGC 1964	710358	05 31.2	-21 59	9*9F		
NGC 1964	729560	05 31.2	-21 59	9*9F		
NGC 1964	765221	05 31.2	-21 59	9*9F		
	182954	05 32.1	-71 06	9*9FF	1	
	189227	05 32.1	-71 06	9*9FF	1	
	183133	05 32.5	-67 43	9*9FF	1	
	187448	05 32.5	-67 43	9*9FF	1	
	241550	05 32.7	-71 03	3*3SS		
	247047	05 32.7	-71 03	3*3SS		
ST 38	194285	05 32.8	-05 26	9*9F		BADGAIN
ST 38	218972	05 32.8	-05 26	9*9F		BADGAIN
ST 38	238389	05 32.8	-05 26	9*9F		BADGAIN
SCHO 0136	278962	05 32.8	-05 34	9*9F		BADGAIN
	194087	05 32.8	-05 35	9*9F	1	BADGAIN
THE2 ORI	195267	05 32.9	-05 27	3*1S		BADGAIN
THE2 ORI	222302	05 32.9	-05 27	3*1S		BADGAIN
THE2 ORI	224851	05 32.9	-05 27	3*1S		BADGAIN
THE2 ORI	279145	05 32.9	-05 27	3*1S		BADGAIN
	222699	05 33.0	-05 12	9*9FF		BADGAIN
	237097	05 33.0	-05 12	9*9FF		BADGAIN
	187947	05 35.5	-67 36	9*9FF	1	
	189209	05 35.5	-67 36	9*9FF	1	

LH120-N063	455975	05 35.7	-66 04	3*3S		
LH120-N063	466558	05 35.7	-66 04	3*3S		
MN 43	735049	05 35.9	-07 12	9*9FF		
	189994	05 36.1	-69 15	9*9FF	1	
	192738	05 36.1	-69 15	9*9FF	1	
NGC 1961	304978	05 36.6	+69 21	9*9F		
NGC 1961	327909	05 36.6	+69 21	9*9F		
NGC 1961	240686	05 36.6	+69 21	9*9FF		
NGC 1961	278131	05 36.6	+69 21	9*9FF		
	794243	05 37.3	+23 49	9*9F		
	797180	05 37.3	+23 49	9*9F		
	190923	05 37.4	+23 51	9*9FF	1	
	192883	05 37.4	+23 51	9*9FF	1	
MRSL 173+02/3	225222	05 37.5	+35 40	9*9F		BADGAIN
MRSL 173+02/3	259329	05 37.5	+35 40	9*9F		BADGAIN
MRSL 173+02/3	266777	05 37.5	+35 40	9*9F		BADGAIN
LBN 0837	784444	05 38.0	+20 20	9*9F		
	680190	05 38.4	-08 09	9*9FF		
	718590	05 38.4	-08 09	9*9FF		
"	189798	05 39.1	-69 07	9*9FF	1	BADGAIN
	192542	05 39.1	-69 07	9*9FF	1	BADGAIN
IC 0434	225441	05 39.2	-01 57	9*9FF		BADGAIN
IC 0434	277394	05 39.2	-01 57	9*9FF		BADGAIN
IC 0434	278765	05 39.2	-01 57	9*9FF		BADGAIN
	185486	05 39.6	-69 31	9*9FF	1	
	190974	05 39.6	-69 31	9*9FF	1	
LH120-N158	241745	05 39.8	-69 37	9*9F		BADGAIN
LH120-N158	243706	05 39.8	-69 37	9*9F		BADGAIN
LH120-N160	197835	05 40.2	-69 40	9*9FF		BADGAIN
LH120-N160	193915	05 40.2	-69 40	9*9FF	1	BADGAIN
LH120-N159	195287	05 40.4	-69 46	9*9FF		BADGAIN
LH120-N159	198627	05 40.4	-69 46	9*9FF		BADGAIN
	236066	05 40.5	-69 46	9*9F		BADGAIN
"	238021	05 40.5	-69 46	9*9F		BADGAIN
	225245	05 43.8	-00 13	9*9F		
	254452	05 43.8	-00 13	9*9F		
"	279154	05 43.8	-00 13	9*9F		
	219007	05 47.6	-69 43	3*3SS		
	211951	05 47.6	-69 43	3*3SS		BADGAIN
2ZW 040	759165	05 53.1	+03 23	9*9F		
2ZW 040	767394	05 53.1	+03 23	9*9F		
	187247	05 57.9	-52 28	9*9F	1	
	188229	05 57.9	-52 28	9*9F	1	
	207059	05 58.8	-75 40	3*3SS		
	209407	05 58.8	-75 40	3*3SS		
ACK 243-25.1	199986	06 00.4	-37 25	3*3SS		
ACK 243-25.1	218606	06 00.4	-37 25	3*3SS		
	239161	06 04.5	+19 28	9*9FF		
	264823	06 04.5	+19 28	9*9FF		
	279930	06 04.5	+19 28	9*9FF		
	215426	06 05.6	+20 31	9*9FF		BADGAIN
	240726	06 05.6	+20 31	9*9FF		BADGAIN
SG 3.250	275020	06 05.6	+20 40	9*9FF		
SG 3.250	288738	06 05.6	+20 40	9*9FF		
	209715	06 10.8	+78 22	9*9F		
	211871	06 10.8	+78 22	9*9F		

NGC 2146	221865	06 10.8	+78 22	9*9FF		
NGC 2146	222658	06 10.8	+78 22	9*9FF		
NGC 2146	223825	06 10.8	+78 22	9*9FF		
NGC 2146	224805	06 10.8	+78 22	9*9FF		
	805600	06 11.0	+12 23	9*9F		
	808343	06 11.0	+12 23	9*9F		
	234439	06 13.8	+22 15	9*9FF		
	237183	06 13.8	+22 15	9*9FF		
NGC 2207	784222	06 14.2	-21 21	9*9F		
NGC 2207	797936	06 14.2	-21 21	9*9F		
	248164	06 14.3	+22 10	9*9FF		
	262665	06 14.3	+22 10	9*9FF		
	278347	06 14.3	+22 10	9*9FF		
	240123	06 14.3	+22 28	9*9FF		
	278149	06 14.3	+22 28	9*9FF		
	250318	06 14.7	+22 24	9*9FF		
	280894	06 14.7	+22 24	9*9FF		
	242673	06 15.0	+22 15	9*9FF		
	281090	06 15.0	+22 15	9*9FF		
HD 44179	224868	06 17.6	-10 37	3*1S		
HD 44179	279947	06 17.6	-10 37	3*1S		
HD 44179	303849	06 17.6	-10 37	9*9F		
HD 44179	326393	06 17.6	-10 37	9*9F		
ACK 247-21.1	223900	06 23.8	-39 50	3*3SS		
ACK 247-21.1	226644	06 23.8	-39 50	3*3SS		
PK 233-16.1	235653	06 25.0	-25 21	3*3SS		
PK 233-16.1	243879	06 25.0	-25 21	3*3SS		
HH 39	233860	06 36.2	+08 54	9*9F		
HH 39	239349	06 36.2	+08 54	9*9F		
SG 3.087	240926	06 36.4	+08 47	9*9F		
SG 3.087	244838	06 36.4	+08 47	9*9F		
SG 3.091	251107	06 38.4	+09 32	9*9FF		
SG 3.091	256595	06 38.4	+09 32	9*9FF		
MCG-06-15-018	303672	06 39.9	-34 42	9*9F		
	259383	06 40.4	-50 55	9*9FF		
	262713	06 40.4	-50 55	9*9FF		
GRA A	237436	06 44.4	-74 11	9*9F		
GRA A	239792	06 44.4	-74 11	9*9F		
MR6 + S308	282296	06 52.1	-23 52	3*1SS		
MR6 + S308	744061	06 52.1	-23 52	9*9F		
MR6 + S308	746216	06 52.1	-23 52	9*9F		
	250707	06 52.2	+39 09	9*9FF		
UGC 3600	242481	06 52.2	+39 09	9*9FF		
UGC 3600	245221	06 52.2	+39 09	9*9FF		
PK 242-11.1	274660	07 00.9	-31 31	3*3SS		
PK 242-11.1	276616	07 00.9	-31 31	3*3SS		
VDB.66N 092	367751	07 01.6	-11 27	9*9F		
NGC 2339	758973	07 05.4	+18 52	9*9F		
NGC 2339	759757	07 05.4	+18 52	9*9F		
	299138	07 06.8	-00 43	9*9F		
	328149	07 06.8	-00 43	9*9F		
	271724	07 07.9	-36 07	9*9FF		
	275844	07 07.9	-36 07	9*9FF		
	278486	07 07.9	-36 07	9*9FF		
	281330	07 07.9	-36 07	9*9FF		
NGC 2276	761557	07 10.5	+85 51	9*9F		

NGC 2276	781153	07 10.5	+85 51	9*9F		
	363068	07 12.8	-48 23	9*9FF		
	365812	07 12.8	-48 23	9*9FF		
	368358	07 12.8	-48 23	9*9FF		
	371102	07 12.8	-48 23	9*9FF		
	288384	07 14.5	-43 52	9*9FF		
	290740	07 14.5	-43 52	9*9FF		
	292704	07 14.5	-43 52	9*9FF		
	302503	07 14.5	-43 52	9*9FF		
	218340	07 16.0	+76 00	9*9F		
	220496	07 16.0	+76 00	9*9F		
NGC 2369	785765	07 16.1	-62 15	9*9F		
NGC 2369	791255	07 16.1	-62 15	9*9F		
MR7+NGC2359	301896	07 16.2	-13 08	9*9F		
MR7+NGC2359	326005	07 16.2	-13 08	9*9F		
CD-44 3318	294272	07 17.8	-44 29	9*9FF		
CD-44 3318	316813	07 17.8	-44 29	9*9FF		
CD-44 3318	362870	07 17.8	-44 29	9*9FF		
CD-44 3318	365614	07 17.8	-44 29	9*9FF		
CD-44 3318	363263	07 17.9	-44 30	3*3S		
CD-44 3318	366006	07 17.9	-44 30	3*3S		
NGC 2336	261858	07 18.5	+80 17	9*9FF		
NGC 2336	270081	07 18.5	+80 17	9*9FF		
	313280	07 18.6	-44 32	9*9FF		
	316024	07 18.6	-44 32	9*9FF		
	218536	07 19.0	+75 49	9*9F		
	220698	07 19.0	+75 49	9*9F		
VY CMA	282494	07 20.9	-25 40	3*3SS		BADGAIN
VY CMA	297982	07 20.9	-25 40	3*3SS		BADGAIN
VY CMA	298373	07 20.9	-25 40	9*9F		
VY CMA	300725	07 20.9	-25 40	9*9F		
VY CMA	770707	07 20.9	-25 40	9*9F		
VY CMA	776194	07 20.9	-25 40	9*9F		
	218732	07 21.0	+75 50	9*9F		
	221280	07 21.0	+75 50	9*9F		
IC 0467	259308	07 21.9	+79 58	9*9FF		
IC 0467	279489	07 21.9	+79 58	9*9FF		
NGC 2377	819893	07 22.6	-09 34	9*9F		
NGC 2377	827723	07 22.6	-09 34	9*9F		
	287009	07 22.9	-24 25	9*9FF		
	328169	07 22.9	-24 25	9*9FF		
NGC 2366	228733	07 23.6	+69 19	9*9FF		
NGC 2366	231482	07 23.6	+69 19	9*9FF		
UGC 3860	256396	07 24.8	+40 52	9*9FF		
UGC 3860	286578	07 24.8	+40 52	9*9FF		
	218931	07 25.0	+75 51	9*9F		
	221084	07 25.0	+75 51	9*9F		
NGC 2392	291290	07 26.2	+21 01	3*3SS		
NGC 2392	758389	07 26.2	+21 01	9*9F		
NGC 2392	761132	07 26.2	+21 01	9*9F		
	395994	07 26.3	-50 58	9*9FF		
	434404	07 26.3	-50 58	9*9FF		
	339340	07 27.9	-41 04	9*9FF		
	173685	07 27.9	-41 04	9*9FF		
	176849	07 27.9	-41 04	9*9FF		
LBN 1041	301424	07 28.0	-18 27	9*9FF		

LBN 1043	328936	07	28.0	-18	27	9*9FF
	225985	07	29.0	+75	33	3*3SS
	239705	07	29.0	+75	33	3*3SS
	368556	07	29.3	-46	53	9*9FF
	371300	07	29.3	-46	53	9*9FF
	374044	07	29.3	-46	53	9*9FF
	393053	07	29.3	-46	53	9*9FF
	331303	07	29.7	-46	40	9*9FF
	333275	07	29.7	-46	40	9*9FF
	398737	07	31.0	-50	39	9*9FF
	401284	07	31.0	-50	39	9*9FF
	406572	07	31.0	-50	39	9*9FF
	410880	07	31.0	-50	39	9*9FF
NGC 2403	239905	07	32.1	+65	43	9*9FF
NGC 2403	242844	07	32.1	+65	43	9*9FF
	393443	07	32.6	-46	50	9*9FF
	395796	07	32.6	-46	50	9*9FF
NGC 2415	829120	07	33.7	+35	21	9*9F
NGC 2415	848712	07	33.7	+35	21	9*9F
NGC 2427	398540	07	35.0	-47	31	9*9FF
NGC 2427	401083	07	35.0	-47	31	9*9FF
NGC 2427	404224	07	35.0	-47	31	9*9FF
	406968	07	37.3	-49	44	9*9FF
	409516	07	37.3	-49	44	9*9FF
	412060	07	37.3	-49	44	9*9FF
	406381	07	37.9	-47	46	9*9FF
	439889	07	37.9	-47	46	9*9FF
UGC 3966	289323	07	38.0	+40	14	9*9FF
UGC 3966	294615	07	38.0	+40	14	9*9FF
	349546	07	38.5	-47	48	9*9FF
	352290	07	38.5	-47	48	9*9FF
UGC 3974	281293	07	39.1	+16	55	9*9FF
UGC 3974	284037	07	39.1	+16	55	9*9FF
	387565	07	39.2	-41	19	9*9FF
	390108	07	39.2	-41	19	9*9FF
	368750	07	39.2	-43	41	9*9FF
	393250	07	39.2	-43	41	9*9FF
PK 231+04.2	301104	07	40.0	-14	36	9*9F
PK 231+04.2	303652	07	40.0	-14	36	9*9F
PK 231+04.2	328545	07	40.0	-14	36	9*9FF
PK 231+04.2	363837	07	40.0	-14	36	9*9FF
	329144	07	40.0	-41	23	9*9FF
	331104	07	40.0	-41	23	9*9FF
	333655	07	40.0	-43	45	9*9FF
	336993	07	40.0	-43	45	9*9FF
	387956	07	40.9	-41	57	9*9FF
	390699	07	40.9	-41	57	9*9FF
	387762	07	41.1	-41	08	9*9FF
	390506	07	41.1	-41	08	9*9FF
	408342	07	41.6	-49	07	9*9FF
	410306	07	41.6	-49	07	9*9FF
	412259	07	41.6	-49	07	9*9FF
	415003	07	41.6	-49	07	9*9FF
	331496	07	41.7	-42	01	9*9FF
	334245	07	41.7	-42	01	9*9FF
	330712	07	41.9	-41	12	9*9FF
	333851	07	41.9	-41	12	9*9FF
	409712	07	42.3	-48	58	9*9FF
	412648	07	42.3	-48	58	9*9FF
NGC 2445	283242	07	43.5	+39	09	9*9F
NGC 2445	283630	07	43.5	+39	09	9*9F
A 24	300901	07	49.0	-03	08	9*9F
A 24	303450	07	49.0	-03	08	9*9F
	374425	07	50.0	-33	08	9*9FF
	415391	07	50.0	-33	08	9*9FF
	361685	07	51.7	-50	09	9*9FF
	416964	07	51.7	-50	09	9*9FF
	420491	07	51.7	-50	09	9*9FF
	422453	07	51.7	-50	09	9*9FF
PK 164+31.1	255789	07	54.0	+53	33	9*9F
PK 164+31.1	258533	07	54.0	+53	33	9*9F
UGC 4115	296971	07	54.2	+14	31	9*9FF
UGC 4115	363413	07	54.2	+14	31	9*9FF
	369908	07	56.2	-33	10	9*9FF
	378731	07	56.2	-33	10	9*9FF
	384219	07	56.3	-35	56	9*9FF
	387364	07	56.3	-35	56	9*9FF
VHE 01	375606	07	59.1	-45	19	9*9FF
VHE 01	415784	07	59.1	-45	19	9*9FF
	383827	08	04.3	-33	45	9*9FF
	357966	08	06.5	-35	53	9*9FF
	363449	08	06.5	-35	53	9*9FF
NGC 2532	379870	08	07.1	+34	06	9*9F
DG 123	366194	08	10.5	-32	56	9*9FF
DG 123	368938	08	10.5	-32	56	9*9FF
	241469	08	13.7	+70	52	9*9FF
	254408	08	13.7	+70	52	9*9FF
VHE 10	420687	08	15.5	-42	05	9*9FF
VHE 10	423430	08	15.5	-42	05	9*9FF
VHE 10	443218	08	15.5	-42	05	9*9FF
VHE 11	423234	08	16.3	-41	57	9*9FF
NGC 2566	784421	08	16.6	-25	21	9*9F
NGC 2566	806167	08	16.6	-25	21	9*9F
KARA.68 052	247950	08	18.0	+71	12	9*9FF
KARA.68 052	250877	08	18.0	+71	12	9*9FF
VHE 128	418927	08	18.5	-49	58	9*9FF
	450671	08	18.7	-62	16	9*9FF
	455777	08	18.7	-62	16	9*9FF
	414218	08	19.6	-49	26	9*9F
	416574	08	19.6	-49	26	9*9F
	443421	08	19.6	-49	28	9*9F
	446159	08	19.6	-49	28	9*9F
	448122	08	19.6	-49	28	9*9F
	367955	08	19.6	-49	30	9*9FF
	369924	08	19.6	-49	30	9*9FF
	414023	08	19.6	-49	34	9*9F
	416180	08	19.6	-49	34	9*9F
	418531	08	19.8	-49	28	9*9FF
	422258	08	19.8	-49	28	9*9FF
	437935	08	19.8	-49	28	9*9FF
	454786	08	19.8	-49	28	9*9FF
VHE 144 + B	417547	08	20.6	-40	16	9*9FF
VHE 144 + B	420879	08	20.6	-40	16	9*9FF
	377768	08	24.3	-50	50	9*9FF
	379725	08	24.3	-50	50	9*9FF
	419124	08	24.3	-50	53	9*9FF
	421867	08	24.3	-50	53	9*9FF
	435977	08	24.3	-50	53	9*9FF
	460869	08	24.3	-50	53	9*9FF
	422062	08	25.0	-50	30	9*9FF
UGC 4426	299906	08	25.1	+42	01	9*9FF
UGC 4426	354774	08	25.1	+42	01	9*9FF
	460084	08	25.1	-50	51	9*9FF
	462236	08	25.1	-50	51	9*9FF
VHE 16	419711	08	26.1	-51	01	9*9FF
VHE 16	460670	08	26.1	-51	01	9*9FF
VHE 16	463809	08	26.1	-51	01	9*9FF
VHE 16	466747	08	26.1	-51	01	9*9FF
VHE 16	419516	08	26.2	-50	59	9*9FF
VHE 16	421672	08	26.2	-50	59	9*9FF
	408919	08	26.8	-33	35	9*9F
	413038	08	26.8	-33	35	9*9F
NGC 2613	369316	08	31.2	-22	48	9*9FF
NGC 2613	408713	08	31.2	-22	48	9*9FF
	465954	08	32.7	-50	07	9*9FF
	469095	08	32.7	-50	07	9*9FF
VELA X	372662	08	33.7	-45	00	9*9F
VELA X	375411	08	33.7	-45	00	9*9F
NGC 2623	792478	08	35.4	+25	56	9*9F
NGC 2623	794048	08	35.4	+25	56	9*9F
VHE 19	385796	08	35.6	-47	01	9*9FF
	408142	08	37.5	-40	58	9*9FF
PK 158+37.1	286559	08	37.7	+58	24	9*9F
PK 158+37.1	288717	08	37.7	+58	24	9*9F
PK 244+12.1	342073	08	38.0	-20	43	9*9F
PK 244+12.1	407347	08	38.0	-20	43	9*9F
UGC 4527	240289	08	38.2	+77	06	9*9FF
UGC 4527	259115	08	38.2	+77	06	9*9FF
	440080	08	39.2	-41	25	9*9FF
	442632	08	40.5	-42	42	9*9FF
NGC 2633	264407	08	42.6	+74	17	9*9FF
NGC 2633	308115	08	42.6	+74	17	9*9FF
	442823	08	42.7	-41	59	9*9FF
CED 106N	441261	08	42.8	-41	07	9*9FF BADGAIN
NGC 2663	369517	08	43.1	-33	37	3*3SS
NGC 2663	380101	08	43.1	-33	37	3*3SS
	447147	08	43.1	-59	43	9*9FF
	449696	08	43.1	-59	43	9*9FF
	441456	08	43.5	-40	57	9*9FF
NGC 2646	253627	08	45.0	+73	39	9*9FF
NGC 2646	258918	08	45.0	+73	39	9*9FF
VHE 218	452427	08	45.4	-43	32	9*9FF
	455374	08	47.2	-60	00	9*9FF
	457341	08	47.2	-60	00	9*9FF
VHE 220 + E	471844	08	49.0	-48	55	9*9FF
NGC 2655	238916	08	49.1	+78	25	9*9FF
NGC 2655	241660	08	49.1	+78	25	9*9FF
NGC 2684	195939	08	51.6	+11	16	9*9F

NGC 2683	332832	08 49.6	+33 36	9*9FF		
NGC 2681	298919	08 50.0	+51 30	9*9FF		
NGC 2681	304793	08 50.0	+51 30	9*9FF		
	461488	08 50.5	-44 02	9*9F		
	463410	08 50.5	-44 02	9*9F		
	466936	08 50.5	-44 02	9*9F		
	494963	08 50.8	-44 09	9*9F		
	497116	08 50.8	-44 09	9*9F		
	499859	08 50.8	-44 09	9*9F		
VHE 22A + B	410100	08 51.0	-48 34	9*9FF		
VHE 22A + B	416768	08 51.0	-48 34	9*9FF		
	462822	08 51.1	-44 02	9*9F		
	469679	08 51.1	-44 02	9*9F		
	467133	08 51.1	-44 02	9*9F	BADGAIN	
	464192	08 51.2	-42 30	9*9F		
	467327	08 51.2	-42 30	9*9F		
	469877	08 51.2	-42 30	9*9F		
	470070	08 51.5	-42 50	9*9F		
	472423	08 51.5	-42 50	9*9F		
	464390	08 51.5	-42 50	9*9F	BADGAIN	
NGC 2685	291269	08 51.7	+58 55	9*9FF		
NGC 2685	300084	08 51.7	+58 55	9*9FF		
	472620	08 51.8	-42 05	9*9F		
	475167	08 51.8	-42 05	9*9F		
	477910	08 51.8	-42 05	9*9F		
	465564	08 51.9	-43 02	9*9F		
	472814	08 51.9	-43 02	9*9F		
	475364	08 51.9	-43 02	9*9F		
	450086	08 52.2	-41 34	9*9FF		
VHE 24	386580	08 53.3	-43 16	9*9FF		
VHE 24	454390	08 53.3	-43 16	9*9FF		
NGC 2693	298135	08 53.4	+51 32	9*9FF		
NGC 2693	300879	08 53.4	+51 32	9*9FF		
	465171	08 53.9	-42 48	9*9F		
	475557	08 53.9	-42 48	9*9F		
	486531	08 53.9	-42 48	9*9F		
	452623	08 54.0	-41 53	9*9FF		
VHE 25B	454587	08 54.8	-43 01	9*9FF		
VHE 25B	456539	08 54.8	-43 01	9*9FF		
	464975	08 55.1	-42 16	9*9F		
	478301	08 55.1	-42 16	9*9F		
	480654	08 55.1	-42 16	9*9F		
	537097	08 55.8	-46 47	9*9F		
	471450	08 55.8	-46 47	9*9FF		
VHE 27B	488885	08 55.9	-42 29	9*9F		
VHE 27B	481044	08 55.9	-42 29	9*9F	BADGAIN	
VHE 27B	483787	08 55.9	-42 29	9*9F	BADGAIN	
VHE 27B	490457	08 56.2	-42 30	9*9F	BADGAIN	
VHE 27B	455958	08 56.2	-42 30	9*9FF	BADGAIN	
VHE 27A	490262	08 56.2	-42 38	9*9F		
VHE 27A	454981	08 56.2	-42 38	9*9FF		
VHE 26	548858	08 56.4	-47 11	9*9F	BADGAIN	
VHE 26	548717	08 56.4	-47 11	9*9FF	BADGAIN	
	531936	08 56.5	-42 25	9*9F		
	536112	08 56.5	-42 25	9*9F		
	518660	08 56.5	-42 25	9*9F		
HERBST 28	885692	08 56.6	-43 14	9*9F		
HERBST 28	888043	08 56.6	-43 14	9*9F		
VHE 28	483397	08 56.6	-43 14	9*9F		
VHE 28	458115	08 56.6	-43 14	9*9FF		
	491628	08 56.7	-43 34	9*9F		
	493588	08 56.7	-43 34	9*9F		
	489082	08 56.7	-43 34	9*9F	BADGAIN	
	489274	08 56.8	-43 35	9*9F	BADGAIN	
	491825	08 56.8	-43 35	9*9F	BADGAIN	
	494372	08 56.8	-43 35	9*9F	BADGAIN	
	453799	08 57.0	-42 34	9*9FF		
	456350	08 57.0	-42 34	9*9FF		
	492018	08 57.0	-43 04	9*9F		
	494569	08 57.0	-43 04	9*9F		
	496527	08 57.0	-43 04	9*9F		
MRSL 267-01/1	459283	08 57.3	-43 31	9*9FF	BADGAIN	
MRSL 267-01/3	406772	08 57.4	-47 19	9*9FF	BADGAIN	
MRSL 267-01/3	408730	08 57.4	-47 19	9*9FF	BADGAIN	
MRSL 265-01/1	492608	08 57.7	-43 35	9*9F	BADGAIN	
MRSL 265-01/1	495942	08 57.7	-43 35	9*9F	BADGAIN	
MRSL 265-01/1	498287	08 57.7	-43 35	9*9F	BADGAIN	
	483595	08 59.6	-44 24	9*9F		
	463213	08 59.6	-44 24	9*9FF		
	490066	09 00.2	-45 26	9*9F		
	470665	09 00.2	-45 26	9*9FF		
0900-40	381676	09 00.3	-40 23	3*1S		
0900-40	383636	09 00.3	-40 23	3*1S		
0900-40	388346	09 00.3	-40 23	3*1S		
0900-40	411467	09 00.3	-40 23	3*1S		
	442239	09 00.5	-44 38	9*9FF		
	448196	09 00.5	-44 38	9*9FF		
NGC 2715	241856	09 01.8	+78 17	9*9FF		
NGC 2715	245388	09 01.8	+78 17	9*9FF		
MRSL 269-01/2	401480	09 01.8	-48 14	9*9FF	BADGAIN	
MRSL 269-01/2	404417	09 01.8	-48 14	9*9FF	BADGAIN	
MRSL 269-01/2	437740	09 01.8	-48 14	9*9FF	BADGAIN	
	496733	09 02.9	-52 35	9*9FF		
	499477	09 02.9	-52 35	9*9FF		
	502220	09 02.9	-52 35	9*9FF		
	504172	09 02.9	-52 35	9*9FF		
	488106	09 07.0	-48 54	9*9FF		
	487325	09 07.8	-48 12	9*9FF		
NGC 2782	761535	09 10.9	+40 19	9*9F		
NGC 2782	772903	09 10.9	+40 19	9*9F		
NGC 2798	767416	09 14.1	+42 13	9*9F		
NGC 2798	768006	09 14.1	+42 13	9*9F		
	319105	09 14.2	+42 12	3*3SS		
	351642	09 14.2	+42 12	3*3SS		
MRSL 270+00/1	449106	09 15.0	-47 44	9*9FF	BADGAIN	
NGC 2832	357525	09 16.8	+33 57	9*9FF		
NGC 2832	389869	09 16.8	+33 57	9*9FF		
NGC 2832	404174	09 16.8	+33 57	9*9FF		
	442418	09 16.8	-46 06	9*9FF		
	444189	09 16.8	-46 06	9*9FF		
VHE 10	408[illegible]	09 16.9	-48 11	9*9FF		
VHE 10	4[illegible]	09 16.9	-48 11	9*9FF		
	465368	09 16.9	-48 15	9*9F		
	467723	09 16.9	-48 15	9*9F		
	480851	09 16.9	-48 15	9*9F		
NGC 2841	299116	09 18.6	+51 11	9*9FF		
NGC 2841	313215	09 18.6	+51 11	9*9FF		
VHE 31A	438326	09 21.5	-48 00	9*9FF		
VHE 31A	440674	09 21.5	-48 00	9*9FF		
	489300	09 24.4	-44 59	9*9FF		
	502989	09 25.5	-50 57	9*9FF		
PK 277-03.1	462628	09 25.5	-55 54	9*9F		
PK 277-03.1	489870	09 25.5	-55 54	9*9F		
NGC 2915	199417	09 26.5	-76 25	9*9FF		
NGC 2915	206080	09 26.5	-76 25	9*9FF		
	504960	09 27.0	-51 23	9*9FF		
NGC 2903	837933	09 29.3	+21 43	9*9F		
NGC 2903	840676	09 29.3	+21 43	9*9F		
A 33	382827	09 36.6	-02 35	9*9F		
	500636	09 39.4	-48 59	9*9FF		
	505343	09 39.4	-48 59	9*9FF		
	507887	09 39.4	-48 59	9*9FF		
NGC 2964	773482	09 40.0	+32 04	9*9F		
NGC 2964	785434	09 40.0	+32 04	9*9F		
NGC 2976	281071	09 43.2	+68 09	9*9FF		
NGC 2976	305758	09 43.2	+68 09	9*9FF		
A 34	383617	09 43.2	-12 56	9*9F		
NGC 2993	871998	09 43.4	-14 08	9*9F		
NGC 2993	888064	09 43.4	-14 08	9*9F		
NGC 2997	409114	09 43.5	-30 58	9*9FF		
NGC 2997	411858	09 43.5	-30 58	9*9FF		
IRC+10216	863004	09 45.3	+13 31	9*9F		
IRC+10216	865746	09 45.3	+13 31	9*9F		
	505156	09 48.9	-51 30	9*9FF		
NGC 3044	839094	09 51.1	+01 49	9*9F		
NGC 3044	850067	09 51.1	+01 49	9*9F		
NGC 3031	280876	09 51.5	+69 18	9*9FF		
NGC 3031	283608	09 51.5	+69 18	9*9FF		
NGC 3034	446480	09 51.7	+69 55	9*9F		
NGC 3034	446874	09 51.7	+69 55	9*9F		
NGC 3034	304189	09 51.7	+69 55	9*9FF		
NGC 3034	308501	09 51.7	+69 55	9*9FF		
UGC 5364	368701	09 56.5	+30 59	9*9FF		
UGC 5364	387511	09 56.5	+30 59	9*9FF		
NGC 3095	886288	09 57.9	-31 19	9*9F		
NGC 3095	888247	09 57.9	-31 19	9*9F		
NGC 3079	812199	09 58.6	+55 55	9*9F		
NGC 3079	756060	09 58.6	+55 55	9*9F		
NGC 3079	769774	09 58.6	+55 55	9*9F		
NGC 3077	305365	09 59.4	+68 58	9*9FF		
NGC 3077	373965	09 59.4	+68 58	9*9FF		
	556699	10 00.4	-57 26	9*9FF		BADGAIN
VHE 32A	542185	10 00.4	-57 26	9*9FF		BADGAIN
VHE 32A	558867	10 00.4	-57 26	9*9FF		BADGAIN
NGC 3109	444780	10 00.8	-25 55	9*9FF		
NGC 3109	447524	10 00.8	-25 55	9*9FF		
VHE 33D	511195	10 01.2	-54 02	9*9FF		
VHE 33D	516528	10 01.2	-54 02	9*9FF		

L-5

NGC 3115	886698	10 02.7	-07 28	9*9F		
	483209	10 04.9	-56 58	9*9FF	BADGAIN	
	492408	10 04.9	-56 58	9*9FF	BADGAIN	
NGC 3175	863768	10 12.4	-28 37	9*9F		
NGC 3175	866510	10 12.4	-28 37	9*9F		
NGC 3175	886484	10 12.4	-28 37	9*9F		
NGC 3147	278902	10 12.7	+73 39	9*9FF		
NGC 3147	281646	10 12.7	+73 39	9*9FF		
NGC 3177	825982	10 13.8	+21 22	9*9F		
NGC 3177	826762	10 13.8	+21 22	9*9F		
VHE 34	524758	10 14.0	-60 03	9*9FF		
VHE 34	580806	10 14.0	-60 03	9*9FF		
WR18+NGC3199	496139	10 15.2	-57 40	9*9F	BADGAIN	
WR18+NGC3199	500056	10 15.2	-57 40	9*9F	BADGAIN	
VHE 35	510451	10 16.6	-60 39	9*9FF		
VHE 35	558072	10 16.6	-60 39	9*9FF		
NGC 3198	340657	10 16.9	+45 48	9*9FF		
NGC 3198	371237	10 16.9	+45 48	9*9FF		
	495354	10 19.8	-57 51	9*9FF	BADGAIN	
	497906	10 19.8	-57 51	9*9FF	BADGAIN	
	555523	10 20.6	-58 53	9*9FF		
	565896	10 20.6	-58 53	9*9FF	BADGAIN	
NGC 3226	818733	10 20.7	+20 08	9*9F		
NGC 3226	821476	10 20.7	+20 08	9*9F		
WRAY 19.22	527292	10 22.3	-57 33	9*9FF	BADGAIN	
WRAY 19.22	551787	10 22.3	-57 33	9*9FF	BADGAIN	
	489674	10 22.4	-57 38	9*9FF	BADGAIN	
	492994	10 22.4	-57 38	9*9FF	BADGAIN	
VHE 36	533575	10 22.5	-57 19	9*9FF	BADGAIN	
VHE 36	543164	10 22.5	-57 19	9*9FF	BADGAIN	
WRAY 19.22	568654	10 22.9	-57 32	9*9FF	BADGAIN	
IC 2574	304776	10 24.7	+68 41	9*9FF		
IC 2574	349668	10 24.7	+68 41	9*9FF		
NGC 3256	862182	10 25.7	-43 39	9*9F		
NGC 3256	885888	10 25.7	-43 39	9*9F		
NGC 3256	492799	10 25.7	-43 39	9*9FF		
NGC 3256	494758	10 25.7	-43 39	9*9FF		
	495551	10 29.5	-57 47	9*9FF	BADGAIN	
	498481	10 29.5	-57 47	9*9FF	BADGAIN	
NGC 3281	886088	10 29.6	-34 36	9*9F		
NGC 3281	886676	10 29.6	-34 36	9*9F		
VHE 39	578442	10 31.6	-59 25	9*9FF	BADGAIN	
VHE 39	581776	10 31.6	-59 25	9*9FF	BADGAIN	
VHE 38	518877	10 31.9	-61 27	9*9FF		
	539649	10 32.4	-64 37	9*9F		
	545724	10 32.4	-64 37	9*9F		
	554344	10 32.4	-64 37	9*9F		
	531211	10 32.4	-64 37	9*9FF		
	549436	10 32.4	-64 37	9*9FF		
	552180	10 32.4	-64 37	9*9FF		
	559053	10 32.4	-64 37	9*9FF		
	498686	10 32.5	-58 30	9*9FF		
	500652	10 32.5	-58 30	9*9FF	BADGAIN	
	519448	10 32.6	-46 21	9*9FF		
	524149	10 32.6	-46 21	9*9FF		
VHE 408	621169	10 33.9	-58 59	9*9F	BADGAIN	
VHE 408	581194	10 33.9	-58 59	9*9FF	BADGAIN	
	583151	10 34.1	-64 31	9*9F		
	550221	10 34.1	-64 31	9*9FF		
	573932	10 34.1	-64 31	9*9FF		
	576676	10 34.1	-64 31	9*9FF		
	579419	10 34.1	-64 31	9*9FF		
VHE 40A	619797	10 34.5	-58 42	9*9F	BADGAIN	
VHE 40A	580594	10 34.5	-58 42	9*9FF	BADGAIN	
	571383	10 34.6	-58 02	9*9FF	BADGAIN	
MRSL 285-00/1	579222	10 35.3	-58 38	9*9FF	BADGAIN	
VHE 41B	579629	10 35.4	-58 26	9*9FF	BADGAIN	
NGC 3310	352417	10 35.7	+53 46	9*9F		
NGC 3310	365746	10 35.7	+53 46	9*9F		
NGC 3310	783488	10 35.7	+53 46	9*9F		
VHE 42B	533952	10 35.7	-57 45	9*9FF	BADGAIN	
VHE 42B	544535	10 35.7	-57 45	9*9FF	BADGAIN	
NGC 3319	368889	10 36.2	+41 57	9*9FF		
NGC 3319	371632	10 36.2	+41 57	9*9FF		
WR22+NGC3372	533372	10 39.4	-59 25	9*9F	BADGAIN	
WR22+NGC3372	535329	10 39.4	-59 25	9*9F	BADGAIN	
WR23+ANON	529257	10 39.7	-58 31	9*9F	BADGAIN	
WR23+ANON	531804	10 39.7	-58 31	9*9F	BADGAIN	
NGC 3347	483192	10 40.5	-36 06	9*9FF		
NGC 3347	485936	10 40.5	-36 06	9*9FF		
	506135	10 40.5	-59 20	9*9FF	BADGAIN	
	508882	10 40.5	-59 20	9*9FF	BADGAIN	
NGC 3344	401234	10 40.8	+25 11	9*9FF		
NGC 3344	420835	10 40.8	+25 11	9*9FF		
NGC 3346	414566	10 41.0	+15 08	9*9F		
	506527	10 41.0	-59 24	9*9FF	BADGAIN	
	525343	10 41.0	-59 24	9*9FF	BADGAIN	
	506331	10 41.1	-59 16	9*9FF	BADGAIN	
	525539	10 41.1	-59 16	9*9FF	BADGAIN	
THE CAR	532201	10 41.2	-64 08	3*1S		
THE CAR	534160	10 41.2	-64 08	3*1S		
THE CAR	536699	10 41.2	-64 08	3*1S		
THE CAR	539062	10 41.2	-64 08	3*1S		
NGC 3351	840273	10 41.3	+11 58	9*9F		
NGC 3351	843016	10 41.3	+11 58	9*9F		
HOFFL 06	550811	10 41.4	-60 00	9*9FF	BADGAIN	
HOFFL 06	554531	10 41.4	-60 00	9*9FF	BADGAIN	
HOFFL 06	568639	10 41.4	-60 00	9*9FF	BADGAIN	
HOFFL 06	574126	10 41.4	-60 00	9*9FF	BADGAIN	
	521606	10 41.6	-59 11	9*9FF	BADGAIN	
	524349	10 41.6	-59 11	9*9FF	BADGAIN	
	506921	10 41.6	-59 20	9*9FF	BADGAIN	
	525930	10 41.6	-59 20	9*9FF	BADGAIN	
	507117	10 41.6	-59 28	9*9FF	BADGAIN	
	516133	10 41.6	-59 28	9*9FF	BADGAIN	
VHA 102	579613	10 41.7	-59 19	9*9FF	BADGAIN	
VHA 102	582357	10 41.7	-59 19	9*9FF	BADGAIN	
VHA 102	584124	10 41.7	-59 19	9*9FF	BADGAIN	
	507707	10 42.1	-59 33	9*9FF	BADGAIN	
	515934	10 42.1	-59 33	9*9FF	BADGAIN	
	518672	10 42.2	-59 07	9*9FF	BADGAIN	
	521414	10 42.2	-59 07	9*9FF	BADGAIN	
	524548	10 42.2	-59 16	9*9FF	BADGAIN	
	526516	10 42.2	-59 16	9*9FF	BADGAIN	
	507314	10 42.2	-59 24	9*9FF	BADGAIN	
	524743	10 42.2	-59 24	9*9FF	BADGAIN	
	521999	10 42.7	-59 20	9*9FF		
	519256	10 42.7	-59 20	9*9FF	BADGAIN	
	507903	10 42.7	-59 29	9*9FF	BADGAIN	
	516718	10 42.7	-59 29	9*9FF	BADGAIN	
	513769	10 42.8	-59 12	9*9FF	BADGAIN	
	516512	10 42.8	-59 12	9*9FF	BADGAIN	
ETA CAR	508090	10 43.1	-59 25	9*9F	BADGAIN	
ETA CAR	510833	10 43.1	-59 25	9*9F	BADGAIN	
	513574	10 43.3	-59 16	9*9FF	BADGAIN	
	516317	10 43.3	-59 16	9*9FF	BADGAIN	
	521805	10 43.3	-59 24	9*9FF		
	519061	10 43.3	-59 24	9*9FF	BADGAIN	
NGC 3359	324182	10 43.4	+63 29	9*9FF		
	508282	10 43.8	-59 20	9*9FF	BADGAIN	
	511026	10 43.8	-59 20	9*9FF	BADGAIN	
NGC 3368	841840	10 44.1	+12 05	9*9F		
NGC 3368	874167	10 44.1	+12 05	9*9F		
	532979	10 46.0	-58 53	3*3SS	BADGAIN	
	534746	10 46.0	-58 53	3*3SS	BADGAIN	
7ZW 347	327318	10 46.3	+65 48	9*9FF		
7ZW 347	365349	10 46.3	+65 48	9*9FF		
NGC 3396	378100	10 47.1	+33 15	9*9FF		
NGC 3396	409661	10 47.1	+33 15	9*9FF		
	330730	10 49.3	-76 49	9*9FF		
	332690	10 49.3	-76 49	9*9FF		
	123168	10 49.3	-76 49	9*9FF 1		
	125717	10 49.3	-76 49	9*9FF 1		
	131205	10 49.3	-76 49	9*9FF 1		
NGC 3437	826373	10 49.9	+23 12	9*9F		
NGC 3437	827157	10 49.9	+23 12	9*9F		
VHE 44	533559	10 50.1	-55 54	9*9FF		
VHE 44	535910	10 50.1	-55 54	9*9FF		
	586080	10 51.0	-59 30	9*9FF		
	589622	10 51.0	-59 30	9*9FF		
	581965	10 51.7	-59 29	9*9FF	BADGAIN	
	587452	10 51.7	-59 29	9*9FF	BADGAIN	
	590392	10 51.7	-59 29	9*9FF	BADGAIN	
VHE 45A + B	641942	10 54.4	-62 46	9*9F		
VHE 45A + B	592939	10 54.4	-62 46	9*9FF		
	330927	10 55.0	-76 51	9*9FF		
	333670	10 55.0	-76 51	9*9FF		
	123364	10 55.0	-76 51	9*9FF 1		
	131401	10 55.0	-76 51	9*9FF 1		
NGC 3486	401631	10 57.7	+29 15	9*9FF		
NGC 3486	447496	10 57.7	+29 15	9*9FF		
VHE 46	539047	10 59.4	-59 35	9*9FF	BADGAIN	
VHE 46	541399	10 59.4	-59 35	9*9FF	BADGAIN	
NGC 3504	827152	11 00.5	+28 15	9*9F		
NGC 3504	889455	11 00.5	+28 15	9*9F		
	259199	11 02.8	-77 39	9*9F		
	261747	11 02.8	-77 39	9*9F		
	185124	11 04.0	-77 02	9*9FF 1		

	147083	11 03.0	-77 02	9*9FF	1	
	622936	11 03.0	-77 30	9*9FF		
	626658	11 03.0	-77 30	9*9FF		
	630376	11 03.0	-77 30	9*9FF		
	638013	11 03.0	-77 30	9*9FF		
	246461	11 03.1	-77 10	9*9F		
	258023	11 03.1	-77 10	9*9F		
	623916	11 03.3	-77 18	9*9FF		
	630576	11 03.3	-77 18	9*9FF		
	639595	11 03.3	-77 18	9*9FF		
	642724	11 03.3	-77 18	9*9FF		
	260180	11 03.7	-76 50	9*9F		
	263513	11 03.7	-76 50	9*9F		
	243329	11 03.8	-77 22	9*9F		
	246655	11 03.8	-77 22	9*9F		
WR40+NCW58	546696	11 04.3	-65 14	9*9F		
WR40+NCW58	549047	11 04.3	-65 14	9*9F		
	637047	11 04.5	-77 02	9*9FF		
	658201	11 04.5	-77 02	9*9FF		
	660944	11 04.5	-77 02	9*9FF		
	681133	11 04.5	-77 02	9*9FF		
	144926	11 04.6	-77 18	9*9FF	1	
	146887	11 04.6	-77 18	9*9FF	1	
	582558	11 05.1	-61 49	9*9F		
	593531	11 05.1	-61 49	9*9F		BADGAIN
	595881	11 05.1	-61 49	9*9F		BADGAIN
	376986	11 05.3	-77 08	9*9F		
	379338	11 05.3	-77 08	9*9F		
	614507	11 05.8	-77 05	9*9FF		
	644684	11 05.8	-77 05	9*9FF		
	656438	11 05.8	-77 05	9*9FF		
	658399	11 05.8	-77 05	9*9FF		
HD 97048	331126	11 06.7	-77 23	9*9F		
HD 97048	333478	11 06.7	-77 23	9*9F		
	112194	11 06.7	-77 24	9*9F	1	
	114743	11 06.7	-77 24	9*9F	1	
	379534	11 06.8	-77 18	9*9F		
	385021	11 06.8	-77 18	9*9F		
	617444	11 07.2	-77 28	9*9F		
	627242	11 07.2	-77 28	9*9F		
	326811	11 08.0	-76 16	9*9FF		
	331319	11 08.0	-76 16	9*9FF		
	123561	11 08.0	-76 16	9*9FF	1	
	131598	11 08.0	-76 16	9*9FF	1	
HD 97300	208045	11 08.3	-76 21	9*9F		
HD 97300	144538	11 08.3	-76 21	9*9F	1	
	246852	11 08.4	-77 06	9*9F		
	259003	11 08.4	-77 06	9*9F		
	259787	11 08.5	-77 21	9*9F		
	261943	11 08.5	-77 21	9*9F		
NGC 3556	755867	11 08.6	+55 57	9*9F		
NGC 3556	758410	11 08.6	+55 57	9*9F		
	260376	11 08.7	-76 27	9*9F		
	263122	11 08.7	-76 27	9*9F		
	638696	11 08.8	-76 36	9*9FF		
	639981	11 08.8	-76 36	9*9FF		

	661734	11 08.8	-76 36	9*9FF		
	670161	11 08.8	-76 36	9*9FF		
VHE 47A+B+C	587843	11 09.1	-61 04	9*9FF		BADGAIN
VHE 47A+B+C	600973	11 09.1	-61 04	9*9FF		BADGAIN
	260573	11 09.5	-76 48	9*9F		
	262534	11 09.5	-76 48	9*9F		
CED 113	527489	11 09.7	-61 02	9*9F		BADGAIN
CED 113	530232	11 09.7	-61 02	9*9F		BADGAIN
UGC 6251	366719	11 10.5	+53 52	9*9FF		
NGC 3587	380642	11 11.9	+55 17	9*9F		
NGC 3587	387697	11 11.9	+55 17	9*9F		
MRSL 291-00/2	593332	11 12.9	-60 53	9*9F		BADGAIN
MRSL 291-00/2	595685	11 12.9	-60 53	9*9F		BADGAIN
MRSL 291-00/2	538073	11 12.9	-60 59	9*9F		BADGAIN
MRSL 291-00/2	543952	11 12.9	-60 59	9*9F		BADGAIN
MRSL 291-00/2	552776	11 12.9	-60 59	9*9F		BADGAIN
	540617	11 13.1	-60 02	9*9F		
	542974	11 13.1	-60 02	9*9F		
	593138	11 13.1	-60 02	9*9F		
NGC 3610	392991	11 15.5	+59 04	9*9FF		
NGC 3621	477705	11 15.8	-32 32	9*9FF		
NGC 3621	488680	11 15.8	-32 32	9*9FF		
CEN X-3	529655	11 19.0	-60 19	3*1S		
CEN X-3	531603	11 19.0	-60 19	3*1S		BADGAIN
NGC 3655	866531	11 20.3	+16 52	9*9F		
NGC 3655	876716	11 20.3	+16 52	9*9F		
VHE 48A	537289	11 21.8	-58 38	9*9FF		
VHE 48A	540032	11 21.8	-58 38	9*9FF		
UGC 6426	500200	11 22.0	+39 02	9*9F		
MSH 11-54	535723	11 22.3	-57 00	9*9F		
MSH 11-54	537873	11 22.3	-57 00	9*9F		
MSH 11-54	540420	11 22.3	-57 00	9*9F		
MSH 11-54	532586	11 22.3	-58 58	9*9F		
MSH 11-54	534549	11 22.3	-58 58	9*9F		
K 1-22	488483	11 24.3	-34 06	9*9F		
K 1-22	491226	11 24.3	-34 06	9*9F		
	383586	11 24.6	+43 15	9*9F		
	404360	11 24.6	+43 15	9*9F		
	417888	11 24.6	+43 15	9*9F		
UGC 6456	280662	11 24.6	+79 16	9*9FF		
UGC 6456	302225	11 24.6	+79 16	9*9FF		
NGC 3683	783687	11 24.7	+57 09	9*9F		
NGC 3683	822868	11 24.7	+57 09	9*9F		
NGC 3690	832665	11 25.7	+58 50	9*9F		
NGC 3690	837756	11 25.7	+58 50	9*9F		
VHE 49	641549	11 26.6	-62 49	9*9F		BADGAIN
VHE 49	614886	11 26.6	-62 49	9*9FF		BADGAIN
VHE 50A + B	617825	11 28.1	-63 33	9*9FF		BADGAIN
VHE 50A + B	621950	11 28.1	-63 33	9*9FF		BADGAIN
NGC 3718	406710	11 29.8	+53 21	9*9FF		
NGC 3718	439249	11 29.8	+53 21	9*9FF		
VHE 51	641352	11 30.3	-63 11	9*9F		BADGAIN
VHE 51	618609	11 30.3	-63 11	9*9FF		BADGAIN
NGC 3738	387494	11 33.1	+54 48	9*9FF		
NGC 3738	401217	11 33.1	+54 48	9*9FF		
NGC 3738	401573	11 33.1	+54 48	9*9FF		

	497887	11 36.6	-37 28	3*3SS		
	499957	11 36.6	-37 28	3*3SS		
NGC 3782	393384	11 36.7	+46 47	9*9FF		
NGC 3810	876909	11 38.4	+11 45	9*9F		
NGC 3893	824630	11 46.0	+48 59	9*9F		
VHE 54	603518	11 46.1	-61 13	9*9FF		
VHE 54	611945	11 46.1	-61 13	9*9FF		
VHE 55	618804	11 46.2	-62 03	9*9FF		
VHE 55	620963	11 46.2	-62 03	9*9FF		
VHE 56	629582	11 47.7	-64 36	9*9FF		
NGC 3918	535128	11 47.8	-56 54	3*3SS		
NGC 3918	537486	11 47.8	-56 54	3*3SS		
UGC 6823	398479	11 48.5	+55 21	9*9F		
UGC 6823	450220	11 48.5	+55 21	9*9F		
UGC 6823	450611	11 48.5	+55 21	9*9F		
NGC 3949	819337	11 51.1	+48 08	9*9F		
NGC 3949	824041	11 51.1	+48 08	9*9F		
	206278	11 52.1	-79 10	9*9FF		
	238813	11 52.1	-79 10	9*9FF		
	331712	11 52.1	-79 10	9*9FF		
NGC 4027	496314	11 56.9	-18 59	9*9F		
NGC 4027	539627	11 56.9	-18 59	9*9F		
NGC 4088	791327	12 03.0	+50 49	9*9F		
NGC 4088	799751	12 03.0	+50 49	9*9F		
NGC 4102	825611	12 03.9	+52 59	9*9F		
NGC 4102	833053	12 03.9	+52 59	9*9F		
NGC 4125	368474	12 05.6	+65 27	9*9FF		
NGC 4125	383767	12 05.6	+65 27	9*9FF		
NGC 4125	398853	12 05.6	+65 27	9*9FF		
NGC 4157	511165	12 08.6	+50 46	9*9F		
NGC 4157	788584	12 08.6	+50 46	9*9F		
NGC 4157	797008	12 08.6	+50 46	9*9F		
NGC 4194	814444	12 11.7	+54 48	9*9F		
	568251	12 12.7	-62 45	9*9F		BADGAIN
	570994	12 12.7	-62 45	9*9F		BADGAIN
NGC 4214	488831	12 13.1	+36 36	9*9F		
NGC 4214	460610	12 13.1	+36 36	9*9FF		
NGC 4236	378473	12 14.3	+69 45	9*9FF		
NGC 4236	383567	12 14.3	+69 45	9*9FF		
NGC 4244	541154	12 15.0	+38 05	9*9F		
NGC 4244	458851	12 15.0	+38 05	9*9FF		
NGC 4254	494719	12 16.3	+14 42	9*9FF		
NGC 4258	395729	12 16.5	+47 35	9*9F		
NGC 4258	406312	12 16.5	+47 35	9*9F		
NGC 4258	474905	12 16.5	+47 35	9*9FF		
NGC 4258	475297	12 16.5	+47 35	9*9FF		
VHE 57A	631346	12 19.5	-63 01	9*9FF		BADGAIN
VHE 57A	634284	12 19.5	-63 01	9*9FF		BADGAIN
NGC 4314	513527	12 20.1	+30 10	9*9FF		
NGC 4314	518631	12 20.1	+30 10	9*9FF		
NGC 4321	475314	12 20.4	+16 06	9*9FF		
NGC 4382	536270	12 22.9	+18 28	9*9FF		
NGC 4382	536463	12 22.9	+18 28	9*9FF		
NGC 4395	461204	12 23.3	+33 49	9*9FF		
NGC 4395	468538	12 23.3	+33 49	9*9FF		
NGC 4438	540574	12 [illegible]	+13 17	9*9FF		

NGC 4438	581357	12 25.2	+13 17	9*9FF		
NGC 4449	461782	12 25.8	+44 22	9*9F		
NGC 4449	483536	12 25.8	+44 22	9*9F		
NGC 4450	497863	12 26.0	+17 22	9*9FF		
NGC 4450	543707	12 26.0	+17 22	9*9FF		
NGC 4490	420426	12 28.2	+41 55	9*9F		
NGC 4490	422778	12 28.2	+41 55	9*9F		
NGC 4486	540381	12 28.3	+12 40	9*9F		
NGC 4486	541557	12 28.3	+12 40	9*9F		
	642527	12 28.8	-79 20	9*9F		
	655658	12 28.8	-79 20	9*9F		
NGC 4559	472183	12 33.5	+28 14	9*9FF		
NGC 4559	480414	12 33.5	+28 14	9*9FF		
NGC 4565	447479	12 33.9	+26 16	9*9FF		
NGC 4565	451019	12 33.9	+26 16	9*9FF		
NGC 4569	546844	12 34.3	+13 26	9*9FF		
NGC 4569	548804	12 34.3	+13 26	9*9FF		
NGC 4592	543129	12 36.7	-00 15	9*9FF		
NGC 4605	368082	12 37.8	+61 53	9*9FF		
NGC 4605	412586	12 37.8	+61 53	9*9FF		
NGC 4631	521361	12 39.7	+32 49	9*9F		
NGC 4631	524104	12 39.7	+32 49	9*9F		
NGC 4631	462187	12 39.7	+32 49	9*9FF		
NGC 4631	522142	12 39.7	+32 49	9*9FF		
FIT.N	146105	12 41.0	-78 32	9*9FF	1	
FIT.N	149045	12 41.0	-78 32	9*9FF	1	
FIT.N	216472	12 41.2	-78 32	9*9FF		
	186482	12 41.2	-78 32	9*9FF	1	
NGC 4656	524885	12 41.5	+32 26	9*9FF		
NGC 4656	527629	12 41.5	+32 26	9*9FF		
NGC 4696	541787	12 45.9	-41 02	3*3SS		
NGC 4696	542373	12 45.9	-41 02	3*3SS		
NGC 4725	489233	12 48.0	+25 46	9*9FF		
NGC 4725	549190	12 48.0	+25 46	9*9FF		
NGC 4736	516650	12 48.5	+41 24	9*9FF		
NGC 4736	535083	12 48.5	+41 24	9*9FF		
	262734	12 50.1	-76 53	9*9F		
	268415	12 50.1	-76 53	9*9F		
NGC 4762	543320	12 50.4	+11 30	9*9FF		
NGC 4762	549589	12 50.4	+11 30	9*9FF		
A 35	536289	12 51.0	-22 35	9*9F		
	145712	12 51.8	-76 25	9*9FF	1	
	147673	12 51.8	-76 25	9*9FF	1	
LT 5	496673	12 53.1	+26 10	9*9F		
LT 5	530383	12 53.1	+26 10	9*9F		
UGC 8058	420815	12 54.1	+57 09	9*9F		
UGC 8058	443550	12 54.1	+57 09	9*9F		
	249601	12 54.1	-77 16	9*9F		
	260771	12 54.1	-77 16	9*9F		
NGC 4826	500006	12 54.3	+21 57	9*9FF		
NGC 4826	508038	12 54.3	+21 57	9*9FF		
	238620	12 54.8	-77 08	9*9FF		
	331334	12 54.8	-77 08	9*9FF		
	182183	12 54.8	-77 09	9*9FF	1	
	145519	12 55.5	-76 52	9*9F	1	
	147479	12 55.5	-76 52	9*9F	1	
	112782	12 55.9	-76 51	9*9FF	1	
	259989	12 56.0	-76 54	9*9F		
	265477	12 56.0	-76 54	9*9F		
	145910	12 56.4	-77 19	9*9FF	1	
	147868	12 56.4	-77 19	9*9FF	1	
	248819	12 58.1	-77 07	9*9F		
	256855	12 58.1	-77 07	9*9F		
	260968	13 00.5	-77 19	9*9F		
	265671	13 00.5	-77 19	9*9F		
	180615	13 01.8	-77 37	9*9FF	1	
	186091	13 01.8	-77 37	9*9FF	1	
NGC 4945	563343	13 02.5	-49 12	9*9F		
NGC 4945	576281	13 02.5	-49 12	9*9F		
	259600	13 02.6	-77 48	9*9F		
	265867	13 02.6	-77 48	9*9F		
	259404	13 03.0	-77 31	9*9F		
	266063	13 03.0	-77 31	9*9F		
UGC 8201	349066	13 04.6	+67 58	9*9FF		
UGC 8201	377097	13 04.6	+67 58	9*9FF		
WR48+ANON	598625	13 04.9	-65 02	9*9F		
WR48+ANON	601172	13 04.9	-65 02	9*9F		
NGC 5005	536052	13 08.6	+37 19	9*9FF		
NGC 5005	536447	13 08.6	+37 19	9*9FF		
NGC 5033	482944	13 11.1	+36 52	9*9FF		
NGC 5033	537425	13 11.1	+36 52	9*9FF		
NGC 5055	469418	13 13.6	+42 18	9*9FF		
NGC 5055	481179	13 13.6	+42 18	9*9FF		
WR52+ANON	585102	13 15.3	-57 52	9*9F		
WR52+ANON	587255	13 15.3	-57 52	9*9F		
VHE 60C	652897	13 15.3	-62 26	9*9FF		BADGAIN
NGC 5068	540016	13 16.2	-20 47	9*9FF		
NGC 5068	542955	13 16.2	-20 47	9*9FF		
NGC 5102	555111	13 19.1	-36 22	9*9FF		
NGC 5102	559817	13 19.1	-36 22	9*9FF		
NGC 5128	560599	13 22.5	-42 45	9*9F		
NGC 5128	566086	13 22.5	-42 45	9*9F		
NGC 5128	568829	13 22.5	-42 45	9*9F		
NGC 5128	583525	13 22.5	-42 45	9*9F		
NGC 5128	589798	13 22.5	-42 45	9*9F		
ALF VIR	619370	13 22.6	-10 54	3*1S		
ALF VIR	619566	13 22.6	-10 54	3*1S		
SER 102.01	583327	13 24.7	-41 13	9*9F		
SER 102.01	600771	13 24.7	-41 13	9*9F		
NGC 5170	593512	13 27.1	-17 42	9*9FF		
NGC 5170	623685	13 27.1	-17 42	9*9FF		
NGC 5204	408653	13 27.7	+58 41	9*9FF		
NGC 5204	456483	13 27.7	+58 41	9*9FF		
NGC 5194	437273	13 27.8	+47 27	9*9FF		
NGC 5194	441976	13 27.8	+47 27	9*9FF		
NGC 5195	480788	13 27.9	+47 32	9*9F		
NGC 5195	495483	13 27.9	+47 32	9*9F		
NGC 5189	11.401	13 30.0	-65 44	9*9F	1	
WR55+RCW78	603915	13 30.1	-62 04	9*9F		BADGAIN
WR55+RCW78	606659	13 30.1	-62 04	9*9F		BADGAIN
NGC 5218	761953	13 30.5	+63 01	9*9F		
NGC 5218	803093	13 30.5	+63 01	9*9F		
NGC 5236	584308	13 34.2	-29 37	9*9FF		
NGC 5236	587052	13 34.2	-29 37	9*9FF		
NGC 5256	819937	13 36.3	+48 32	9*9F		
MCG-06-30-025	619974	13 46.4	-35 49	9*9F		
NGC 5430	764697	13 59.1	+59 34	9*9F		
NGC 5430	772925	13 59.1	+59 34	9*9F		
NGC 5408	622719	14 00.3	-41 10	9*9F		
NGC 5408	625263	14 00.3	-41 10	9*9F		
	508221	14 00.7	+54 31	9*9F		
	534084	14 00.7	+54 31	9*9F		
	534280	14 00.7	+54 34	9*9F		
	534672	14 00.7	+54 34	9*9F		
	534476	14 00.8	+54 36	9*9F		
	534868	14 00.8	+54 36	9*9F		
	532722	14 01.2	+54 29	9*9F		
	533114	14 01.2	+54 29	9*9F		
NGC 5457	442363	14 01.5	+54 36	9*9FF		
NGC 5457	448252	14 01.5	+54 36	9*9FF		
	489213	14 01.5	+54 50	9*9F		
	497830	14 01.5	+54 50	9*9F		
	669555	14 01.5	-66 48	9*9F		
	671908	14 01.5	-66 48	9*9F		
	532918	14 01.9	+54 33	9*9F		
	535064	14 01.9	+54 33	9*9F		
	530949	14 02.1	+54 36	9*9F		
	532321	14 02.1	+54 36	9*9F		
	489016	14 02.7	+54 38	9*9F		
	530362	14 02.7	+54 38	9*9F		
NGC 5474	493319	14 03.3	+53 54	9*9FF		
NGC 5474	496456	14 03.3	+53 54	9*9FF		
	390231	14 03.8	+54 42	9*9FF		
	393368	14 03.8	+54 42	9*9FF		
	144752	14 09.3	-65 06	9*9FF	1	
	181598	14 09.3	-65 06	9*9FF	1	
	182381	14 09.3	-65 06	9*9FF	1	
	184343	14 09.3	-65 06	9*9FF	1	
	185909	14 09.3	-65 06	9*9FF	1	
NGC 5544	549383	14 15.0	+36 48	9*9F		
NGC 5544	552128	14 15.0	+36 48	9*9F		
	387878	14 18.2	+56 57	9*9FF		
	390621	14 18.2	+56 57	9*9FF		
	627612	14 24.8	-46 05	9*9F		
	630162	14 24.8	-46 05	9*9F		
	716781	14 39.7	-58 25	9*9F		BADGAIN
	719525	14 39.7	-58 25	9*9F		BADGAIN
	666609	14 39.7	-58 32	9*9FF		BADGAIN
	673467	14 39.7	-58 32	9*9FF		BADGAIN
	625037	14 42.4	+02 10	9*9F		
	626605	14 42.4	+02 10	9*9F		
	123183	14 44.4	-65 04	9*9FF	1	
	125731	14 44.4	-65 04	9*9FF	1	
	131219	14 44.4	-65 04	9*9FF	1	
	125745	14 55.5	-47 04	9*9FF	1	
	131423	14 55.5	-47 04	9*9FF	1	
NGC 5820	470196	14 57.2	+54 05	9*9F		
NGC 5820	533690	14 57.2	+54 05	9*9F		

	623506	14 57.7	-48 06	9*9F		
	626249	14 57.7	-48 06	9*9F		
	144164	14 59.3	-63 12	9*9FF	1	
	148075	14 59.3	-63 12	9*9FF	1	
	164341	14 59.5	-72 26	9*9F	1	
	164537	14 59.5	-72 26	9*9F	1	
	164733	15 00.5	-72 15	9*9F	1	
	164929	15 00.5	-72 15	9*9F	1	
NGC 5850	681669	15 04.6	+01 44	9*9F		
NGC 5866	390425	15 05.1	+55 57	9*9FF		
NGC 5866	410610	15 05.1	+55 57	9*9FF		
NGC 5866	499000	15 05.1	+55 57	9*9FF		
NGC 5866	505273	15 05.1	+55 57	9*9FF		
	637220	15 05.3	-51 27	9*9F		
	645449	15 05.3	-51 27	9*9F		
UGC 9749	361016	15 08.2	+67 23	9*9FF		
MSH 15-52	153373	15 10.0	-58 57	9*9F	1	BADGAIN
NGC 5907	410022	15 14.6	+56 30	9*9FF		
NGC 5907	423152	15 14.6	+56 30	9*9FF		
NGC 5907	449812	15 14.6	+56 30	9*9FF		
NGC 5907	493512	15 14.6	+56 30	9*9FF		
NGC 5907	498804	15 14.6	+56 30	9*9FF		
	146903	15 14.8	-56 29	9*9FF	1	BADGAIN
	149255	15 14.8	-56 29	9*9FF	1	BADGAIN
NGC 5929	540948	15 24.3	+41 51	3*3SS		
NGC 5929	544866	15 24.3	+41 51	3*3SS		
NGC 5962	620717	15 34.2	+16 46	9*9F		
NGC 5962	661669	15 34.2	+16 46	9*9F		
	145729	15 40.7	-53 57	9*9FF	1	BADGAIN
	147690	15 40.7	-53 57	9*9FF	1	BADGAIN
NGC 5967	674654	15 41.9	-75 31	9*9F		
NGC 5967	688569	15 41.9	-75 31	9*9F		
NGC 5967	691312	15 41.9	-75 31	9*9F		
	161998	15 45.0	-54 33	9*9FF	1	BADGAIN
	167487	15 45.0	-54 33	9*9FF	1	BADGAIN
	167291	15 49.2	-54 29	9*9FF	1	BADGAIN
	170035	15 49.2	-54 29	9*9FF	1	BADGAIN
NGC 6015	493904	15 50.7	+62 27	9*9F		
NGC 6015	497625	15 50.7	+62 27	9*9F		
MSH 15-57	152985	15 51.8	-53 09	9*9F	1	BADGAIN
MSH 15-57	155729	15 51.8	-53 09	9*9F	1	BADGAIN
	162195	15 52.0	-52 35	9*9FF	1	BADGAIN
	146710	15 59.7	-53 02	9*9FF	1	BADGAIN
	149062	15 59.7	-53 02	9*9FF	1	BADGAIN
	696330	16 03.2	+66 38	9*9F		
	696524	16 03.2	+66 38	9*9F		
WR 72	736357	16 03.2	-35 37	9*9F		
WR 72	743020	16 03.2	-35 37	9*9F		
	167684	16 06.5	-51 59	9*9FF	1	BADGAIN
	170428	16 06.5	-51 59	9*9FF	1	BADGAIN
	173763	16 13.5	-51 52	9*9FF	1	BADGAIN
	176900	16 13.5	-51 52	9*9FF	1	BADGAIN
	702862	16 13.8	-50 25	9*9F		BADGAIN
	759879	16 13.8	-50 25	9*9F		BADGAIN
	169841	16 15.9	-50 57	9*9FF	1	BADGAIN
	172585	16 15.9	-50 57	9*9FF	1	BADGAIN

	707567	16 16.4	-57 17	9*9F		
	710703	16 16.4	-57 17	9*9F		
	156123	16 18.4	-49 59	9*9FF	1	BADGAIN
	177094	16 18.4	-49 59	9*9FF	1	BADGAIN
MRSL 332-01/2	672098	16 20.6	-51 25	9*9F		BADGAIN
MRSL 332-01/2	677584	16 20.6	-51 25	9*9F		BADGAIN
	143396	16 24.0	-24 32	9*9F	1	BADGAIN
	143592	16 24.2	-24 22	9*9F	1	BADGAIN
NGC 6181	675382	16 30.2	+19 56	9*9F		
NGC 6181	689295	16 30.2	+19 56	9*9F		
	170227	16 30.8	-67 02	3*3SS	1	
	172775	16 30.8	-67 02	3*3SS	1	
TAU SCO	149060	16 32.8	-24 07	3*1S	1	BADGAIN
	149100	16 34.4	-10 29	3*1S	1	
	147500	16 34.5	-46 06	9*9FF	1	BADGAIN
	149654	16 34.5	-46 06	9*9FF	1	BADGAIN
	224333	16 36.3	-46 07	9*9FF		BADGAIN
	227077	16 36.3	-46 07	9*9FF		BADGAIN
	172196	16 36.3	-46 08	9*9FF	1	BADGAIN
	176704	16 36.3	-46 08	9*9FF	1	BADGAIN
	677384	16 36.5	-45 35	9*9F		BADGAIN
	695217	16 36.5	-45 35	9*9F		BADGAIN
NGC 6207	623840	16 41.3	+36 56	9*9F		
NGC 6207	631482	16 41.3	+36 56	9*9F		
VHE 74	778679	16 45.1	-48 00	9*9F		BADGAIN
VHE 74	719317	16 45.1	-48 00	9*9FF		BADGAIN
NGC 6215	754393	16 46.8	-58 55	9*9F		
NGC 6215	757136	16 46.8	-58 55	9*9F		
NGC 6221	721871	16 48.4	-59 08	9*9F		
NGC 6221	724418	16 48.4	-59 08	9*9F		
NGC 6221	754984	16 48.4	-59 08	9*9F		
NGC 6221	758307	16 48.4	-59 08	9*9F		
	169487	16 48.7	+05 04	9*9F	1	
	161216	16 54.7	-50 32	9*9FF	1	
	163960	16 54.7	-50 32	9*9FF	1	
VHE 79A	778880	16 55.3	-46 03	9*9F		BADGAIN
VHE 79A	724216	16 55.3	-46 03	9*9FF		BADGAIN
VHE 77	779857	16 55.5	-40 32	9*9F		BADGAIN
VHE 77	722060	16 55.5	-40 32	9*9FF		BADGAIN
	219092	16 56.0	+35 25	3*1SS		
	144409	16 56.0	+39 25	3*1SS	1	
	219423	16 58.8	-79 47	9*9FF		
	222168	16 58.8	-79 47	9*9FF		
	230403	16 58.8	-79 47	9*9FF		
	240787	16 58.8	-79 47	9*9FF		
B 049	232377	16 59.4	-33 12	9*9FF		
B 049	240610	16 59.4	-33 12	9*9FF		
B 049	173379	16 59.4	-33 12	9*9FF	1	
M 2-9	164978	17 02.9	-10 05	3*1S	1	
M 2-9	185950	17 02.9	-10 05	3*1S	1	
	701284	17 11.0	-39 42	9*9F		BADGAIN
	757717	17 11.0	-39 42	9*9F		BADGAIN
NGC 6340	281443	17 11.3	+72 22	9*9FF		
NGC 6340	284180	17 11.3	+72 22	9*9FF		
NGC 6340	358267	17 11.3	+72 22	9*9FF		
NGC 6340	391194	17 11.3	+72 22	9*9FF		

	222365	17 11.8	-77 49	9*9FF		
	241766	17 11.8	-77 49	9*9FF		
	244120	17 11.8	-77 49	9*9FF		
	258041	17 11.8	-77 49	9*9FF		
NGC 6300	771049	17 12.3	-62 46	9*9F		
NGC 6300	773985	17 12.3	-62 46	9*9F		
	247067	17 14.9	-77 06	9*9FF		
	257842	17 14.9	-77 06	9*9FF		
	260198	17 14.9	-77 06	9*9FF		
	268624	17 14.9	-77 06	9*9FF		
MRSL 351+00/4	199643	17 16.6	-35 55	9*9FF		BADGAIN
MRSL 351+00/4	783966	17 16.6	-35 55	9*9FF		BADGAIN
MRSL 351+00/4	174554	17 16.6	-35 55	9*9FF	1	BADGAIN
	174358	17 16.9	-35 52	9*9FF	1	BADGAIN
	194155	17 16.9	-35 52	9*9FF	1	BADGAIN
MRSL 348-01/1	695018	17 16.9	-38 54	9*9F		BADGAIN
MRSL 348-01/1	698348	17 16.9	-38 54	9*9F		BADGAIN
NGC 6334	781422	17 17.1	-35 49	9*9F		BADGAIN
NGC 6334	783576	17 17.1	-35 49	9*9F		BADGAIN
NGC 6334	248840	17 17.1	-35 49	9*9FF		BADGAIN
	174162	17 17.3	-35 46	9*9FF	1	BADGAIN
	191411	17 17.3	-35 46	9*9FF	1	BADGAIN
	173966	17 17.5	-35 44	9*9FF	1	BADGAIN
	188667	17 17.5	-35 44	9*9FF	1	BADGAIN
	203592	17 17.9	-00 56	9*9F		
	173791	17 17.9	-00 56	9*9F	1	
	181072	17 19.2	+57 57	9*9FF	1	
	184012	17 19.2	+57 57	9*9FF	1	
	246674	17 25.8	-76 32	9*9FF		
	257646	17 25.8	-76 32	9*9FF		
	261563	17 25.8	-76 32	9*9FF		
	263532	17 25.8	-76 32	9*9FF		
	782589	17 29.8	-33 36	9*9F		BADGAIN
	785336	17 29.8	-33 36	9*9F		BADGAIN
NGC 6384	180665	17 30.0	+07 05	9*9FF	1	
NGC 6384	183802	17 30.0	+07 05	9*9FF	1	
NGC 6384	260638	17 30.0	+07 06	9*9FF		
CALFIELD	175521	17 36.4	-56 54	9*9FF	1	
CALFIELD	178072	17 37.7	-52 55	9*9FF	1	
CALFIELD	177878	17 38.8	-48 55	9*9FF	1	
CALFIELD	188857	17 39.7	-44 55	9*9FF	1	
PK 045+24.1	203017	17 40.3	+21 28	3*3SS		
PK 045+24.1	216344	17 40.3	+21 28	3*3SS		
CALFIELD	262558	17 40.5	-40 55	9*9FF		
CALFIELD	265302	17 40.5	-40 55	9*9FF		
CALFIELD	196898	17 41.2	-36 55	9*9FF		
CALFIELD	251586	17 41.9	-32 55	9*9FF		BADGAIN
CALFIELD	261397	17 41.9	-32 55	9*9FF		BADGAIN
	175713	17 42.2	-64 38	9*9FF	1	
	178457	17 42.2	-64 38	9*9FF	1	
CALFIELD	261202	17 42.4	-32 55	9*9FF		BADGAIN
	248649	17 42.7	-44 30	9*9FF		
PK 051+25.1	202824	17 43.0	+27 20	3*1SS		
PK 051+25.1	216540	17 43.0	+27 20	3*1SS		
	261005	17 43.0	-24 55	9*9FF		BADGAIN
CALFIELD	202015	17 43.5	-20 55	9*9FF		

CALFIELD	201822	17 44.0	-16 55	9*9FF		
CALFIELD	201629	17 44.4	-12 55	9*9FF		
CALFIELD	194183	17 44.9	-08 56	9*9FF	1	
CALFIELD	191439	17 45.3	-04 56	9*9FF	1	
CALFIELD	188695	17 45.7	-00 56	9*9FF	1	
NGC 6503	228715	17 50.0	+70 09	9*9FF		
NGC 6503	232041	17 50.0	+70 09	9*9FF		
NGC 6503	356502	17 50.0	+70 09	9*9FF		
NGC 6503	385120	17 50.0	+70 09	9*9FF		
A 43	204775	17 51.2	+10 38	3*3SS		
PK 053+24.1	203210	17 52.3	+28 00	3*3SS		
PK 053+24.1	205371	17 52.3	+28 00	3*3SS		
PK 053+24.1	207331	17 52.3	+28 00	3*3SS		
NGC 6543	198721	17 58.6	+66 38	3*3SS		
NGC 6543	201075	17 58.6	+66 38	3*3SS		
NGC 6543	357874	17 58.6	+66 38	3*3SS		
NGC 6543	360228	17 58.6	+66 38	3*3SS		
NGC 6543	364539	17 58.6	+66 38	3*3SS		
NGC 6543	367879	17 58.6	+66 38	3*3SS		
NGC 6543	369635	17 58.6	+66 38	3*3SS		
NGC 6543	199113	17 58.6	+66 38	9*9F		
NGC 6543	206561	17 58.6	+66 38	9*9F		
NGC 6543	240867	17 58.6	+66 38	9*9F		
NGC 6543	250662	17 58.6	+66 38	9*9F		
NGC 6543	270264	17 58.6	+66 38	9*9F		
NGC 6543	284767	17 58.6	+66 38	9*9F		
NGC 6543	293983	17 58.6	+66 38	9*9F		
NGC 6543	326517	17 58.6	+66 38	9*9F		
NGC 6543	329067	17 58.6	+66 38	9*9F		
NGC 6543	331223	17 58.6	+66 38	9*9F		
NGC 6543	333184	17 58.6	+66 38	9*9F		
NGC 6543	337296	17 58.6	+66 38	9*9F		
NGC 6543	340635	17 58.6	+66 38	9*9F		
NGC 6543	361990	17 58.6	+66 38	9*9F		
NGC 6543	362386	17 58.6	+66 38	9*9F		
NGC 6543	362975	17 58.6	+66 38	9*9F		
NGC 6543	364147	17 58.6	+66 38	9*9F		
NGC 6543	364734	17 58.6	+66 38	9*9F		
NGC 6543	365133	17 58.6	+66 38	9*9F		
NGC 6543	374340	17 58.6	+66 38	9*9F		
NGC 6543	375516	17 58.6	+66 38	9*9F		
NGC 6543	377869	17 58.6	+66 38	9*9F		
NGC 6543	378454	17 58.6	+66 38	9*9F		
	210614	17 59.3	-46 40	9*9FF		
NGC 6574	763161	18 09.6	+14 58	9*9F		
NGC 6574	766492	18 09.6	+14 58	9*9F		
NGC 6572	204185	18 09.7	+06 50	3*3SS		
NGC 6572	238878	18 09.7	+06 50	3*3SS		
CN 3-1	203791	18 15.2	+10 08	3*3SS		
CN 3-1	239468	18 15.2	+10 08	3*3SS		
	216099	18 19.0	-56 39	3*3SS		
	257260	18 19.0	-56 39	3*3SS		
	281956	18 19.0	-56 39	3*3SS		
NGC 6643	222644	18 21.2	+74 33	9*9FF		
NGC 6643	224601	18 21.2	+74 33	9*9FF		
CRL 2155	196348	18 24.0	+23 27	3*1S		
CRL 2155	198316	18 24.0	+23 27	3*1S		
	780596	18 25.7	+24 15	9*9F		
	787648	18 25.7	+24 15	9*9F		
	240048	18 27.3	+01 13	9*9F		
	289248	18 27.3	+01 13	9*9F		
	741812	18 27.3	+01 13	9*9F		
	783731	18 28.8	+22 01	9*9F		
A 46	205568	18 29.2	+26 53	3*3SS		
A 46	207526	18 29.2	+26 53	3*3SS		
	817028	18 29.9	+39 56	9*9F		
	791170	18 31.7	+37 18	9*9F		
	820751	18 31.7	+37 18	9*9F		
	783532	18 35.8	+28 00	9*9F		
CALFIELD	262995	18 36.2	+15 53	9*9FF		
CALFIELD	262796	18 37.5	+11 59	9*9FF		
CALFIELD	271613	18 38.7	+08 08	9*9FF		
PK 056+14.1	225162	18 39.1	+26 52	3*3SS		
PK 056+14.1	236930	18 39.1	+26 52	3*3SS		
CALFIELD	265334	18 39.9	+04 20	9*9FF		
CALFIELD	263570	18 41.1	+00 32	9*9FF		BADGAIN
WR 121	783554	18 41.6	-03 51	9*9F		BADGAIN
CALFIELD	291597	18 42.3	-03 14	9*9FF		BADGAIN
29.9-0.0	259053	18 43.4	-02 43	9*9F		BADGAIN
29.9-0.0	254358	18 43.5	-02 44	9*9FF		BADGAIN
29.9-0.0	276310	18 43.5	-02 44	9*9FF		BADGAIN
30.9-0.1	259449	18 45.1	-01 49	9*9F		BADGAIN
30.8-0.1	256702	18 45.2	-01 58	9*9F		BADGAIN
30.8-0.1	259250	18 45.2	-01 58	9*9F		BADGAIN
HU 2-1	224970	18 47.6	+20 47	3*3SS		
HU 2-1	233202	18 47.6	+20 47	3*3SS		
NGC 6699	328601	18 47.8	-57 23	9*9F		
M 1-64	234581	18 48.2	+35 11	3*3SS		
M 1-64	236539	18 48.2	+35 11	3*3SS		
	239852	18 50.8	+01 11	9*9FF		BADGAIN
	242005	18 50.8	+01 11	9*9FF		BADGAIN
NGC 6720	224581	18 51.7	+32 58	3*3SS		
NGC 6720	233009	18 51.7	+32 58	3*3SS		
NGC 6720	298860	18 51.7	+32 58	9*9F		
NGC 6720	307092	18 51.7	+32 58	9*9F		
20-2.1	261026	18 52.3	+05 58	9*9F		
20-2.1	289643	18 52.3	+05 58	9*9F		
	242799	18 53.6	+07 50	9*9F		BADGAIN
	262204	18 53.6	+07 50	9*9F		BADGAIN
PK 035-00.1	239270	18 55.6	+01 35	9*9FF		BADGAIN
PK 035-00.1	242203	18 55.6	+01 35	9*9FF		BADGAIN
PK 078+18.1	243792	18 58.0	+48 24	3*3SS		
PK 078+18.1	245753	18 58.0	+48 24	3*3SS		
NGC 6744	210998	19 05.0	-63 56	9*9FF		
NGC 6744	216296	19 05.0	-63 56	9*9FF		
NGC 6744	221972	19 05.0	-63 56	9*9FF		
NGC 6744	224715	19 05.0	-63 56	9*9FF		
NGC 6751	771243	19 07.1	-57 08	9*9F		
NGC 6751	781823	19 07.1	-57 08	9*9F		
	249662	19 07.8	+09 01	9*9FF		BADGAIN
	254563	19 07.8	+09 01	9*9FF		BADGAIN
	255150	19 07.9	+09 01	9*9FF		BADGAIN
	279845	19 07.9	+09 01	9*9FF		BADGAIN
SS 433	261222	19 09.4	+04 54	9*9F		
SS 433	322764	19 09.4	+04 54	9*9F		
IC 4837	341740	19 11.2	-54 45	9*9F		
MIL 76	259072	19 12.0	+11 04	9*9FF		BADGAIN
MIL 76	285332	19 12.0	+11 04	9*9FF		BADGAIN
NGC 6835	863095	19 15.8	-12 42	9*9F		
LDN 0723	243982	19 16.0	+19 08	9*9FF		
LDN 0723	249274	19 16.0	+19 08	9*9FF		
LDN 0723	257307	19 16.0	+19 08	9*9FF		
HH 32A + B	251614	19 18.1	+10 56	9*9FF		
HH 32A + B	253775	19 18.1	+10 56	9*9FF		BADGAIN
HH 32A + B	293372	19 18.1	+10 56	9*9FF		BADGAIN
HH 32A + B	310027	19 18.1	+10 56	9*9FF		BADGAIN
	254957	19 21.4	+14 24	9*9FF		BADGAIN
	258485	19 21.4	+14 24	9*9FF		BADGAIN
VY 2-2	248871	19 22.0	+00 10	3*3SS		
VY 2-2	258466	19 22.0	+00 10	3*3SS		
	256299	19 27.9	-17 47	9*9FF		
	343529	19 27.9	-17 47	9*9FF		
MRSL 053+00/1	259845	19 28.1	+18 09	9*9FF		BADGAIN
MRSL 053+00/1	262589	19 28.1	+18 09	9*9FF		BADGAIN
MRSL 053+00/1	326104	19 28.1	+18 13	9*9FF		BADGAIN
MRSL 053+00/1	328061	19 28.1	+18 13	9*9FF		BADGAIN
A 62	260833	19 30.9	+10 30	9*9F		
A 62	326493	19 30.9	+10 30	9*9F		
BD+30 3639	262023	19 32.8	+30 24	3*1S		
BD+30 3639	263981	19 32.8	+30 24	3*1S		
BD+30 3639	312578	19 32.8	+30 24	9*9F		
BD+30 3639	315322	19 32.8	+30 24	9*9F		
M 1-92	262414	19 34.3	+29 26	3*1S		
M 1-92	268867	19 34.3	+29 26	3*1S		
M 1-92	265935	19 34.3	+29 26	9*9F		
M 1-92	268485	19 34.3	+29 26	9*9F		
M 1-92	307286	19 34.3	+29 26	9*9F		
M 1-92	312773	19 34.3	+29 26	9*9F		
LDN 0663	257102	19 34.6	+07 27	9*9FF		
LDN 0663	262397	19 34.6	+07 27	9*9FF		
	232951	19 35.9	-69 55	9*9FF		
	238248	19 35.9	-69 55	9*9FF		
	233147	19 37.1	-68 53	9*9FF		
	238635	19 37.1	-68 53	9*9FF		
	268287	19 37.6	+21 28	3*3SS		BADGAIN
	277104	19 37.6	+21 28	3*3SS		BADGAIN
	329044	19 37.6	+21 28	9*9F		
	315517	19 37.6	+21 28	9*9F		BADGAIN
NGC 6808	763213	19 38.5	-70 45	9*9F		
NGC 6808	781046	19 38.5	-70 45	9*9F		
NGC 6810	782213	19 39.3	-58 46	9*9F		
NGC 6810	785937	19 39.3	-58 46	9*9F		
HM SGE	270822	19 39.7	+16 38	3*1S		
HM SGE	273970	19 39.7	+16 38	3*1S		
HM SGE	329236	19 39.7	+16 38	9*9F		
HM SGE	331788	19 39.7	+16 38	9*9F		
	276517	19 41.1	+23 17	9*9FF		BADGAIN
	279850	19 41.1	+23 17	9*9FF		BADGAIN

NGC 6826	299458	19 43.5	+50 24	3*3SS		
NGC 6826	301613	19 43.5	+50 24	3*3SS		
NGC 6826	384713	19 43.5	+50 24	3*3SS		
NGC 6826	389812	19 43.5	+50 24	3*3SS		
NGC 6826	320437	19 43.5	+50 24	9*9F		
NGC 6826	322396	19 43.5	+50 24	9*9F		
MRSL 060-00/1	276715	19 44.2	+24 28	9*9FF	BADGAIN	
MRSL 060-00/1	284545	19 44.2	+24 28	9*9FF	BADGAIN	
	294351	19 46.3	+18 05	9*9F		
	299054	19 46.3	+18 05	9*9F		
	246480	19 46.9	-67 51	9*9FF		
	255294	19 46.9	-67 51	9*9FF		
NGC 6833	298879	19 48.4	+48 50	3*1S		
NGC 6833	300839	19 48.4	+48 50	3*1S		
NGC 6833	376870	19 48.4	+48 50	3*1S		
NGC 6833	380789	19 48.4	+48 50	3*1S		
	863072	19 48.6	+32 47	9*9F		
	865028	19 48.6	+32 47	9*9F		
CTB 80 (C)	286717	19 51.1	+32 45	3*3SS		
CTB 80 (C)	288668	19 51.1	+32 45	3*3SS		
2CG 065+00	286908	19 52.4	+29 15	9*9FF		
2CG 065+00	330997	19 52.4	+29 15	9*9FF		
V1016 CYG	287885	19 55.3	+39 41	3*1S		
V1016 CYG	290629	19 55.3	+39 41	3*1S		
	335706	19 56.3	+31 14	9*9FF		
	343546	19 56.3	+31 14	9*9FF		
CYG X-1	286519	19 56.4	+35 04	3*1S		
CYG X-1	289268	19 56.4	+35 04	3*1S		
MRSL 068+01/1	291810	19 56.7	+31 17	9*9FF		
MRSL 068+01/1	328255	19 56.7	+31 17	9*9FF		
NGC 6853	282592	19 57.5	+22 35	3*3SS	BADGAIN	
NGC 6853	288079	19 57.5	+22 35	3*3SS	BADGAIN	
NGC 6853	282399	19 57.5	+22 35	9*9F		
NGC 6853	285143	19 57.5	+22 35	9*9F		
VV 072	291032	19 57.7	+40 36	3*3SS		
VV 072	291228	19 57.7	+40 36	3*3SS		
VV 072	301412	19 57.7	+40 36	3*3SS		
VV 072	303960	19 57.7	+40 36	3*3SS		
LBN 0158	293181	19 58.4	+33 07	9*9F	BADGAIN	
LBN 0158	333161	19 58.4	+33 07	9*9F	BADGAIN	
	295341	19 59.0	+33 21	9*9FF	BADGAIN	
	297886	19 59.0	+33 21	9*9FF	BADGAIN	
	356288	19 59.0	+33 24	9*9F	BADGAIN	
	359029	19 59.0	+33 24	9*9F	BADGAIN	
	299851	19 59.2	+33 02	9*9FF		
	304540	19 59.2	+33 02	9*9FF	BADGAIN	
ON 3	295725	19 59.8	+33 25	9*9FF	BADGAIN	
ON 3	298666	19 59.8	+33 25	9*9FF	BADGAIN	
ON 3	290437	19 59.9	+33 24	3*3SS	BADGAIN	
ON 3	292392	19 59.9	+33 24	3*3SS	BADGAIN	
ON 3	323555	19 59.9	+33 24	9*9F	BADGAIN	
ON 3	325912	19 59.9	+33 24	9*9F	BADGAIN	
ON 3	339826	19 59.9	+33 24	9*9F	BADGAIN	
	384311	20 00.0	+35 10	9*9F	BADGAIN	
	384415	20 00.0	+35 10	9*9F	BADGAIN	
	413716	20 00.0	+35 10	9*9F	BADGAIN	

VDB.66N 128	364516	20 02.6	+32 05	9*9F	BADGAIN	
VDB.66N 128	369611	20 02.6	+32 05	9*9F	BADGAIN	
	320810	20 08.2	+31 22	9*9F	BADGAIN	LDN 1157
	334529	20 08.2	+31 22	9*9F	BADGAIN	LDN 1157
	331592	20 08.4	+36 02	9*9F		LDN 1147/8
	334336	20 08.4	+36 02	9*9F		LDN 1147/8
NGC 6884	329445	20 08.8	+46 18	9*9F		LDN 1149/51
NGC 6884	332191	20 08.8	+46 18	9*9F		LDN 1149/51
NGC 6884	385696	20 08.8	+46 18	9*9F		NML CYG
NGC 6884	388047	20 08.8	+46 18	9*9F		NML CYG
FG SGE	293959	20 09.7	+20 11	3*3SS		NML CYG
FG SGE	296311	20 09.7	+20 11	3*3SS		NML CYG
MRSL 075+02/1	347861	20 10.3	+38 12	9*9F		IC 5052
MRSL 075+02/1	350605	20 10.3	+38 12	9*9F		IC 5052
CTB 87	306702	20 14.3	+37 01	9*9F		IC 5052
CTB 87	309642	20 14.3	+37 01	9*9F		IC 5052
IC 4997	298469	20 17.9	+16 34	3*1S		LDN 1076
IC 4997	301213	20 17.9	+16 34	3*1S		LDN 1076
	417050	20 19.8	+37 20	9*9F	BADGAIN	
	419792	20 19.8	+37 20	9*9F	BADGAIN	
	382745	20 20.8	+37 22	9*9FF		
	320418	20 20.8	+37 22	9*9FF	BADGAIN	NGC 7008
	323162	20 20.8	+37 22	9*9FF	BADGAIN	NGC 7008
	410771	20 20.8	+37 22	9*9FF	BADGAIN	NGC 7008
	327084	20 23.2	+39 01	9*9FF	BADGAIN	NGC 7008
	339626	20 23.2	+39 01	9*9FF	BADGAIN	
MRSL 076-00/1	327477	20 25.6	+37 13	9*9F	BADGAIN	
MRSL 076-00/1	337080	20 25.6	+37 13	9*9F	BADGAIN	
MRSL 076-00/1	361579	20 25.6	+37 13	9*9F	BADGAIN	
NGC 6921	763742	20 26.4	+25 34	9*9F		AFGL 2688
NGC 6921	765703	20 26.4	+25 34	9*9F		AFGL 2688
ACK 078+00.1	325326	20 27.6	+40 01	9*9F	BADGAIN	CED 187
ACK 078+00.1	342570	20 27.6	+40 01	9*9F	BADGAIN	CED 187
A 71	334743	20 30.8	+47 11	9*9F		CED 187
A 71	337484	20 30.8	+47 11	9*9F		CED 187
A 71	387262	20 30.8	+47 11	9*9F		CED 187
A 71	405888	20 30.8	+47 11	9*9F		NGC 7013
LDN 1094	462339	20 32.0	+63 50	9*9FF		NGC 7013
LDN 1094	464498	20 32.0	+63 50	9*9FF		
NGC 6946	405304	20 33.8	+59 59	9*9FF		
NGC 6946	413736	20 33.8	+59 59	9*9FF		
NGC 6946	419219	20 33.8	+59 59	9*9FF		
NGC 6946	421962	20 33.8	+59 59	9*9FF		LDN 1173
LDN 1100	510157	20 34.0	+63 50	9*9FF		LDN 1173
LDN 1100	519751	20 34.0	+63 50	9*9FF		
	416671	20 35.3	+67 43	9*9F		
	422158	20 35.3	+67 43	9*9F		
	510546	20 35.3	+67 43	9*9F		
	521127	20 35.3	+67 43	9*9F		
NGC 6951	755501	20 36.6	+65 56	9*9F		
NGC 6951	758244	20 36.6	+65 56	9*9F		NGC 7029
LBN 0311	342960	20 36.8	+42 25	9*9FF	BADGAIN	NGC 7029
LBN 0311	345130	20 36.8	+42 25	9*9FF	BADGAIN	T CEP
	342176	20 37.1	+42 18	9*9FF	BADGAIN	LDN 0970
	345423	20 37.1	+42 18	9*9FF	BADGAIN	LDN 0970
	341784	20 37.3	+42 09	9*9FF	BADGAIN	LDN 0970

	352376	20 37.3	+42 09	9*9FF	BADGAIN	
	372750	20 37.3	+42 09	9*9FF	BADGAIN	
	510744	20 39.0	+67 50	9*9FF		
	540342	20 39.0	+67 50	9*9FF		
	555025	20 40.0	+67 10	9*9FF		
	588743	20 40.0	+67 10	9*9FF		
	415091	20 41.0	+57 20	9*9FF		
	435680	20 41.0	+57 20	9*9FF		
	338062	20 44.6	+39 56	3*3SS	BADGAIN	
	340021	20 44.6	+39 56	3*3SS	BADGAIN	
	369812	20 44.6	+39 56	9*9F		
	375299	20 44.6	+39 56	9*9F	BADGAIN	
	230003	20 47.4	-69 23	9*9FF		
	232752	20 47.4	-69 23	9*9FF		
	236087	20 47.4	-69 23	9*9FF		
	238828	20 47.4	-69 23	9*9FF		
	489578	20 48.2	+59 40	9*9FF		
	495843	20 48.2	+59 40	9*9FF		
	456658	20 59.0	+67 57	9*9F		
	489189	20 59.0	+67 57	9*9F		
	541511	20 59.0	+67 57	9*9F		
	410790	20 59.1	+54 21	9*9F		
	414504	20 59.1	+54 21	9*9F		
	417443	20 59.1	+54 21	9*9F		
	419991	20 59.1	+54 21	9*9F		
	395308	20 59.8	+68 01	9*9F		
	410990	20 59.8	+68 01	9*9F		
	551314	20 59.8	+68 01	9*9F		
	558166	20 59.8	+68 01	9*9F		
	350796	21 00.3	+36 30	3*1S		
	348647	21 00.3	+36 30	3*1S	BADGAIN	
	565819	21 01.0	+67 58	3*3S	BADGAIN	
	354538	21 01.0	+67 58	9*9FF		
	357282	21 01.0	+67 58	9*9FF		
	563267	21 01.0	+67 58	9*9FF		
	567385	21 01.0	+67 58	9*9FF		
	366870	21 01.4	+29 42	9*9F		
	370198	21 01.4	+29 42	9*9F		
	388250	21 01.8	+67 42	9*9F		
	421570	21 01.8	+67 42	9*9F		
	560718	21 01.8	+67 42	9*9F		
	588929	21 01.8	+67 42	9*9F		
	548956	21 04.0	+67 30	9*9FF		
	562284	21 04.0	+67 30	9*9FF		
	517597	21 06.9	+52 14	9*9F		
	519558	21 06.9	+52 14	9*9F		
	519361	21 07.6	+52 08	9*9F	BADGAIN	
	542289	21 07.6	+52 08	9*9F	BADGAIN	
	508384	21 07.6	+52 20	9*9F		
	516614	21 07.6	+52 20	9*9F		
	293127	21 08.5	-49 30	9*9FF		
	295871	21 08.5	-49 30	9*9FF		
	290878	21 08.8	+68 17	9*9FF		
	379011	21 10.7	+47 10	9*9F		
	441[illegible]	21 10.7	+47 10	9*9F		
	466051	21 10.7	+47 10	9*9F		

LDN 0970	492901	21 10.7	+47 10	9*9F		
	467819	21 10.8	+52 49	9*9F		
	470172	21 10.8	+52 49	9*9F		
	506037	21 10.8	+52 49	9*9F		
FRITS	262346	21 19.8	-69 57	3*3SS		
FRITS	271166	21 19.8	-69 57	3*3SS		
	491729	21 20.0	+52 03	9*9F		
LDN 1080	494266	21 20.0	+56 20	9*9FF		
LDN 1080	497213	21 20.0	+56 20	9*9FF		
	469190	21 20.5	+52 07	9*9F		
	514259	21 20.5	+52 07	9*9F		
	516810	21 20.5	+52 07	9*9F		
	507993	21 20.7	+52 24	9*9F		
	512110	21 20.7	+52 24	9*9F		
	514854	21 20.7	+52 24	9*9F		
	470369	21 20.9	+52 17	9*9F		
	507798	21 20.9	+52 17	9*9F		
	515632	21 20.9	+52 17	9*9F		
	514063	21 21.2	+52 14	9*9F		
	518576	21 21.2	+52 14	9*9F		
	515829	21 21.8	+52 24	9*9F		
	517793	21 21.8	+52 24	9*9F		
	520535	21 21.8	+52 24	9*9F		
	515049	21 22.2	+52 19	9*9F		
	517007	21 22.2	+52 19	9*9F		
	518969	21 22.2	+52 19	9*9F		
	509170	21 22.3	+52 29	9*9F		
	516221	21 22.3	+52 29	9*9F		
	518381	21 22.3	+52 29	9*9F		
LDN 1014	423520	21 22.4	+49 46	9*9F		
LDN 1014	457823	21 22.4	+49 46	9*9F		
LDN 1014	460566	21 22.4	+49 46	9*9F		
IC 5117	409795	21 30.6	+44 22	3*1S		
IC 5117	412159	21 30.6	+44 22	3*1S		
IC 5117	439008	21 30.6	+44 22	9*9F		
IC 5117	493880	21 30.6	+44 22	9*9F		
	422735	21 30.6	+55 41	9*9F		
	446254	21 30.6	+55 41	9*9F		
	474283	21 30.6	+55 41	9*9F		
	479770	21 30.6	+55 41	9*9F		
NGC 7083	263326	21 31.9	-64 08	9*9FF		
NGC 7083	268238	21 31.9	-64 08	9*9FF		
	387849	21 37.7	+57 55	9*9FF		
	411766	21 37.7	+57 55	9*9FF		
	435485	21 37.7	+57 55	9*9FF		
	502116	21 37.7	+57 55	9*9FF		
LDN 1110/1	502889	21 38.0	+57 40	9*9FF		
LDN 1110/1	504849	21 38.0	+57 40	9*9FF		
	409998	21 38.2	+50 01	9*9F		
	461352	21 38.2	+50 01	9*9F		
KHAV 748	499754	21 38.8	+57 39	9*9FF		
KHAV 748	502301	21 38.8	+57 39	9*9FF		
SCHO 1326	423131	21 39.8	+56 24	9*9F		
SCHO 1326	491924	21 39.8	+56 24	9*9F		
SCHO 1326	494075	21 39.8	+56 24	9*9F		
LDN 1104	411177	21 40.7	+56 30	9*9F		
LDN 1104	418428	21 40.7	+56 30	9*9F		
LDN 1104	495644	21 40.7	+56 30	9*9F		
LDN 1104	497800	21 40.7	+56 30	9*9F		
HH-103	390796	21 41.3	+65 50	9*9F		
HH-103	408633	21 41.3	+65 50	9*9F		
HH-103	546014	21 41.3	+65 50	9*9F		
HH-103	594806	21 41.3	+65 50	9*9F		
CED 196	379230	21 42.0	+65 53	9*9FF		
CED 196	390009	21 42.0	+65 53	9*9FF		
CED 196	494678	21 42.0	+65 53	9*9FF		
CED 196	497422	21 42.0	+65 53	9*9FF		
B 164	421765	21 44.9	+50 52	9*9FF		
B 164	454674	21 44.9	+50 52	9*9FF		
NGC 7130	886816	21 45.3	-35 11	9*9F		
	414891	21 45.4	+47 18	9*9FF		
	448994	21 45.4	+47 18	9*9FF		
NGC 7137	377445	21 45.9	+21 56	9*9F		
NGC 7137	379603	21 45.9	+21 56	9*9F		
BD+46 3471	456242	21 50.7	+46 59	3*3S		
BD+46 3471	464871	21 50.7	+46 59	3*3S		
BD+46 3471	459194	21 50.7	+46 59	9*9F		
BD+46 3471	461534	21 50.7	+46 59	9*9F		
LBN 0424	455853	21 52.0	+46 58	9*9FF		
LBN 0424	458598	21 52.0	+46 58	9*9FF		
B 170	413930	21 56.9	+58 42	9*9FF		
B 170	416475	21 56.9	+58 42	9*9FF		
B 170	504067	21 56.9	+58 42	9*9FF		
B 170	506810	21 56.9	+58 42	9*9FF		
NGC 7177	383916	21 58.3	+17 30	9*9F		
NGC 7177	386467	21 58.3	+17 30	9*9F		
IC 5152	304100	21 59.6	-51 32	9*9FF		
IC 5152	312332	21 59.6	-51 32	9*9FF		
LDN 1166	507201	22 04.0	+59 20	9*9FF		
LDN 1166	531501	22 04.0	+59 20	9*9FF		
LDN 1164	531307	22 05.0	+58 55	9*9FF		
LDN 1164	554237	22 05.0	+58 55	9*9FF		
NGC 7205	839224	22 05.2	-57 41	9*9F		
NGC 7205	841967	22 05.2	-57 41	9*9F		
NGC 7217	411157	22 05.6	+31 07	9*9FF		
NGC 7217	415676	22 05.6	+31 07	9*9FF		
CED 201	561489	22 12.3	+70 00	9*9FF		
CED 201	572658	22 12.3	+70 00	9*9FF		
IC 5179	864873	22 13.2	-37 06	9*9F		
IC 5179	870356	22 13.2	-37 06	9*9F		
NGC 7241	866995	22 13.5	+18 59	9*9F		
NGC 7241	870418	22 13.5	+18 59	9*9F		
	555419	22 17.7	+63 04	9*9F	BADGAIN	
	613616	22 17.7	+63 04	9*9F	BADGAIN	
IC 5201	327722	22 18.3	-46 19	9*9FF		
IC 5201	325858	22 18.3	-46 19	9*9FF		
IC 5201	336834	22 18.3	-46 19	9*9FF		
	348056	22 20.6	+37 22	9*9F		
	377846	22 20.6	+37 22	9*9F		
MF 2-2	456048	22 20.6	+47 33	3*1S		
MF 2-2	460159	22 20.6	+47 33	3*1S		
NGC 7320	419391	22 33.8	+33 42	9*9F		
NGC 7320	421162	22 33.8	+33 42	9*9F		
NGC 7331	420964	22 34.8	+34 09	9*9FF		
NGC 7331	458860	22 34.8	+34 09	9*9FF		
	507003	22 46.2	+57 49	9*9FF	BADGAIN	
	536793	22 46.2	+57 49	9*9FF	BADGAIN	
MRSL 108-00/1	558548	22 47.5	+59 39	9*9FF		
MRSL 108-00/1	583630	22 47.5	+59 39	9*9FF		
	553064	22 54.3	+61 46	9*9F	BADGAIN	
	594213	22 54.3	+61 46	9*9F	BADGAIN	
NGC 7424	355849	22 54.5	-41 20	9*9FF		
NGC 7424	364078	22 54.5	-41 20	9*9FF		
COU 99	555809	22 55.2	+62 25	9*9F		
COU 99	553457	22 55.2	+62 25	9*9F	BADGAIN	
	543848	22 55.7	+58 33	9*9FF		
	546396	22 55.7	+58 33	9*9FF		
	547190	22 56.0	+62 21	9*9F	BADGAIN	
	581676	22 56.0	+62 21	9*9F	BADGAIN	
NGC 7463	416647	22 59.4	+15 43	9*9F		
NGC 7463	416840	22 59.4	+15 43	9*9F		
NGC 7469	872679	23 00.7	+08 36	9*9F		
NGC 7469	875421	23 00.7	+08 36	9*9F		
NGC 7479	420753	23 02.4	+12 03	9*9F		
NGC 7479	422711	23 02.4	+12 03	9*9F		
LDN 1222	547577	23 02.7	+61 33	9*9F		
LDN 1222	550321	23 02.7	+61 33	9*9F		
MRSL 110+00/1	546993	23 03.1	+59 59	9*9F		
MRSL 110+00/1	585597	23 03.1	+59 59	9*9F		
NGC 7496	890936	23 07.0	-43 42	9*9F		
NGC 7496	896422	23 07.0	-43 42	9*9F		
	572269	23 08.5	+62 07	9*9F		
	596960	23 08.5	+62 07	9*9F		
NGC 7541	885416	23 12.2	+04 16	9*9F		
NGC 7541	888158	23 12.2	+04 16	9*9F		
NGC 7552	364274	23 13.4	-42 51	9*9FF		
NGC 7552	369761	23 13.4	-42 51	9*9FF		
NGC 7582	881527	23 15.6	-42 39	9*9F		
NGC 7582	884270	23 15.6	-42 39	9*9F		
NGC 7590	885249	23 16.2	-42 31	9*9F		
NGC 7590	887404	23 16.2	-42 31	9*9F		
NGC 7640	499162	23 19.7	+40 34	9*9FF		
NGC 7640	501903	23 19.7	+40 34	9*9FF		
CAS A	553262	23 21.2	+58 33	9*9F		
CAS A	586376	23 21.2	+58 33	9*9F		
NGC 7662	494853	23 23.5	+42 16	3*3SS		
NGC 7662	497000	23 23.5	+42 16	3*3SS		
NGC 7662	468389	23 23.5	+42 16	9*9F		
NGC 7662	471133	23 23.5	+42 16	9*9F		
	146008	23 23.5	+74 01	9*9F	1	
	149732	23 23.5	+74 01	9*9F	1	
	328480	23 23.8	+74 01	9*9F		
	330636	23 23.8	+74 01	9*9F		
	361405	23 23.8	+74 01	9*9F		
	113472	23 23.8	+74 01	9*9F	1	
HR 12	552080	23 24.0	+57 54	3*1S		
HR 12	556194	23 24.0	+57 54	3*1S		
IC 5332	384397	23 33.8	-36 21	9*9F		

D-083608
C-023043

```
TAPESCAN 4.4 - TAPE ANALYSIS AND COPYING PROGRAM          09/09/91    7:50:40.9   INPUT VOL=JJ0002   (LAST MOD-24OCT88)    PAGE   1
OPTIONS IN EFFECT: LIST001,NOHEX

C2148-T1  IRAS-DAX Chopped  Photometric Channel                    00010000  CPCFT1 : 489 observations  RA : 00 to 07 h
TAPEMARK NO 0001                BLOCK LENGTHS:  MIN=00160  MAX=00160  AVG=00160    NUMBER OF BLOCKS=000001
SIMPLE  =                  T / SIMPLE FITS FORMAT ( HEADER VERSION D1 850214) BITPIX  =                  16 / PIXEL VALUES: 2-BYT
TAPEMARK NO 0002                BLOCK LENGTHS:  MIN=14400  MAX=14400  AVG=14400    NUMBER OF BLOCKS=000001
SIMPLE  =                  T / SIMPLE FITS FORMAT ( HEADER VERSION D1 850214) BITPIX  =                  16 / PIXEL VALUES: 2-BYT
TAPEMARK NO 0003                BLOCK LENGTHS:  MIN=14400  MAX=14400  AVG=14400    NUMBER OF BLOCKS=000001
SIMPLE  =                  T / SIMPLE FITS FORMAT ( HEADER VERSION D1 850214) BITPIX  =                  16 / PIXEL VALUES: 2-BYT
TAPEMARK NO 0004                BLOCK LENGTHS:  MIN=14400  MAX=14400  AVG=14400    NUMBER OF BLOCKS=000001
SIMPLE  =                  T / SIMPLE FITS FORMAT ( HEADER VERSION D1 850214) BITPIX  =                  16 / PIXEL VALUES: 2-BYT
TAPEMARK NO 0005                BLOCK LENGTHS:  MIN=14400  MAX=14400  AVG=14400    NUMBER OF BLOCKS=000001
SIMPLE  =                  T / SIMPLE FITS FORMAT ( HEADER VERSION D1 850214) BITPIX  =                  16 / PIXEL VALUES: 2-BYT
TAPEMARK NO 0006                BLOCK LENGTHS:  MIN=11520  MAX=11520  AVG=11520    NUMBER OF BLOCKS=000001
SIMPLE  =                  T / SIMPLE FITS FORMAT ( HEADER VERSION D1 850214) BITPIX  =                  16 / PIXEL VALUES: 2-BYT
TAPEMARK NO 0007                BLOCK LENGTHS:  MIN=11520  MAX=11520  AVG=11520    NUMBER OF BLOCKS=000001
SIMPLE  =                  T / SIMPLE FITS FORMAT ( HEADER VERSION D1 850214) BITPIX  =                  16 / PIXEL VALUES: 2-BYT
TAPEMARK NO 0008                BLOCK LENGTHS:  MIN=14400  MAX=14400  AVG=14400    NUMBER OF BLOCKS=000001
SIMPLE  =                  T / SIMPLE FITS FORMAT ( HEADER VERSION D1 850214) BITPIX  =                  16 / PIXEL VALUES: 2-BYT
TAPEMARK NO 0009                BLOCK LENGTHS:  MIN=14400  MAX=14400  AVG=14400    NUMBER OF BLOCKS=000001
SIMPLE  =                  T / SIMPLE FITS FORMAT ( HEADER VERSION D1 850214) BITPIX  =                  16 / PIXEL VALUES: 2-BYT
TAPEMARK NO 0010                BLOCK LENGTHS:  MIN=11520  MAX=11520  AVG=11520    NUMBER OF BLOCKS=000001
SIMPLE  =                  T / SIMPLE FITS FORMAT ( HEADER VERSION D1 850214) BITPIX  =                  16 / PIXEL VALUES: 2-BYT
TAPEMARK NO 0011                BLOCK LENGTHS:  MIN=11520  MAX=11520  AVG=11520    NUMBER OF BLOCKS=000001
SIMPLE  =                  T / SIMPLE FITS FORMAT ( HEADER VERSION D1 850214) BITPIX  =                  16 / PIXEL VALUES: 2-BYT
TAPEMARK NO 0012                BLOCK LENGTHS:  MIN=14400  MAX=14400  AVG=14400    NUMBER OF BLOCKS=000001
SIMPLE  =                  T / SIMPLE FITS FORMAT ( HEADER VERSION D1 850214) BITPIX  =                  16 / PIXEL VALUES: 2-BYT
TAPEMARK NO 0013                BLOCK LENGTHS:  MIN=14400  MAX=14400  AVG=14400    NUMBER OF BLOCKS=000001
SIMPLE  =                  T / SIMPLE FITS FORMAT ( HEADER VERSION D1 850214) BITPIX  =                  16 / PIXEL VALUES: 2-BYT
TAPEMARK NO 0014                BLOCK LENGTHS:  MIN=14400  MAX=14400  AVG=14400    NUMBER OF BLOCKS=000001
```

```
SIMPLE  =                    T / SIMPLE FITS FORMAT ( HEADER VERSION D1 850214) BITPIX  =                    16 / PIXEL VALUES: 2-BYT
TAPEMARK NO 0967                 BLOCK LENGTHS:  MIN=11520  MAX=11520  AVG=11520    NUMBER OF BLOCKS=000001
SIMPLE  =                    T / SIMPLE FITS FORMAT ( HEADER VERSION D1 850214) BITPIX  =                    16 / PIXEL VALUES: 2-BYT
TAPEMARK NO 0968                 BLOCK LENGTHS:  MIN=14400  MAX=14400  AVG=14400    NUMBER OF BLOCKS=000001
SIMPLE  =                    T / SIMPLE FITS FORMAT ( HEADER VERSION D1 850214) BITPIX  =                    16 / PIXEL VALUES: 2-BYT
TAPEMARK NO 0969                 BLOCK LENGTHS:  MIN=14400  MAX=14400  AVG=14400    NUMBER OF BLOCKS=000001
SIMPLE  =                    T / SIMPLE FITS FORMAT ( HEADER VERSION D1 850214) BITPIX  =                    16 / PIXEL VALUES: 2-BYT
TAPEMARK NO 0970                 BLOCK LENGTHS:  MIN=14400  MAX=14400  AVG=14400    NUMBER OF BLOCKS=000001
SIMPLE  =                    T / SIMPLE FITS FORMAT ( HEADER VERSION D1 850214) BITPIX  =                    16 / PIXEL VALUES: 2-BYT
TAPEMARK NO 0971                 BLOCK LENGTHS:  MIN=14400  MAX=14400  AVG=14400    NUMBER OF BLOCKS=000001
SIMPLE  =                    T / SIMPLE FITS FORMAT ( HEADER VERSION D1 850214) BITPIX  =                    16 / PIXEL VALUES: 2-BYT
TAPEMARK NO 0972                 BLOCK LENGTHS:  MIN=14400  MAX=14400  AVG=14400    NUMBER OF BLOCKS=000001
SIMPLE  =                    T / SIMPLE FITS FORMAT ( HEADER VERSION D1 850214) BITPIX  =                    16 / PIXEL VALUES: 2-BYT
TAPEMARK NO 0973                 BLOCK LENGTHS:  MIN=14400  MAX=14400  AVG=14400    NUMBER OF BLOCKS=000001
SIMPLE  =                    T / SIMPLE FITS FORMAT ( HEADER VERSION D1 850214) BITPIX  =                    16 / PIXEL VALUES: 2-BYT
TAPEMARK NO 0974                 BLOCK LENGTHS:  MIN=14400  MAX=14400  AVG=14400    NUMBER OF BLOCKS=000001
SIMPLE  =                    T / SIMPLE FITS FORMAT ( HEADER VERSION D1 850214) BITPIX  =                    16 / PIXEL VALUES: 2-BYT
TAPEMARK NO 0975                 BLOCK LENGTHS:  MIN=14400  MAX=14400  AVG=14400    NUMBER OF BLOCKS=000001
SIMPLE  =                    T / SIMPLE FITS FORMAT ( HEADER VERSION D1 850214) BITPIX  =                    16 / PIXEL VALUES: 2-BYT
TAPEMARK NO 0976                 BLOCK LENGTHS:  MIN=14400  MAX=14400  AVG=14400    NUMBER OF BLOCKS=000001
SIMPLE  =                    T / SIMPLE FITS FORMAT ( HEADER VERSION D1 850214) BITPIX  =                    16 / PIXEL VALUES: 2-BYT
TAPEMARK NO 0977                 BLOCK LENGTHS:  MIN=14400  MAX=14400  AVG=14400    NUMBER OF BLOCKS=000001
SIMPLE  =                    T / SIMPLE FITS FORMAT ( HEADER VERSION D1 850214) BITPIX  =                    16 / PIXEL VALUES: 2-BYT
TAPEMARK NO 0978                 BLOCK LENGTHS:  MIN=14400  MAX=14400  AVG=14400    NUMBER OF BLOCKS=000001
SIMPLE  =                    T / SIMPLE FITS FORMAT ( HEADER VERSION D1 850214) BITPIX  =                    16 / PIXEL VALUES: 2-BYT
TAPEMARK NO 0979                 BLOCK LENGTHS:  MIN=14400  MAX=14400  AVG=14400    NUMBER OF BLOCKS=000001
C2148-T2  IRAS-DAX Chopped  Photometric Channel                          00010000  CPCFT2 : 624 observations  RA : 08 to 15 h
TAPEMARK NO 0980                 BLOCK LENGTHS:  MIN=00160  MAX=00160  AVG=00160    NUMBER OF BLOCKS=000001
```

```
TAPESCAN 4.4 - TAPE ANALYSIS AND COPYING PROGRAM          09/09/91    7:50:40.9   INPUT VOL=JJ0002   (LAST MOD-24OCT88)    PAGE 160
SIMPLE  =                    T / SIMPLE FITS FORMAT ( HEADER VERSION D1 850214) BITPIX  =                    16 / PIXEL VALUES: 2-BYT
TAPEMARK NO 2227                  BLOCK LENGTHS:  MIN=14400  MAX=14400  AVG=14400    NUMBER OF BLOCKS=000001
SIMPLE  =                    T / SIMPLE FITS FORMAT ( HEADER VERSION D1 850214) BITPIX  =                    16 / PIXEL VALUES: 2-BYT
TAPEMARK NO 2228                  BLOCK LENGTHS:  MIN=14400  MAX=14400  AVG=14400    NUMBER OF BLOCKS=000001
C2148-T3  IRAS-DAX Chopped   Photometric Channel                          00010000  CPCFT3 : 395 observations  RA : 16 to 23 h
TAPEMARK NO 2229                  BLOCK LENGTHS:  MIN=00160  MAX=00160  AVG=00160    NUMBER OF BLOCKS=000001
SIMPLE  =                    T / SIMPLE FITS FORMAT ( HEADER VERSION D1 850214) BITPIX  =                    16 / PIXEL VALUES: 2-BYT
TAPEMARK NO 2230                  BLOCK LENGTHS:  MIN=11520  MAX=11520  AVG=11520    NUMBER OF BLOCKS=000001
SIMPLE  =                    T / SIMPLE FITS FORMAT ( HEADER VERSION D1 850214) BITPIX  =                    16 / PIXEL VALUES: 2-BYT
TAPEMARK NO 2231                  BLOCK LENGTHS:  MIN=11520  MAX=11520  AVG=11520    NUMBER OF BLOCKS=000001
SIMPLE  =                    T / SIMPLE FITS FORMAT ( HEADER VERSION D1 850214) BITPIX  =                    16 / PIXEL VALUES: 2-BYT
TAPEMARK NO 2232                  BLOCK LENGTHS:  MIN=11520  MAX=11520  AVG=11520    NUMBER OF BLOCKS=000001
SIMPLE  =                    T / SIMPLE FITS FORMAT ( HEADER VERSION D1 850214) BITPIX  =                    16 / PIXEL VALUES: 2-BYT
TAPEMARK NO 2233                  BLOCK LENGTHS:  MIN=11520  MAX=11520  AVG=11520    NUMBER OF BLOCKS=000001
SIMPLE  =                    T / SIMPLE FITS FORMAT ( HEADER VERSION D1 850214) BITPIX  =                    16 / PIXEL VALUES: 2-BYT
TAPEMARK NO 2234                  BLOCK LENGTHS:  MIN=14400  MAX=14400  AVG=14400    NUMBER OF BLOCKS=000001
SIMPLE  =                    T / SIMPLE FITS FORMAT ( HEADER VERSION D1 850214) BITPIX  =                    16 / PIXEL VALUES: 2-BYT
TAPEMARK NO 2235                  BLOCK LENGTHS:  MIN=14400  MAX=14400  AVG=14400    NUMBER OF BLOCKS=000001
SIMPLE  =                    T / SIMPLE FITS FORMAT ( HEADER VERSION D1 850214) BITPIX  =                    16 / PIXEL VALUES: 2-BYT
TAPEMARK NO 2236                  BLOCK LENGTHS:  MIN=11520  MAX=11520  AVG=11520    NUMBER OF BLOCKS=000001
SIMPLE  =                    T / SIMPLE FITS FORMAT ( HEADER VERSION D1 850214) BITPIX  =                    16 / PIXEL VALUES: 2-BYT
TAPEMARK NO 2237                  BLOCK LENGTHS:  MIN=11520  MAX=11520  AVG=11520    NUMBER OF BLOCKS=000001
SIMPLE  =                    T / SIMPLE FITS FORMAT ( HEADER VERSION D1 850214) BITPIX  =                    16 / PIXEL VALUES: 2-BYT
TAPEMARK NO 2238                  BLOCK LENGTHS:  MIN=11520  MAX=11520  AVG=11520    NUMBER OF BLOCKS=000001
SIMPLE  =                    T / SIMPLE FITS FORMAT ( HEADER VERSION D1 850214) BITPIX  =                    16 / PIXEL VALUES: 2-BYT
TAPEMARK NO 2239                  BLOCK LENGTHS:  MIN=11520  MAX=11520  AVG=11520    NUMBER OF BLOCKS=000001
SIMPLE  =                    T / SIMPLE FITS FORMAT ( HEADER VERSION D1 850214) BITPIX  =                    16 / PIXEL VALUES: 2-BYT
TAPEMARK NO 2240                  BLOCK LENGTHS:  MIN=11520  MAX=11520  AVG=11520    NUMBER OF BLOCKS=000001
```

D-083698
C-028093

LECTURE V4.0 C.D.S. 18.04.89 16:53:15

2nd file (1st tape) 18.04.8

Lrecl= 80. Blksize= ~~2880.~~
Lecture partielle: 30 enreg. puis 1 ,tous les 1000.
Conversion ASCII -> EBCDIC. (code ASCII détecte automatiquement).

```
         1         2         3         4         5         6         7         8         9
12345678901234567890123456789012345678901234567890123456789012345678901234567890123456789012345678
--------------------------------------------------------------------------------------------------
SIMPLE  =                    T / SIMPLE FITS FORMAT ( HEADER VERSION D1 850214)
BITPIX  =                   16 / PIXEL VALUES: 2-BYTE TWOS-COMPLEMENT INTEGERS
NAXIS   =                    3 / NUMBER OF AXES IN THE DATA ARRAY
NAXIS1  =                   44 / NUMBER OF PIXELS/ROW  (RA) (COLUMNS)
NAXIS2  =                   53 / NUMBER OF ROWS        (DEC)
NAXIS3  =                    2 / NUMBER OF WAVELENGTHS (LAMBDA)
CTYPE1  = 'RA      '           /
CRVAL1  =          3.10000E+00 / COORDINATE TRANSFORMATIONS:
CRPIX1  =          2.30000E+01 /  X OF PIXEL = ( COLUMN - CRPIX1 )*CDELT1
CDELT1  =         -5.55556E-03 /  Y OF PIXEL = ( ROW - CRPIX2 )*CDELT2
CTYPE2  = 'DEC     '           / TRANSFORMATIONS BETWEEN (X,Y) AND (RA,DEC):
CRVAL2  =         -3.94667E+01 /  APPROXIMATE (FAR FROM THE CELESTIAL POLES):
CRPIX2  =          2.90000E+01 /   X = (CRVAL1 - RA)*COS(CRVAL2)
CDELT2  =          5.55556E-03 /   Y = DEC - CRVAL2
CTYPE3  = 'LAMBDA  '           /  EXACT:
CRPIX3  =          1.00000E+00 /   X = SIN(CRVAL1 - RA)*COS(DEC)
CRVAL3  =          5.00000E-05 /   Y = ( SIN(DEC)*COS(CRVAL2) ) -
CDELT3  =          5.00000E-05 /       ( COS(DEC)*SIN(CRVAL2)*COS(RA-CRVAL1) )
BSCALE  =          5.59164E-03 / DATA SCALE FACTOR (REAL=TAPE*BSCALE+BZERO)
BZERO   =          1.96742E+02 / DATA OFFSET VALUE
BUNIT   = 'MJY / SR'           / BRIGHTNESS UNITS
BLANK   =                -32767 / TAPE PIXEL VALUE ASSIGNED TO UNDEFINED VALUE
DATE-OBS= '01/06/83'           / DATE OF OBSERVATION       (JE 1983.416210)
TIME-OBS= '06:29:02'           / TIME OF OBSERVATION
INSTRUME= 'IRAS-CPC'           / INSTRUMENT USED IN OBSERVATION
ORIGIN  = 'ROG-GRON'           / NAME OF INSTITUTE THAT PRODUCED THIS FILE
OBJECT  = 'NGC 0055    '       / NAME OF THE OBSERVED OBJECT
COMMENT  IRAS CPC CLEAN IMAGE
COMMENT
COMMENT  START OF SCAN AT (COL,ROW)=( 5,26) TO (COL,ROW)=(20,49) IN 10 SECONDS.
```

Dernier enregistrement du fichier:

Nombre d'enregistrements = 180

LECTURE V4.0 C.D.S. 18.04.89 16:53:28 979th file (1st tape) 18.04.89

Lrecl= 80. Blksize= ~~2880~~.
Lecture partielle: 30 enreg. puis 1 ,tous les 1000.
Conversion ASCII -> EBCDIC. (code ASCII détecte automatiquement).

```
         1         2         3         4         5         6         7         8         9
123456789012345678901234567890123456789012345678901234567890123456789012345678901234567890123456789
-----------------------------------------------------------------------------------------------------
SIMPLE  =                    T / SIMPLE FITS FORMAT ( HEADER VERSION D1 850214)
BITPIX  =                   16 / PIXEL VALUES: 2-BYTE TWOS-COMPLEMENT INTEGERS
NAXIS   =                    3 / NUMBER OF AXES IN THE DATA ARRAY
NAXIS1  =                   48 / NUMBER OF PIXELS/ROW  (RA) (COLUMNS)
NAXIS2  =                   55 / NUMBER OF ROWS        (DEC)
NAXIS3  =                    2 / NUMBER OF WAVELENGTHS (LAMBDA)
CTYPE1  = 'RA      '           /
CRVAL1  =          1.19767E+02 / COORDINATE TRANSFORMATIONS:
CRPIX1  =          2.50000E+01 /  X OF PIXEL = ( COLUMN - CRPIX1 )*CDELT1
CDELT1  =         -5.55556E-03 /  Y OF PIXEL = ( ROW - CRPIX2 )*CDELT2
CTYPE2  = 'DEC     '           / TRANSFORMATIONS BETWEEN (X,Y) AND (RA,DEC):
CRVAL2  =         -4.53167E+01 /  APPROXIMATE (FAR FROM THE CELESTIAL POLES):
CRPIX2  =          3.30000E+01 /   X = (CRVAL1 - RA)*COS(CRVAL2)
CDELT2  =          5.55556E-03 /   Y = DEC - CRVAL2
CTYPE3  = 'LAMBDA  '           /  EXACT:
CRPIX3  =          1.00000E+00 /   X = SIN(CRVAL1 - RA)*COS(DEC)
CRVAL3  =          5.00000E-05 /   Y = ( SIN(DEC)*COS(CRVAL2) ) -
CDELT3  =          5.00000E-05 /       ( COS(DEC)*SIN(CRVAL2)*COS(RA-CRVAL1) )
BSCALE  =          1.00533E-02 / DATA SCALE FACTOR (REAL=TAPE*BSCALE+BZERO)
BZERO   =          3.40339E+02 / DATA OFFSET VALUE
BUNIT   = 'MJY / SR'           / BRIGHTNESS UNITS
BLANK   =                -32767 / TAPE PIXEL VALUE ASSIGNED TO UNDEFINED VALUE
DATE-OBS= '01/06/83'           / DATE OF OBSERVATION       (JE 1983.415784)
TIME-OBS= '02:45:04'           / TIME OF OBSERVATION
INSTRUME= 'IRAS-CPC'           / INSTRUMENT USED IN OBSERVATION
ORIGIN  = 'ROG-GRON'           / NAME OF INSTITUTE THAT PRODUCED THIS FILE
OBJECT  = 'VHE 01      '       / NAME OF THE OBSERVED OBJECT
COMMENT  IRAS CPC RAW IMAGE :NO DEGLITCHING, NO GAINCORRECTION APPLIED.
COMMENT
COMMENT  START OF SCAN AT (COL,ROW)=(25,49) TO (COL,ROW)=(44,29) IN 10 SECONDS.
```

Dernier enregistrement du fichier:

Nombre d'enregistrements = 180

LECTURE V4.0 C.D.S. 18.04.89 16:56:41 981st file (1st tape) 18.04.89

Lrecl= 80. Blksize= ~~2880~~.
Lecture partielle: 30 enreg. puis 1 ,tous les 1000.
Conversion ASCII -> EBCDIC. (code ASCII détecte automatiquement).

```
         1         2         3         4         5         6         7         8         9
12345678901234567890123456789012345678901234567890123456789012345678901234567890123456789012345678
--------------------------------------------------------------------------------------------------
SIMPLE  =                    T / SIMPLE FITS FORMAT ( HEADER VERSION D1 850214)
BITPIX  =                   16 / PIXEL VALUES: 2-BYTE TWOS-COMPLEMENT INTEGERS
NAXIS   =                    3 / NUMBER OF AXES IN THE DATA ARRAY
NAXIS1  =                   45 / NUMBER OF PIXELS/ROW  (RA) (COLUMNS)
NAXIS2  =                   55 / NUMBER OF ROWS        (DEC)
NAXIS3  =                    2 / NUMBER OF WAVELENGTHS (LAMBDA)
CTYPE1  = 'RA      '           /
CRVAL1  =          1.21067E+02 / COORDINATE TRANSFORMATIONS:
CRPIX1  =          2.30000E+01 /  X OF PIXEL = ( COLUMN - CRPIX1 )*CDELT1
CDELT1  =         -5.55556E-03 /  Y OF PIXEL = ( ROW - CRPIX2 )*CDELT2
CTYPE2  = 'DEC     '           / TRANSFORMATIONS BETWEEN (X,Y) AND (RA,DEC):
CRVAL2  =         -3.37500E+01 /  APPROXIMATE (FAR FROM THE CELESTIAL POLES):
CRPIX2  =          3.30000E+01 /   X = (CRVAL1 - RA)*COS(CRVAL2)
CDELT2  =          5.55556E-03 /   Y = DEC - CRVAL2
CTYPE3  = 'LAMBDA  '           /  EXACT:
CRPIX3  =          1.00000E+00 /   X = SIN(CRVAL1 - RA)*COS(DEC)
CRVAL3  =          5.00000E-05 /   Y = ( SIN(DEC)*COS(CRVAL2) ) -
CDELT3  =          5.00000E-05 /       ( COS(DEC)*SIN(CRVAL2)*COS(RA-CRVAL1) )
BSCALE  =          2.05755E-03 / DATA SCALE FACTOR (REAL=TAPE*BSCALE+BZERO)
BZERO   =          7.92493E+01 / DATA OFFSET VALUE
BUNIT   = 'MJY / SR'           / BRIGHTNESS UNITS
BLANK   =                -32767 / TAPE PIXEL VALUE ASSIGNED TO UNDEFINED VALUE
DATE-OBS= '20/05/83'           / DATE OF OBSERVATION       (JE 1983.383827)
TIME-OBS= '10:36:36'           / TIME OF OBSERVATION
INSTRUME= 'IRAS-CPC'           / INSTRUMENT USED IN OBSERVATION
ORIGIN  = 'ROG-GRON'           / NAME OF INSTITUTE THAT PRODUCED THIS FILE
OBJECT  = '            '       / NAME OF THE OBSERVED OBJECT
COMMENT  IRAS CPC CLEAN IMAGE
COMMENT  NOSSEAFTER
COMMENT  START OF SCAN AT (COL,ROW)=(28,48) TO (COL,ROW)=(41,24) IN 10 SECONDS.
```

Dernier enregistrement du fichier:

Nombre d'enregistrements = 180

LECTURE V4.0 C.D.S. 18.04.89 16:56:50 2228th file (1st tape) 18.04.89

Lrecl= 80. Blksize= 2880.
Lecture partielle: 30 enreg. puis 1 ,tous les 1000.
Conversion ASCII -> EBCDIC. (code ASCII détecté automatiquement).

```
         1         2         3         4         5         6         7         8         9
123456789012345678901234567890123456789012345678901234567890123456789012345678901234567890123456
--------------------------------------------------------------------------------------------------
SIMPLE  =                    T / SIMPLE FITS FORMAT ( HEADER VERSION D1 850214)
BITPIX  =                   16 / PIXEL VALUES: 2-BYTE TWOS-COMPLEMENT INTEGERS
NAXIS   =                    3 / NUMBER OF AXES IN THE DATA ARRAY
NAXIS1  =                   48 / NUMBER OF PIXELS/ROW  (RA) (COLUMNS)
NAXIS2  =                   52 / NUMBER OF ROWS        (DEC)
NAXIS3  =                    2 / NUMBER OF WAVELENGTHS (LAMBDA)
CTYPE1  = 'RA      '           /
CRVAL1  =          2.37667E+02 / COORDINATE TRANSFORMATIONS:
CRPIX1  =          2.40000E+01 /  X OF PIXEL = ( COLUMN - CRPIX1 )*CDELT1
CDELT1  =         -5.55556E-03 /  Y OF PIXEL = ( ROW - CRPIX2 )*CDELT2
CTYPE2  = 'DEC     '           / TRANSFORMATIONS BETWEEN (X,Y) AND (RA,DEC):
CRVAL2  =          6.24500E+01 /  APPROXIMATE (FAR FROM THE CELESTIAL POLES):
CRPIX2  =          3.00000E+01 /   X = (CRVAL1 - RA)*COS(CRVAL2)
CDELT2  =          5.55556E-03 /   Y = DEC - CRVAL2
CTYPE3  = 'LAMBDA  '           /  EXACT:
CRPIX3  =          1.00000E+00 /   X = SIN(CRVAL1 - RA)*COS(DEC)
CRVAL3  =          5.00000E-05 /   Y = ( SIN(DEC)*COS(CRVAL2) ) -
CDELT3  =          5.00000E-05 /       ( COS(DEC)*SIN(CRVAL2)*COS(RA-CRVAL1) )
BSCALE  =          1.61789E-03 / DATA SCALE FACTOR (REAL=TAPE*BSCALE+BZERO)
BZERO   =          6.46202E+01 / DATA OFFSET VALUE
BUNIT   = 'MJY / SR'           / BRIGHTNESS UNITS
BLANK   =                -32767 / TAPE PIXEL VALUE ASSIGNED TO UNDEFINED VALUE
DATE-OBS= '01/07/83'           / DATE OF OBSERVATION       (JE 1983.497625)
TIME-OBS= '00:10:12'           / TIME OF OBSERVATION
INSTRUME= 'IRAS-CPC'           / INSTRUMENT USED IN OBSERVATION
ORIGIN  = 'ROG-GRON'           / NAME OF INSTITUTE THAT PRODUCED THIS FILE
OBJECT  = 'NGC 6015      '     / NAME OF THE OBSERVED OBJECT
COMMENT  IRAS CPC RAW IMAGE :NO DEGLITCHING, NO GAINCORRECTION APPLIED.
COMMENT
COMMENT  START OF SCAN AT (COL,ROW)=(22,48) TO (COL,ROW)=(32,40) IN 10 SECONDS.
```

Dernier enregistrement du fichier:

Nombre d'enregistrements = 180

LECTURE V4.0 C.D.S. 18.04.89 16:59:35 2nd file (2nd tape) 18.04.8

Lrecl= 80. Blksize= ~~2880~~.
Lecture partielle: 30 enreg. puis 1 ,tous les 1000.
Conversion ASCII -> EBCDIC. (code ASCII détecte automatiquement).

```
         1         2         3         4         5         6         7         8         9
123456789012345678901234567890123456789012345678901234567890123456789012345678901234567890123456
--------------------------------------------------------------------------------------------------
SIMPLE  =                    T / SIMPLE FITS FORMAT ( HEADER VERSION D1 850214)
BITPIX  =                   16 / PIXEL VALUES: 2-BYTE TWOS-COMPLEMENT INTEGERS
NAXIS   =                    3 / NUMBER OF AXES IN THE DATA ARRAY
NAXIS1  =                   40 / NUMBER OF PIXELS/ROW  (RA) (COLUMNS)
NAXIS2  =                   51 / NUMBER OF ROWS        (DEC)
NAXIS3  =                    2 / NUMBER OF WAVELENGTHS (LAMBDA)
CTYPE1  = 'RA      '           /
CRVAL1  =          2.40800E+02 / COORDINATE TRANSFORMATIONS:
CRPIX1  =          2.10000E+01 /  X OF PIXEL = ( COLUMN - CRPIX1 )*CDELT1
CDELT1  =         -5.55556E-03 /  Y OF PIXEL = ( ROW - CRPIX2 )*CDELT2
CTYPE2  = 'DEC     '           / TRANSFORMATIONS BETWEEN (X,Y) AND (RA,DEC):
CRVAL2  =          6.66333E+01 /  APPROXIMATE (FAR FROM THE CELESTIAL POLES):
CRPIX2  =          3.00000E+01 /   X = (CRVAL1 - RA)*COS(CRVAL2)
CDELT2  =          5.55556E-03 /   Y = DEC - CRVAL2
CTYPE3  = 'LAMBDA  '           /  EXACT:
CRPIX3  =          1.00000E+00 /   X = SIN(CRVAL1 - RA)*COS(DEC)
CRVAL3  =          5.00000E-05 /   Y = ( SIN(DEC)*COS(CRVAL2) ) -
CDELT3  =          5.00000E-05 /       ( COS(DEC)*SIN(CRVAL2)*COS(RA-CRVAL1) )
BSCALE  =          7.13531E-04 / DATA SCALE FACTOR (REAL=TAPE*BSCALE+BZERO)
BZERO   =          3.46445E+01 / DATA OFFSET VALUE
BUNIT   = 'MJY / SR'           / BRIGHTNESS UNITS
BLANK   =                -32767 / TAPE PIXEL VALUE ASSIGNED TO UNDEFINED VALUE
DATE-OBS= '11/09/83'           / DATE OF OBSERVATION       (JE 1983.696330)
TIME-OBS= '14:00:49'           / TIME OF OBSERVATION
INSTRUME= 'IRAS-CPC'           / INSTRUMENT USED IN OBSERVATION
ORIGIN  = 'ROG-GRON'           / NAME OF INSTITUTE THAT PRODUCED THIS FILE
OBJECT  = '            '       / NAME OF THE OBSERVED OBJECT
COMMENT  IRAS CPC CLEAN IMAGE
COMMENT
COMMENT  START OF SCAN AT (COL,ROW)=(36,37) TO (COL,ROW)=(32,24) IN 10 SECONDS.
```

Dernier enregistrement du fichier:

Nombre d'enregistrements = 144

LECTURE V4.0 C.D.S. 18.04.89 16:59:42 791st file (2nd tape) 18.04.89

Lrecl= 80. Blksize= 2880.
Lecture partielle: 30 enreg. puis 1 ,tous les 1000.
Conversion ASCII -> EBCDIC. (code ASCII détecte automatiquement).

```
         1         2         3         4         5         6         7         8         9
12345678901234567890123456789012345678901234567890123456789012345678901234567890123456789012345678901234567
-------------------------------------------------------------------------------------------------------------
SIMPLE  =                    T / SIMPLE FITS FORMAT ( HEADER VERSION D1 850214)
BITPIX  =                   16 / PIXEL VALUES: 2-BYTE TWOS-COMPLEMENT INTEGERS
NAXIS   =                    3 / NUMBER OF AXES IN THE DATA ARRAY
NAXIS1  =                   45 / NUMBER OF PIXELS/ROW  (RA) (COLUMNS)
NAXIS2  =                   51 / NUMBER OF ROWS        (DEC)
NAXIS3  =                    2 / NUMBER OF WAVELENGTHS (LAMBDA)
CTYPE1  = 'RA      '          /
CRVAL1  =          3.58500E+02 / COORDINATE TRANSFORMATIONS:
CRPIX1  =          2.30000E+01 /  X OF PIXEL = ( COLUMN - CRPIX1 )*CDELT1
CDELT1  =         -5.55556E-03 /  Y OF PIXEL = ( ROW - CRPIX2 )*CDELT2
CTYPE2  = 'DEC     '          / TRANSFORMATIONS BETWEEN (X,Y) AND (RA,DEC):
CRVAL2  =          5.82500E+01 /  APPROXIMATE (FAR FROM THE CELESTIAL POLES):
CRPIX2  =          2.80000E+01 /   X = (CRVAL1 - RA)*COS(CRVAL2)
CDELT2  =          5.55556E-03 /   Y = DEC - CRVAL2
CTYPE3  = 'LAMBDA  '          /  EXACT:
CRPIX3  =          1.00000E+00 /   X = SIN(CRVAL1 - RA)*COS(DEC)
CRVAL3  =          5.00000E-05 /   Y = ( SIN(DEC)*COS(CRVAL2) ) -
CDELT3  =          5.00000E-05 /       ( COS(DEC)*SIN(CRVAL2)*COS(RA-CRVAL1) )
BSCALE  =          3.21897E-03 / DATA SCALE FACTOR (REAL=TAPE*BSCALE+BZERO)
BZERO   =          1.22663E+02 / DATA OFFSET VALUE
BUNIT   = 'MJY / SR'           / BRIGHTNESS UNITS
BLANK   =                -32767 / TAPE PIXEL VALUE ASSIGNED TO UNDEFINED VALUE
DATE-OBS= '29/07/83'           / DATE OF OBSERVATION       (JE 1983.575012)
TIME-OBS= '06:32:37'           / TIME OF OBSERVATION
INSTRUME= 'IRAS-CPC'           / INSTRUMENT USED IN OBSERVATION
ORIGIN  = 'ROG-GRON'           / NAME OF INSTITUTE THAT PRODUCED THIS FILE
OBJECT  = 'LDN 1253     '      / NAME OF THE OBSERVED OBJECT
COMMENT  IRAS CPC RAW IMAGE :NO DEGLITCHING, NO GAINCORRECTION APPLIED.
COMMENT
COMMENT  START OF SCAN AT (COL,ROW)=( 4,27) TO (COL,ROW)=(13,37) IN 10 SECONDS.
```

Dernier enregistrement du fichier:

Nombre d'enregistrements = 180

LECTURE V4.0 C.D.S. 18.04.89 17:00:52 792nd file (2nd tape) 18.04.89

Lrecl= 80. Blksize= 2880.
Lecture partielle: 30 enreg. puis 1 .tous les 1000.
Conversion ASCII -> EBCDIC. (code ASCII détecte automatiquement).

```
         1         2         3         4         5         6         7         8         9
123456789012345678901234567890123456789012345678901234567890123456789012345678901234567890123456789
-----------------------------------------------------------------------------------------------------
XTENSION = 'TABLE   '           / CPC (IRAS) list of observations on tape
BITPIX   =                    8 /
NAXIS    =                    2 / 2D table
NAXIS1   =                   40 / max number of characters per row
NAXIS2   =                 1508 / number of rows (observations)
TFIELDS  =                    8 / number of fields per row
EXTNAME  = 'CPC-OBS '           /
EXTVER   =                    2 / Second version of the list

TTYPE1   = 'OBJ.NAME'           / astronomical name of object
TBCOL1   =                    1 / max 13 char
TFORM1   = 'A13     '           /

TTYPE2   = 'TIME OBS'           / time of observation
TBCOL2   =                   14 / 1 unit is about 31.6 sec time
TFORM2   = 'I6      '           /
TUNIT2   = 'MICRO.YR'           / fraction of year since 1983.0

TTYPE3   = 'RAH     '           / Right Ascension; hour part
TBCOL3   =                   20 /
TFORM3   = 'I3      '           /
TUNIT3   = 'HR      '           /

TTYPE4   = 'RAM     '           / Right Ascension; minutes and decimal fraction
TBCOL4   =                   23 /
TFORM4   = 'F5.1    '           /
TUNIT4   = 'MIN     '           /

TTYPE5   = 'DECDSIGN'           / Declination sign
TBCOL5   =                   28 /
```

Dernier enregistrement du fichier:

Nombre d'enregistrements = 828

2nd file (1st tape)


```
Lrecl=   80. Blksize= ~~2880.~~
Lecture partielle:    30 enreg. puis   1 ,tous les  1000.
Conversion ASCII -> EBCDIC. (code ASCII détecte automatiquement).

         1         2         3         4         5         6         7         8         9        10        11        12        13
1234567890123456789012345678901234567890123456789012345678901234567890123456789012345678901234567890123456789012345678901234567890123456789012
--------------------------------------------------------------------------------------------------------------------------------------------
SIMPLE  =                    T / SIMPLE FITS FORMAT ( HEADER VERSION D1 850214)
BITPIX  =                   16 / PIXEL VALUES: 2-BYTE TWOS-COMPLEMENT INTEGERS
NAXIS   =                    3 / NUMBER OF AXES IN THE DATA ARRAY
NAXIS1  =                   44 / NUMBER OF PIXELS/ROW  (RA) (COLUMNS)
NAXIS2  =                   53 / NUMBER OF ROWS        (DEC)
NAXIS3  =                    2 / NUMBER OF WAVELENGTHS (LAMBDA)
CTYPE1  = 'RA      '           /
CRVAL1  =          3.10000E+00 / COORDINATE TRANSFORMATIONS:
CRPIX1  =          2.30000E+01 /  X OF PIXEL = ( COLUMN - CRPIX1 )*CDELT1
CDELT1  =         -5.55556E-03 /  Y OF PIXEL = ( ROW - CRPIX2 )*CDELT2
CTYPE2  = 'DEC     '           / TRANSFORMATIONS BETWEEN (X,Y) AND (RA,DEC):
CRVAL2  =         -3.94667E+01 /  APPROXIMATE (FAR FROM THE CELESTIAL POLES):
CRPIX2  =          2.90000E+01 /   X = (CRVAL1 - RA)*COS(CRVAL2)
CDELT2  =          5.55556E-03 /   Y = DEC - CRVAL2
CTYPE3  = 'LAMBDA  '           /  EXACT:
CRPIX3  =          1.00000E+00 /   X = SIN(CRVAL1 - RA)*COS(DEC)
CRVAL3  =          5.00000E-05 /   Y = ( SIN(DEC)*COS(CRVAL2) ) -
CDELT3  =          5.00000E-05 /       ( COS(DEC)*SIN(CRVAL2)*COS(RA-CRVAL1) )
BSCALE  =          5.59164E-03 / DATA SCALE FACTOR (REAL=TAPE*BSCALE+BZERO)
BZERO   =          1.96742E+02 / DATA OFFSET VALUE
BUNIT   = 'MJY / SR'           / BRIGHTNESS UNITS
BLANK   =                -32767 / TAPE PIXEL VALUE ASSIGNED TO UNDEFINED VALUE
DATE-OBS= '01/06/83'           / DATE OF OBSERVATION       (JE 1983.416210)
TIME-OBS= '06:29:02'           / TIME OF OBSERVATION
INSTRUME= 'IRAS-CPC'           / INSTRUMENT USED IN OBSERVATION
ORIGIN  = 'ROG-GRON'           / NAME OF INSTITUTE THAT PRODUCED THIS FILE
OBJECT  = 'NGC 0055    '       / NAME OF THE OBSERVED OBJECT
COMMENT  IRAS CPC CLEAN IMAGE
COMMENT
COMMENT  START OF SCAN AT (COL,ROW)=( 5,26) TO (COL,ROW)=(20,49) IN 10 SECONDS.

Dernier enregistrement du fichier:


Nombre d'enregistrements =      180
```

```
Lrecl=   80. Blksize= 2880.
Lecture partielle:    30 enreg. puis   1 ,tous les  1000.
Conversion ASCII -> EBCDIC. (code ASCII détecte automatiquement).

         1         2         3         4         5         6         7         8         9        10        11        12        13
1234567890123456789012345678901234567890123456789012345678901234567890123456789012345678901234567890123456789012345678901234567890123456789012
--------------------------------------------------------------------------------------------------------------------------------------------
SIMPLE  =                    T / SIMPLE FITS FORMAT ( HEADER VERSION D1 850214)
BITPIX  =                   16 / PIXEL VALUES: 2-BYTE TWOS-COMPLEMENT INTEGERS
NAXIS   =                    3 / NUMBER OF AXES IN THE DATA ARRAY
NAXIS1  =                   48 / NUMBER OF PIXELS/ROW  (RA) (COLUMNS)
NAXIS2  =                   55 / NUMBER OF ROWS        (DEC)
NAXIS3  =                    2 / NUMBER OF WAVELENGTHS (LAMBDA)
CTYPE1  = 'RA      '           /
CRVAL1  =          1.19767E+02 / COORDINATE TRANSFORMATIONS:
CRPIX1  =          2.50000E+01 /  X OF PIXEL = ( COLUMN - CRPIX1 )*CDELT1
CDELT1  =         -5.55556E-03 /  Y OF PIXEL = ( ROW - CRPIX2 )*CDELT2
CTYPE2  = 'DEC     '           / TRANSFORMATIONS BETWEEN (X,Y) AND (RA,DEC):
CRVAL2  =         -4.53167E+01 /  APPROXIMATE (FAR FROM THE CELESTIAL POLES):
CRPIX2  =          3.30000E+01 /   X = (CRVAL1 - RA)*COS(CRVAL2)
CDELT2  =          5.55556E-03 /   Y = DEC - CRVAL2
CTYPE3  = 'LAMBDA  '           /  EXACT:
CRPIX3  =          1.00000E+00 /   X = SIN(CRVAL1 - RA)*COS(DEC)
CRVAL3  =          5.00000E-05 /   Y = ( SIN(DEC)*COS(CRVAL2) ) -
CDELT3  =          5.00000E-05 /       ( COS(DEC)*SIN(CRVAL2)*COS(RA-CRVAL1) )
BSCALE  =          1.00533E-02 / DATA SCALE FACTOR (REAL=TAPE*BSCALE+BZERO)
BZERO   =          3.40339E+02 / DATA OFFSET VALUE
BUNIT   = 'MJY / SR'           / BRIGHTNESS UNITS
BLANK   =                -32767 / TAPE PIXEL VALUE ASSIGNED TO UNDEFINED VALUE
DATE-OBS= '01/06/83'           / DATE OF OBSERVATION       (JE 1983.415784)
TIME-OBS= '02:45:04'           / TIME OF OBSERVATION
INSTRUME= 'IRAS-CPC'           / INSTRUMENT USED IN OBSERVATION
ORIGIN  = 'ROG-GRON'           / NAME OF INSTITUTE THAT PRODUCED THIS FILE
OBJECT  = 'VHE 01      '       / NAME OF THE OBSERVED OBJECT
COMMENT  IRAS CPC RAW IMAGE :NO DEGLITCHING, NO GAINCORRECTION APPLIED.
COMMENT
COMMENT  START OF SCAN AT (COL,ROW)=(25,49) TO (COL,ROW)=(44,29) IN 10 SECONDS.

Dernier enregistrement du fichier:


Nombre d'enregistrements =     180
```

```
                    Lrecl=   80. Blksize= ~~2880~~.
                    Lecture partielle:    30 enreg. puis   1 ,tous les  1000.
                    Conversion ASCII -> EBCDIC. (code ASCII détecte automatiquement).

         1         2         3         4         5         6         7         8         9         10        11        12        13
1234567890123456789012345678901234567890123456789012345678901234567890123456789012345678901234567890123456789012345678901234567890123456789012
--------------------------------------------------------------------------------------------------------------------------------------------
SIMPLE  =                    T / SIMPLE FITS FORMAT ( HEADER VERSION D1 850214)
BITPIX  =                   16 / PIXEL VALUES: 2-BYTE TWOS-COMPLEMENT INTEGERS
NAXIS   =                    3 / NUMBER OF AXES IN THE DATA ARRAY
NAXIS1  =                   45 / NUMBER OF PIXELS/ROW  (RA) (COLUMNS)
NAXIS2  =                   55 / NUMBER OF ROWS        (DEC)
NAXIS3  =                    2 / NUMBER OF WAVELENGTHS (LAMBDA)
CTYPE1  = 'RA      '           /
CRVAL1  =           1.21067E+02 / COORDINATE TRANSFORMATIONS:
CRPIX1  =           2.30000E+01 /  X OF PIXEL = ( COLUMN - CRPIX1 )*CDELT1
CDELT1  =          -5.55556E-03 /  Y OF PIXEL = ( ROW - CRPIX2 )*CDELT2
CTYPE2  = 'DEC     '            / TRANSFORMATIONS BETWEEN (X,Y) AND (RA,DEC):
CRVAL2  =          -3.37500E+01 /  APPROXIMATE (FAR FROM THE CELESTIAL POLES):
CRPIX2  =           3.30000E+01 /   X = (CRVAL1 - RA)*COS(CRVAL2)
CDELT2  =           5.55556E-03 /   Y = DEC - CRVAL2
CTYPE3  = 'LAMBDA  '            /  EXACT:
CRPIX3  =           1.00000E+00 /   X = SIN(CRVAL1 - RA)*COS(DEC)
CRVAL3  =           5.00000E-05 /   Y = ( SIN(DEC)*COS(CRVAL2) ) -
CDELT3  =           5.00000E-05 /       ( COS(DEC)*SIN(CRVAL2)*COS(RA-CRVAL1) )
BSCALE  =           2.05755E-03 / DATA SCALE FACTOR (REAL=TAPE*BSCALE+BZERO)
BZERO   =           7.92493E+01 / DATA OFFSET VALUE
BUNIT   = 'MJY / SR'            / BRIGHTNESS UNITS
BLANK   =                -32767 / TAPE PIXEL VALUE ASSIGNED TO UNDEFINED VALUE
DATE-OBS= '20/05/83'            / DATE OF OBSERVATION       (JE 1983.383827)
TIME-OBS= '10:36:36'            / TIME OF OBSERVATION
INSTRUME= 'IRAS-CPC'            / INSTRUMENT USED IN OBSERVATION
ORIGIN  = 'ROG-GRON'            / NAME OF INSTITUTE THAT PRODUCED THIS FILE
OBJECT  = '                '    / NAME OF THE OBSERVED OBJECT
COMMENT  IRAS CPC CLEAN IMAGE
COMMENT  NOSSEAFTER
COMMENT  START OF SCAN AT (COL,ROW)=(28,48) TO (COL,ROW)=(41,24) IN 10 SECONDS.

Dernier enregistrement du fichier:


Nombre d'enregistrements =      180
```

```
                    Lrecl=   80. Blksize= 2880.
                    Lecture partielle:    30 enreg. puis   1 ,tous les  1000.
                    Conversion ASCII -> EBCDIC. (code ASCII détecte automatiquement).

          1         2         3         4         5         6         7         8         9         10        11        12        13
1234567890123456789012345678901234567890123456789012345678901234567890123456789012345678901234567890123456789012345678901234567890123456789012
--------------------------------------------------------------------------------------------------------------------------------------------
SIMPLE  =                    T / SIMPLE FITS FORMAT ( HEADER VERSION D1 850214)
BITPIX  =                   16 / PIXEL VALUES: 2-BYTE TWOS-COMPLEMENT INTEGERS
NAXIS   =                    3 / NUMBER OF AXES IN THE DATA ARRAY
NAXIS1  =                   48 / NUMBER OF PIXELS/ROW  (RA) (COLUMNS)
NAXIS2  =                   52 / NUMBER OF ROWS        (DEC)
NAXIS3  =                    2 / NUMBER OF WAVELENGTHS (LAMBDA)
CTYPE1  = 'RA      '           /
CRVAL1  =          2.37667E+02 / COORDINATE TRANSFORMATIONS:
CRPIX1  =          2.40000E+01 /  X OF PIXEL = ( COLUMN - CRPIX1 )*CDELT1
CDELT1  =         -5.55556E-03 /  Y OF PIXEL = ( ROW - CRPIX2 )*CDELT2
CTYPE2  = 'DEC     '           / TRANSFORMATIONS BETWEEN (X,Y) AND (RA,DEC):
CRVAL2  =          6.24500E+01 /  APPROXIMATE (FAR FROM THE CELESTIAL POLES):
CRPIX2  =          3.00000E+01 /   X = (CRVAL1 - RA)*COS(CRVAL2)
CDELT2  =          5.55556E-03 /   Y = DEC - CRVAL2
CTYPE3  = 'LAMBDA  '           /  EXACT:
CRPIX3  =          1.00000E+00 /   X = SIN(CRVAL1 - RA)*COS(DEC)
CRVAL3  =          5.00000E-05 /   Y = ( SIN(DEC)*COS(CRVAL2) ) -
CDELT3  =          5.00000E-05 /       ( COS(DEC)*SIN(CRVAL2)*COS(RA-CRVAL1) )
BSCALE  =          1.61789E-03 / DATA SCALE FACTOR (REAL=TAPE*BSCALE+BZERO)
BZERO   =          6.46202E+01 / DATA OFFSET VALUE
BUNIT   = 'MJY / SR'           / BRIGHTNESS UNITS
BLANK   =                -32767 / TAPE PIXEL VALUE ASSIGNED TO UNDEFINED VALUE
DATE-OBS= '01/07/83'           / DATE OF OBSERVATION       (JE 1983.497625)
TIME-OBS= '00:10:12'           / TIME OF OBSERVATION
INSTRUME= 'IRAS-CPC'           / INSTRUMENT USED IN OBSERVATION
ORIGIN  = 'ROG-GRON'           / NAME OF INSTITUTE THAT PRODUCED THIS FILE
OBJECT  = 'NGC 6015      '     / NAME OF THE OBSERVED OBJECT
COMMENT  IRAS CPC RAW IMAGE :NO DEGLITCHING, NO GAINCORRECTION APPLIED.
COMMENT
COMMENT  START OF SCAN AT (COL,ROW)=(22,48) TO (COL,ROW)=(32,40) IN 10 SECONDS.

Dernier enregistrement du fichier:


Nombre d'enregistrements =      180
```

```
LECTURE   V4.0     C.D.S.     18.04.89   16:59:35   2nd file (2nd tape)                18.04.89   16:59:35     Page   1

                   Lrecl=   80. Blksize= ~~2880~~.
                   Lecture partielle:    30 enreg. puis   1 ,tous les  1000.
                   Conversion ASCII -> EBCDIC. (code ASCII détecte automatiquement).

         1         2         3         4         5         6         7         8         9        10        11        12        13
12345678901234567890123456789012345678901234567890123456789012345678901234567890123456789012345678901234567890123456789012
--------------------------------------------------------------------------------------------------------------------------------
SIMPLE  =                    T / SIMPLE FITS FORMAT ( HEADER VERSION D1 850214)
BITPIX  =                   16 / PIXEL VALUES: 2-BYTE TWOS-COMPLEMENT INTEGERS
NAXIS   =                    3 / NUMBER OF AXES IN THE DATA ARRAY
NAXIS1  =                   40 / NUMBER OF PIXELS/ROW  (RA) (COLUMNS)
NAXIS2  =                   51 / NUMBER OF ROWS        (DEC)
NAXIS3  =                    2 / NUMBER OF WAVELENGTHS (LAMBDA)
CTYPE1  = 'RA      '          /
CRVAL1  =          2.40800E+02 / COORDINATE TRANSFORMATIONS:
CRPIX1  =          2.10000E+01 /  X OF PIXEL = ( COLUMN - CRPIX1 )*CDELT1
CDELT1  =         -5.55556E-03 /  Y OF PIXEL = ( ROW - CRPIX2 )*CDELT2
CTYPE2  = 'DEC     '          / TRANSFORMATIONS BETWEEN (X,Y) AND (RA,DEC):
CRVAL2  =          6.66333E+01 /  APPROXIMATE (FAR FROM THE CELESTIAL POLES):
CRPIX2  =          3.00000E+01 /   X = (CRVAL1 - RA)*COS(CRVAL2)
CDELT2  =          5.55556E-03 /   Y = DEC - CRVAL2
CTYPE3  = 'LAMBDA  '          /  EXACT:
CRPIX3  =          1.00000E+00 /   X = SIN(CRVAL1 - RA)*COS(DEC)
CRVAL3  =          5.00000E-05 /   Y = ( SIN(DEC)*COS(CRVAL2) ) -
CDELT3  =          5.00000E-05 /       ( COS(DEC)*SIN(CRVAL2)*COS(RA-CRVAL1) )
BSCALE  =          7.13531E-04 / DATA SCALE FACTOR (REAL=TAPE*BSCALE+BZERO)
BZERO   =          3.46445E+01 / DATA OFFSET VALUE
BUNIT   = 'MJY / SR'           / BRIGHTNESS UNITS
BLANK   =               -32767 / TAPE PIXEL VALUE ASSIGNED TO UNDEFINED VALUE
DATE-OBS= '11/09/83'           / DATE OF OBSERVATION       (JE 1983.696330)
TIME-OBS= '14:00:49'           / TIME OF OBSERVATION
INSTRUME= 'IRAS-CPC'           / INSTRUMENT USED IN OBSERVATION
ORIGIN  = 'ROG-GRON'           / NAME OF INSTITUTE THAT PRODUCED THIS FILE
OBJECT  = '            '       / NAME OF THE OBSERVED OBJECT
COMMENT  IRAS CPC CLEAN IMAGE
COMMENT
COMMENT  START OF SCAN AT (COL,ROW)=(36,37) TO (COL,ROW)=(32,24) IN 10 SECONDS.

Dernier enregistrement du fichier:


Nombre d'enregistrements =     144
```

791st file (2nd tape)


```
                Lrecl=   80. Blksize= 2880.
                Lecture partielle:    30 enreg. puis   1 ,tous les  1000.
                Conversion ASCII -> EBCDIC. (code ASCII détecte automatiquement).

         1         2         3         4         5         6         7         8         9         10        11        12        13
1234567890123456789012345678901234567890123456789012345678901234567890123456789012345678901234567890123456789012345678901234567890123456789012
--------------------------------------------------------------------------------------------------------------------------------------------
SIMPLE  =                    T / SIMPLE FITS FORMAT ( HEADER VERSION D1 850214)
BITPIX  =                   16 / PIXEL VALUES: 2-BYTE TWOS-COMPLEMENT INTEGERS
NAXIS   =                    3 / NUMBER OF AXES IN THE DATA ARRAY
NAXIS1  =                   45 / NUMBER OF PIXELS/ROW  (RA) (COLUMNS)
NAXIS2  =                   51 / NUMBER OF ROWS        (DEC)
NAXIS3  =                    2 / NUMBER OF WAVELENGTHS (LAMBDA)
CTYPE1  = 'RA      '           /
CRVAL1  =          3.58500E+02 / COORDINATE TRANSFORMATIONS:
CRPIX1  =          2.30000E+01 /  X OF PIXEL = ( COLUMN - CRPIX1 )*CDELT1
CDELT1  =         -5.55556E-03 /  Y OF PIXEL = ( ROW - CRPIX2 )*CDELT2
CTYPE2  = 'DEC     '           / TRANSFORMATIONS BETWEEN (X,Y) AND (RA,DEC):
CRVAL2  =          5.82500E+01 /  APPROXIMATE (FAR FROM THE CELESTIAL POLES):
CRPIX2  =          2.80000E+01 /   X = (CRVAL1 - RA)*COS(CRVAL2)
CDELT2  =          5.55556E-03 /   Y = DEC - CRVAL2
CTYPE3  = 'LAMBDA  '           /  EXACT:
CRPIX3  =          1.00000E+00 /   X = SIN(CRVAL1 - RA)*COS(DEC)
CRVAL3  =          5.00000E-05 /   Y = ( SIN(DEC)*COS(CRVAL2) ) -
CDELT3  =          5.00000E-05 /       ( COS(DEC)*SIN(CRVAL2)*COS(RA-CRVAL1) )
BSCALE  =          3.21897E-03 / DATA SCALE FACTOR (REAL=TAPE*BSCALE+BZERO)
BZERO   =          1.22663E+02 / DATA OFFSET VALUE
BUNIT   = 'MJY / SR'           / BRIGHTNESS UNITS
BLANK   =                -32767 / TAPE PIXEL VALUE ASSIGNED TO UNDEFINED VALUE
DATE-OBS= '29/07/83'           / DATE OF OBSERVATION       (JE 1983.575012)
TIME-OBS= '06:32:37'           / TIME OF OBSERVATION
INSTRUME= 'IRAS-CPC'           / INSTRUMENT USED IN OBSERVATION
ORIGIN  = 'ROG-GRON'           / NAME OF INSTITUTE THAT PRODUCED THIS FILE
OBJECT  = 'LDN 1253    '       / NAME OF THE OBSERVED OBJECT
COMMENT  IRAS CPC RAW IMAGE :NO DEGLITCHING, NO GAINCORRECTION APPLIED.
COMMENT
COMMENT  START OF SCAN AT (COL,ROW)=( 4,27) TO (COL,ROW)=(13,37) IN 10 SECONDS.

Dernier enregistrement du fichier:


Nombre d'enregistrements =      180
```

```
Lrecl=   80. Blksize= 2880.
Lecture partielle:    30 enreg. puis   1 ,tous les  1000.
Conversion ASCII -> EBCDIC. (code ASCII détecte automatiquement).

         1         2         3         4         5         6         7         8         9         10        11        12        13
.345678901234567890123456789012345678901234567890123456789012345678901234567890123456789012345678901234567890123456789012345678901234567890123456789012
XTENSION = 'TABLE   '           / CPC (IRAS) list of observations on tape
BITPIX   =                    8 /
NAXIS    =                    2 / 2D table
NAXIS1   =                   40 / max number of characters per row
NAXIS2   =                 1508 / number of rows (observations)
TFIELDS  =                    8 / number of fields per row
EXTNAME  = 'CPC-OBS '           /
EXTVER   =                    2 / Second version of the list

TTYPE1   = 'OBJ.NAME'           / astronomical name of object
TBCOL1   =                    1 / max 13 char
TFORM1   = 'A13     '           /

TTYPE2   = 'TIME OBS'           / time of observation
TBCOL2   =                   14 / 1 unit is about 31.6 sec time
TFORM2   = 'I6      '           /
TUNIT2   = 'MICRO.YR'           / fraction of year since 1983.0

TTYPE3   = 'RAH     '           / Right Ascension; hour part
TBCOL3   =                   20 /
TFORM3   = 'I3      '           /
TUNIT3   = 'HR      '           /

TTYPE4   = 'RAM     '           / Right Ascension; minutes and decimal fraction
TBCOL4   =                   23 /
TFORM4   = 'F5.1    '           /
TUNIT4   = 'MIN     '           /

TTYPE5   = 'DECDSIGN'           / Declination sign
TBCOL5   =                   28 /

Dernier enregistrement du fichier:


Nombre d'enregistrements =     828
```

```
TAPESCAN 4.4 - TAPE ANALYSIS AND COPYING PROGRAM          09/09/91    7:50:40.9   INPUT VOL=JJ0002   (LAST MOD-24OCT88)    PAGE   1
OPTIONS IN EFFECT: LIST001,NOHEX

C2148-T1  IRAS-DAX Chopped  Photometric Channel                        00010000  CPCFT1 : 489 observations  RA : 00 to 07 h
TAPEMARK NO 0001                 BLOCK LENGTHS:  MIN=00160  MAX=00160  AVG=00160    NUMBER OF BLOCKS=000001
SIMPLE  =                    T / SIMPLE FITS FORMAT ( HEADER VERSION D1 850214) BITPIX  =                    16 / PIXEL VALUES: 2-BYT
TAPEMARK NO 0002                 BLOCK LENGTHS:  MIN=14400  MAX=14400  AVG=14400    NUMBER OF BLOCKS=000001
SIMPLE  =                    T / SIMPLE FITS FORMAT ( HEADER VERSION D1 850214) BITPIX  =                    16 / PIXEL VALUES: 2-BYT
TAPEMARK NO 0003                 BLOCK LENGTHS:  MIN=14400  MAX=14400  AVG=14400    NUMBER OF BLOCKS=000001
SIMPLE  =                    T / SIMPLE FITS FORMAT ( HEADER VERSION D1 850214) BITPIX  =                    16 / PIXEL VALUES: 2-BYT
TAPEMARK NO 0004                 BLOCK LENGTHS:  MIN=14400  MAX=14400  AVG=14400    NUMBER OF BLOCKS=000001
SIMPLE  =                    T / SIMPLE FITS FORMAT ( HEADER VERSION D1 850214) BITPIX  =                    16 / PIXEL VALUES: 2-BYT
TAPEMARK NO 0005                 BLOCK LENGTHS:  MIN=14400  MAX=14400  AVG=14400    NUMBER OF BLOCKS=000001
SIMPLE  =                    T / SIMPLE FITS FORMAT ( HEADER VERSION D1 850214) BITPIX  =                    16 / PIXEL VALUES: 2-BYT
TAPEMARK NO 0006                 BLOCK LENGTHS:  MIN=11520  MAX=11520  AVG=11520    NUMBER OF BLOCKS=000001
SIMPLE  =                    T / SIMPLE FITS FORMAT ( HEADER VERSION D1 850214) BITPIX  =                    16 / PIXEL VALUES: 2-BYT
TAPEMARK NO 0007                 BLOCK LENGTHS:  MIN=11520  MAX=11520  AVG=11520    NUMBER OF BLOCKS=000001
SIMPLE  =                    T / SIMPLE FITS FORMAT ( HEADER VERSION D1 850214) BITPIX  =                    16 / PIXEL VALUES: 2-BYT
TAPEMARK NO 0008                 BLOCK LENGTHS:  MIN=14400  MAX=14400  AVG=14400    NUMBER OF BLOCKS=000001
SIMPLE  =                    T / SIMPLE FITS FORMAT ( HEADER VERSION D1 850214) BITPIX  =                    16 / PIXEL VALUES: 2-BYT
TAPEMARK NO 0009                 BLOCK LENGTHS:  MIN=14400  MAX=14400  AVG=14400    NUMBER OF BLOCKS=000001
SIMPLE  =                    T / SIMPLE FITS FORMAT ( HEADER VERSION D1 850214) BITPIX  =                    16 / PIXEL VALUES: 2-BYT
TAPEMARK NO 0010                 BLOCK LENGTHS:  MIN=11520  MAX=11520  AVG=11520    NUMBER OF BLOCKS=000001
SIMPLE  =                    T / SIMPLE FITS FORMAT ( HEADER VERSION D1 850214) BITPIX  =                    16 / PIXEL VALUES: 2-BYT
TAPEMARK NO 0011                 BLOCK LENGTHS:  MIN=11520  MAX=11520  AVG=11520    NUMBER OF BLOCKS=000001
SIMPLE  =                    T / SIMPLE FITS FORMAT ( HEADER VERSION D1 850214) BITPIX  =                    16 / PIXEL VALUES: 2-BYT
TAPEMARK NO 0012                 BLOCK LENGTHS:  MIN=14400  MAX=14400  AVG=14400    NUMBER OF BLOCKS=000001
SIMPLE  =                    T / SIMPLE FITS FORMAT ( HEADER VERSION D1 850214) BITPIX  =                    16 / PIXEL VALUES: 2-BYT
TAPEMARK NO 0013                 BLOCK LENGTHS:  MIN=14400  MAX=14400  AVG=14400    NUMBER OF BLOCKS=000001
SIMPLE  =                    T / SIMPLE FITS FORMAT ( HEADER VERSION D1 850214) BITPIX  =                    16 / PIXEL VALUES: 2-BYT
TAPEMARK NO 0014                 BLOCK LENGTHS:  MIN=14400  MAX=14400  AVG=14400    NUMBER OF BLOCKS=000001
```

```
SIMPLE  =                    T / SIMPLE FITS FORMAT ( HEADER VERSION D1 850214) BITPIX  =                    16 / PIXEL VALUES: 2-BYT
TAPEMARK NO 0967                  BLOCK LENGTHS:  MIN=11520  MAX=11520  AVG=11520    NUMBER OF BLOCKS=000001
SIMPLE  =                    T / SIMPLE FITS FORMAT ( HEADER VERSION D1 850214) BITPIX  =                    16 / PIXEL VALUES: 2-BYT
TAPEMARK NO 0968                  BLOCK LENGTHS:  MIN=14400  MAX=14400  AVG=14400    NUMBER OF BLOCKS=000001
SIMPLE  =                    T / SIMPLE FITS FORMAT ( HEADER VERSION D1 850214) BITPIX  =                    16 / PIXEL VALUES: 2-BYT
TAPEMARK NO 0969                  BLOCK LENGTHS:  MIN=14400  MAX=14400  AVG=14400    NUMBER OF BLOCKS=000001
SIMPLE  =                    T / SIMPLE FITS FORMAT ( HEADER VERSION D1 850214) BITPIX  =                    16 / PIXEL VALUES: 2-BYT
TAPEMARK NO 0970                  BLOCK LENGTHS:  MIN=14400  MAX=14400  AVG=14400    NUMBER OF BLOCKS=000001
SIMPLE  =                    T / SIMPLE FITS FORMAT ( HEADER VERSION D1 850214) BITPIX  =                    16 / PIXEL VALUES: 2-BYT
TAPEMARK NO 0971                  BLOCK LENGTHS:  MIN=14400  MAX=14400  AVG=14400    NUMBER OF BLOCKS=000001
SIMPLE  =                    T / SIMPLE FITS FORMAT ( HEADER VERSION D1 850214) BITPIX  =                    16 / PIXEL VALUES: 2-BYT
TAPEMARK NO 0972                  BLOCK LENGTHS:  MIN=14400  MAX=14400  AVG=14400    NUMBER OF BLOCKS=000001
SIMPLE  =                    T / SIMPLE FITS FORMAT ( HEADER VERSION D1 850214) BITPIX  =                    16 / PIXEL VALUES: 2-BYT
TAPEMARK NO 0973                  BLOCK LENGTHS:  MIN=14400  MAX=14400  AVG=14400    NUMBER OF BLOCKS=000001
SIMPLE  =                    T / SIMPLE FITS FORMAT ( HEADER VERSION D1 850214) BITPIX  =                    16 / PIXEL VALUES: 2-BYT
TAPEMARK NO 0974                  BLOCK LENGTHS:  MIN=14400  MAX=14400  AVG=14400    NUMBER OF BLOCKS=000001
SIMPLE  =                    T / SIMPLE FITS FORMAT ( HEADER VERSION D1 850214) BITPIX  =                    16 / PIXEL VALUES: 2-BYT
TAPEMARK NO 0975                  BLOCK LENGTHS:  MIN=14400  MAX=14400  AVG=14400    NUMBER OF BLOCKS=000001
SIMPLE  =                    T / SIMPLE FITS FORMAT ( HEADER VERSION D1 850214) BITPIX  =                    16 / PIXEL VALUES: 2-BYT
TAPEMARK NO 0976                  BLOCK LENGTHS:  MIN=14400  MAX=14400  AVG=14400    NUMBER OF BLOCKS=000001
SIMPLE  =                    T / SIMPLE FITS FORMAT ( HEADER VERSION D1 850214) BITPIX  =                    16 / PIXEL VALUES: 2-BYT
TAPEMARK NO 0977                  BLOCK LENGTHS:  MIN=14400  MAX=14400  AVG=14400    NUMBER OF BLOCKS=000001
SIMPLE  =                    T / SIMPLE FITS FORMAT ( HEADER VERSION D1 850214) BITPIX  =                    16 / PIXEL VALUES: 2-BYT
TAPEMARK NO 0978                  BLOCK LENGTHS:  MIN=14400  MAX=14400  AVG=14400    NUMBER OF BLOCKS=000001
SIMPLE  =                    T / SIMPLE FITS FORMAT ( HEADER VERSION D1 850214) BITPIX  =                    16 / PIXEL VALUES: 2-BYT
TAPEMARK NO 0979                  BLOCK LENGTHS:  MIN=14400  MAX=14400  AVG=14400    NUMBER OF BLOCKS=000001
C2148-T2  IRAS-DAX Chopped  Photometric Channel                          00010000  CPCFT2 : 624 observations  RA : 08 to 15 h
TAPEMARK NO 0980                  BLOCK LENGTHS:  MIN=00160  MAX=00160  AVG=00160    NUMBER OF BLOCKS=000001
```

```
SIMPLE  =                    T / SIMPLE FITS FORMAT ( HEADER VERSION D1 850214) BITPIX  =                    16 / PIXEL VALUES: 2-BYT
TAPEMARK NO 2227                  BLOCK LENGTHS:  MIN=14400  MAX=14400  AVG=14400    NUMBER OF BLOCKS=000001
SIMPLE  =                    T / SIMPLE FITS FORMAT ( HEADER VERSION D1 850214) BITPIX  =                    16 / PIXEL VALUES: 2-BYT
TAPEMARK NO 2228                  BLOCK LENGTHS:  MIN=14400  MAX=14400  AVG=14400    NUMBER OF BLOCKS=000001
C2148-T3  IRAS-DAX Chopped  Photometric Channel                          00010000  CPCFT3 : 395 observations  RA : 16 to 23 h
TAPEMARK NO 2229                  BLOCK LENGTHS:  MIN=00160  MAX=00160  AVG=00160    NUMBER OF BLOCKS=000001
SIMPLE  =                    T / SIMPLE FITS FORMAT ( HEADER VERSION D1 850214) BITPIX  =                    16 / PIXEL VALUES: 2-BYT
TAPEMARK NO 2230                  BLOCK LENGTHS:  MIN=11520  MAX=11520  AVG=11520    NUMBER OF BLOCKS=000001
SIMPLE  =                    T / SIMPLE FITS FORMAT ( HEADER VERSION D1 850214) BITPIX  =                    16 / PIXEL VALUES: 2-BYT
TAPEMARK NO 2231                  BLOCK LENGTHS:  MIN=11520  MAX=11520  AVG=11520    NUMBER OF BLOCKS=000001
SIMPLE  =                    T / SIMPLE FITS FORMAT ( HEADER VERSION D1 850214) BITPIX  =                    16 / PIXEL VALUES: 2-BYT
TAPEMARK NO 2232                  BLOCK LENGTHS:  MIN=11520  MAX=11520  AVG=11520    NUMBER OF BLOCKS=000001
SIMPLE  =                    T / SIMPLE FITS FORMAT ( HEADER VERSION D1 850214) BITPIX  =                    16 / PIXEL VALUES: 2-BYT
TAPEMARK NO 2233                  BLOCK LENGTHS:  MIN=11520  MAX=11520  AVG=11520    NUMBER OF BLOCKS=000001
SIMPLE  =                    T / SIMPLE FITS FORMAT ( HEADER VERSION D1 850214) BITPIX  =                    16 / PIXEL VALUES: 2-BYT
TAPEMARK NO 2234                  BLOCK LENGTHS:  MIN=14400  MAX=14400  AVG=14400    NUMBER OF BLOCKS=000001
SIMPLE  =                    T / SIMPLE FITS FORMAT ( HEADER VERSION D1 850214) BITPIX  =                    16 / PIXEL VALUES: 2-BYT
TAPEMARK NO 2235                  BLOCK LENGTHS:  MIN=14400  MAX=14400  AVG=14400    NUMBER OF BLOCKS=000001
SIMPLE  =                    T / SIMPLE FITS FORMAT ( HEADER VERSION D1 850214) BITPIX  =                    16 / PIXEL VALUES: 2-BYT
TAPEMARK NO 2236                  BLOCK LENGTHS:  MIN=11520  MAX=11520  AVG=11520    NUMBER OF BLOCKS=000001
SIMPLE  =                    T / SIMPLE FITS FORMAT ( HEADER VERSION D1 850214) BITPIX  =                    16 / PIXEL VALUES: 2-BYT
TAPEMARK NO 2237                  BLOCK LENGTHS:  MIN=11520  MAX=11520  AVG=11520    NUMBER OF BLOCKS=000001
SIMPLE  =                    T / SIMPLE FITS FORMAT ( HEADER VERSION D1 850214) BITPIX  =                    16 / PIXEL VALUES: 2-BYT
TAPEMARK NO 2238                  BLOCK LENGTHS:  MIN=11520  MAX=11520  AVG=11520    NUMBER OF BLOCKS=000001
SIMPLE  =                    T / SIMPLE FITS FORMAT ( HEADER VERSION D1 850214) BITPIX  =                    16 / PIXEL VALUES: 2-BYT
TAPEMARK NO 2239                  BLOCK LENGTHS:  MIN=11520  MAX=11520  AVG=11520    NUMBER OF BLOCKS=000001
SIMPLE  =                    T / SIMPLE FITS FORMAT ( HEADER VERSION D1 850214) BITPIX  =                    16 / PIXEL VALUES: 2-BYT
TAPEMARK NO 2240                  BLOCK LENGTHS:  MIN=11520  MAX=11520  AVG=11520    NUMBER OF BLOCKS=000001
```

```
$NOP
$NOP
$NOP
$NOP
$NOP ================================ LIST OF GAILOUT1
$EXE TPLIST BS

INPUT PARAMETERS ARE:  AS SR=1=1

 TAPE NO.   1              FILE NO.   1
 RECORD   1                LENGTH   160
C2148-T1  IRAS-DAX Chopped  Photometric Channel                          00010000  CPCFT1  : 489 obse
rvations  RA : 00 to 07 h                          00020000

***** JOB DONE.
$EXE TPLIST BS

INPUT PARAMETERS ARE:  AS SR=1=1 1 1 980

 TAPE NO.   1              FILE NO.   980
 RECORD   1                LENGTH   160
C2148-T2  IRAS-DAX Chopped  Photometric Channel                          00010000  CPCFT2  : 624 obse
rvations  RA : 08 to 15 h                          00020000

***** JOB DONE.
$EXE TPLIST BS

INPUT PARAMETERS ARE:  AS SR=1=1 1 1 2229

 TAPE NO.   1              FILE NO.   2229
 RECORD   1                LENGTH   160
C2148-T3  IRAS-DAX Chopped  Photometric Channel                          00010000  CPCFT3  : 395 obse
rvations  RA : 16 to 23 h                          00020000

***** JOB DONE.
$WEO LPS
$$
$ASS IN HT1
```

Julian date of observation - 1983.0

Object name / Right Ascension / Declination / Observation Type

NGC 0055 / 41621 / 12.4 / -39 28 / 9*9FF

```
NGC 0055      418954 00 12.4 -39 28 9*9FFN
GC 0134      505582 00 27.9 -33 32 9*9F NGC 0134      459723 00 27.9 -33 32 9*9FFM 31      501126
00 37.8 +40 26 9*9FFM 31      536988 00 37.8 +40 26 9*9FFM 31      561290 00 37.8 +40 26 9*9F
FM 31      564425 00 37.8 +40 26 9*9FFM 31      550495 00 39.5 +41 04 9*9FFM 31      60106
9 00 39.5 +41 04 9*9FFM 31      605768 00 39.5 +41 04 9*9FFM 31      635943 00 39.5 +41 04 9*
9FFM 31      537185 00 39.5 +40 54 9*9FFM 31      539929 00 39.6 +40 54 9*9FFM 31      547
751 00 39.6 +40 54 9*9FFM 31      551882 00 39.6 +40 54 9*9FFM 31      119366 00 40.0 +40 59
9*9FFM 31      124461 00 40.0 +40 59 9*9FFM 31      499552 00 40.0 +41 00 9*9FFM 31      5
00531 00 40.0 +41 00 9*9FFM 31      502490 00 40.0 +41 00 9*9FFM 31      503079 00 40.0 +41 0
0 9*9FFM 31      499943 00 40.4 +41 05 9*9FFM 31      510330 00 40.4 +41 05 9*9FFM 31
510919 00 40.4 +41 05 9*9FFM 31      545416 00 40.4 +41 05 9*9FFM 31      636138 00 40.5 +40
55 9*9FFM 31      635729 00 40.5 +40 55 9*9FFM 31      551691 00 41.5 +41 04 9*9FFM 31
567168 00 41.5 +41 04 9*9FFM 31      578336 00 41.5 +41 04 9*9FFM 31      581079 00 41.5 +
41 04 9*9FFM 31      592052 00 41.9 +41 10 9*9FFM 31      594196 00 41.9 +41 10 9*9FFM 31
596359 00 41.9 +41 10 9*9FFM 31      598912 00 41.9 +41 10 9*9FF      599703 00 41.9
+67 57 9*9F M 31      534443 00 42.2 +41 16 9*9FFM 31      598715 00 42.2 +41 16 9*9FFM 31
600676 00 42.2 +41 16 9*9FFM 31      602832 00 42.2 +41 16 9*9FFM 31      603025 00 42
.5 +41 22 9*9FFM 31      633210 00 42.5 +41 22 9*9FFM 31      635335 00 42.5 +41 22 9*9FFM 31
510525 00 42.7 +41 38 9*9FFM 31      549525 00 42.7 +41 38 9*9FFM 31      551490 00
42.7 +41 38 9*9FFM 31      558731 00 42.7 +41 38 9*9FF      592655 00 43.2 +69 59 9*9F
596377 00 43.2 +69 59 9*9F      603623 00 48.6 +69 03 9*9F NGC 0300      435416 0
0 52.5 -37 57 9*9FFNGC 0300      467957 00 52.5 -37 57 9*9FFACK 125-47.1 504246 00 57.3 +15 28 9*9F
ACK 125-47.1 515220 00 57.3 +15 28 9*9F IC 1613      489534 01 02.2 +01 51 9*9FFIC 1613      497758
01 02.2 +01 51 9*9FFIRC+10011      535972 01 03.8 +12 19 9*9FFIRC+10011      555580 01 03.8 +12 19 9*9
FFNGC 0474      523159 01 06.7 +35 27 9*9FFNGC 0474      525997 01 06.7 +35 27 9*9FFNGC 0474      5154
59 01 17.5 +03 09 9*9FFNGC 0474      520895 01 17.5 +03 09 9*9FFM 33      502098 01 30.4 +30 39 9
*9FFM 33      506986 01 30.4 +30 39 9*9FFM 33      508364 01 30.4 +30 39 9*9FFM 33      51
7177 01 30.4 +30 39 9*9FFM 33      482102 01 31.0 +30 24 9*9FFM 33      484845 01 31.0 +30 24
9*9FFM 33      498563 01 31.0 +30 24 9*9FFM 33      499347 01 31.0 +30 24 9*9FFM 33
501111 01 31.0 +30 24 9*9FFM 33      516017 01 31.0 +30 31 9*9FFM 33      506793 01 31.0 +30
31 9*9FFM 33      508758 01 31.0 +30 31 9*9FFM 33      509341 01 31.0 +30 31 9*9FF
513106 01 31.6 +30 31 9*9FF      503268 01 31.6 +30 31 9*9FF      504049 01 31.6 +3
0 31 9*9FF      506598 01 31.6 +30 31 9*9FFNGC 0613      502644 01 32.0 -29 40 9*9F NGC 0628
531291 01 34.0 +15 32 9*9FFNGC 0628      534034 01 34.0 +15 32 9*9FFUGC 1176      536778 01 37.5
+15 39 9*9FFUGC 1176      541862 01 37.5 +15 39 9*9FFNGC 0643B      765965 01 38.4 -75 16 9*9F NGC 064
3B      773414 01 38.4 -75 16 9*9F NGC 65171      597541 01 39.2 +51 19 9*9F NGC 65071      600285 01 39.
2 +51 19 9*9F NGC 0660      531486 01 40.4 +13 23 9*9FFNGC 0660      539521 01 40.4 +13 23 9*9FFNGC 0
782      386330 01 56.0 -58 02 9*9FFNGC 0782      383074 01 56.0 -58 02 9*9FF      233127 01 5
7.0 -57 04 9*9F NGC 0777      555984 01 57.4 +31 11 9*9F NGC 0777      564214 01 57.4 +31 11 9*9F NGC
0784      587337 01 58.4 +28 36 9*9F NGC 0784      599681 01 58.4 +28 36 9*9F NGC 0891      577932 02
19.4 +42 07 9*9F NGC 0891      580676 02 19.4 +42 07 9*9F NGC 0891      125051 02 19.4 +42 07 9*9FFN
GC 0891      142363 02 19.4 +42 07 9*9FFNGC 0925      581655 02 24.3 +33 21 9*9F NGC 0925      583417
02 24.3 +33 21 9*9F NGC 0925      586161 02 24.3 +33 21 9*9F NGC 0925      588904 02 24.3 +33 21 9*9F
UGC 2035      587531 02 31.5 +29 32 9*9F UGC 2035      591451 02 31.5 +29 32 9*9F NGC 1986      50577
5 02 31.6 -39 15 9*9F MAFFEI 1      206976 02 32.6 +59 26 9*9FFMAFFEI 1      209916 02 32.6 +59 26 9*
9FFMAFFEI 2      207175 02 38.1 +59 23 9*9FFMAFFEI 2      212660 02 38.1 +59 23 9*9FF      232
21 02 43.7 -62 43 9*9F NGC 1097      558293 02 44.2 -30 29 9*9FF      631060 02 48.6 +69 03
9*9F      633799 02 48.6 +69 03 9*9F      595571 02 51.2 +41 23 9*9F      6
33394 02 51.2 +41 23 9*9F NGC 1140      582418 02 52.1 -10 14 9*9F NGC 1140      585556 02 52.1 -10 1
4 9*9F ACK 255-59.1 499700 02 55.2 -44 22 9*9F ACK 255-59.1 502443 02 55.2 -44 22 9*9F
150139 02 59.4 +60 16 9*9F NGC 1169      216980 03 00.2 +46 11 9*9FFNGC 1169      219730 03 00.2 +46
11 9*9FF      165214 03 03.5 +58 19 9*9F      168563 03 03.5 +58 19 9*9F NGC 1291
497737 03 15.8 -41 18 9*9FFNGC 1291      500873 03 15.5 -41 18 9*9FF      198959 03 16.5 +
```

```
$NOP
$NOP
$NOP
$NOP
$NOP ========================================= LIST OF GAILOUT1
$EXE TPLIST BS

INPUT PARAMETERS ARE:  AS SR=1=1

 TAPE NO.   1              FILE NO.   1
 RECORD   1                LENGTH   150
C2148-T1  IRAS-DAX Chopped  Photometric Channel                                  10010000  CPCFT1 : 489 obse
rvations  RA : [illegible] to [illegible] h                                  10020001

***** JOB DONE.
$EXE TPLIST BS

INPUT PARAMETERS ARE:  AS SR=1=1 1 1 3020

 TAPE NO.   1              FILE NO.   3020
 RECORD   1                LENGTH   3168
XTENSION = 'TABLE   '           / CPC (IRAS) list of observations on tape        BITPIX   =
          8 /                                                   NAXIS    =                    2 / 2D ta
ble                                   NAXIS1   =                   40 / max number of characters
 per row                NAXIS2   =                 1598 / number of rows (observations)
   TFIELDS  =                    8 / number of fields per row                    EXTNAME  = 'CPC
-OBS '          /                                                   EXTVER   =                    2 / S
econd version of the list
                        TTYPE1   = 'OBJ.NAME'          / astronomical name of object
       TBCOL1   =                    1 / max 13 char                                    TFORM1   =
'A13     '          /
                                          TTYPE2   = 'TIME OBS'          / time of observat
ion                          TBCOL2   =                   14 / 1 unit is about 31.6 sec time
)          TFORM2   = 'I6      '          /                                                TUNIT2
  = 'MICRO.YR'          / fraction of year since 1983.0
                                          TTYPE3   = 'RAH     '          / Right Ascens
ion; hour part                    TBCOL3   =                   28 /
                TFORM3   = 'I3      '          /                                                TUN
IT3   = 'HR      '          /
                                          TTYPE4   = 'RAM     '          / Right As
cension; minutes and decimal fraction  TBCOL4   =                   23 /
                TFORM4   = 'F5.1    '          /
 TUNIT4   = 'MIN     '          /
                                          TTYPE5   = 'DECDSIGN'          / Decl
ination sign                         TBCOL5   =                   28 /
                TFORM5   = 'A2      '          / (' +' or ' -')
CD      '          / Declination; degree part (unsigned)          TBCOL6   =                    TTYPE6   = 'DE
                                          TFORM6   = 'I2      '          /                    30 /
                TUNIT6   = 'DEG                   /
 'DECM    '          / Declination; minutes part                    TBCOL7   =                    TTYPE7   =
2 /                                       TFORM7   = 'I3      '          /                    3
                TUNIT7   = 'ARC.MIN '          /
   = 'RASTER  '          / type of raster scan used                    TBCOL8   =                    TTYPE8
   35 /                                       TFORM8   = 'A6      '          / (' 9*9F ' o
r ' 9*9FF' )
}          ORIGIN   = 'ROS-GRON'          / Laboratory of Space Research, Groningen          DA
E      = '11/04/85'          / creation date of this file                    TITLE    = 'CPC-IRAS'
                                          END
```